



# Hidden Capacities of the EMO Quay Wall in the Port of Rotterdam

BSc Thesis of J.M. Verstijnen

Port of Rotterdam





Project Hidden Capacities of the EMO Quay Wall in the Port of Rotterdam  
Document BSc Thesis of J.M. Verstijnen  
Status Unverified (no rights can be claimed from unverified, non-approved, documents)  
Submission Date 22 December 2016  
Reference -

Client Port of Rotterdam  
Project code RT78-49  
Project Leader P. Quist, MSc  
Project Director -

Author(s) J.M. Verstijnen  
Checked by D.J. Jaspers Focks, MSc  
Approved by -

BSc Thesis for the study Land and Water Management at University of Applied Sciences  
Van Hall Larenstein in Velp

Keywords Quay walls, Geotechnical, GWW

Address Witteveen+Bos Raadgevende ingenieurs B.V.  
Van Twickelostraat 2  
P.O. Box 233  
7400 AE Deventer  
The Netherlands  
+31 570 69 79 11  
www.witteveenbos.com  
CoC 38020751

The Quality management system of Witteveen+Bos has been approved based on ISO 9001.

© Witteveen+Bos

No part of this document may be reproduced and/or published in any form, without prior written permission of Witteveen+Bos Consulting engineers, nor may it be used for any work other than that for which it was manufactured without such permission, unless otherwise agreed in writing. Witteveen+Bos Consulting engineers does not accept liability for any damage arising out of or related to changing the content of the document provided by Witteveen+Bos Consulting engineers.



## Preface

In front of you is my graduation thesis whereon I've been working on for the past four months. The thesis is part of the BSc study Land- and Water Management at the University of Applied Sciences Van Hall-Larenstein in Velp. The thesis has been made under supervision of Dirk Jan Jaspers Focks of Witteveen+Bos Consulting Engineers, in the Department of Geotechnical Engineering.

I was doing my internship at this same group when I informed if there was a possibility to do my final project as well. I had already insinuated that I wanted to continue studying at the university when I would be finished with my bachelor. So, it was decided that the research should have a technical point of view. I wanted the subject to be in the professional field of geotechnical, but should have an interface with water. Dirk Jan suggested writing the thesis about the behaviour of quay walls, which I thought was really interesting and met the proposed conditions. After four months of working on the subject I would like to express my gratitude towards a few people. First of all: Dirk Jan Jaspers Focks as he was my daily supervisor at Witteveen+Bos. Whenever he had time he would give extensive answers to all of my questions about quay walls and soil models. Thereby I would like to thank my colleagues of the Department of Geotechnics, especially Floris, Thomas and Arny as they helped with me with the theory of Plaxis and the Plaxis calculations when I couldn't get it running.

I would express my gratitude to my parents as they always supporting my decisions during my years of studying in Velp. And to Nienke, as she gave me mental support all the way from the USA. Last but not least, I also would like to thank my roommates, as they needed to listen to my frustrations when my models didn't work and provided company during the evenings and weekends.

Deventer, the Netherlands  
December 2016

Bart Verstijnen



## Summary

The demand for bigger, quicker and cheaper transportation costs is as high as it has ever been. Enormous cargo and bulk ships are the results of these demands, resulting in equally massive infrastructure to facilitate these kinds of vessels. As quay walls grow bigger and bigger, there is a growing interest in the behaviour of these structures to ensure that they are both safe and economical.

Quay walls are complex civil structures with a lot of uncertainties within the design process. The purpose of the research is to determine the actual behaviour of the quay wall and to compare it with the models that have been used to design the construction. By comparing these results, it is possible to back-calculate the safety of the structure and its potential hidden capacities. Hidden capacities are additional capacities generated by making conservative decisions during the design process to ensure a safe design, e.g. assumption that the soil is weaker than in reality. The main research question of the thesis is: How does the (potential) hidden capacity of the quay wall relate to the comparison of the actual behaviour and the calculated models? The EMO quay wall in Rotterdam, the Netherlands will be used as a case study, because periodic measurements on this quay wall have been taken over the last 5 years.

The design models and the measurement data have been collected over the past 5 years are compared to determine the hidden capacities of the quay wall and its safety. A new model has been set up due to absence of the model that originally has been used. The process of creating this design is the same as a normal design process, except the dimensions and parameters of the structure were already known. A starting point memo has been set up to summarise all of the uncertainties. A Finite Element Method calculation has been performed with the use of Plaxis. Plaxis is capable of calculating complex geometries with highly specified boundary conditions and extensive construction / load phases. Both static and dynamic calculations have been performed and gave various results.

The Port of Rotterdam has released various kinds of measurement data of the quay wall. Continuous measurements of anchor forces and periodical measurements of the deformations of the combi wall and deformation bolts have been made. In an earlier research it has been stated that a correction factor has to be applied on the anchor forces to eliminate the effect of the groundwater temperature on the anchor forces. After the correction, the anchor forces vary between the 294 kN and 505 kN. The anchor forces both increase and decrease over time, which implies loading and unloading of the structure. Deformations suggest the same over time, as the combi wall varies between 64 mm and 25 mm and the deformation bolts vary between the 10 mm and -14 mm horizontally and between the 23 mm and -5 mm vertically. A comparison of the measured and calculated values has been made to check the consistency of the calculated values next to the measured ones. The results of the static calculation give relatively close values to the measurements, but are more varied and larger on average. The dynamic results of the load combinations give higher results, but don't match with the measurements when plotted over time. The fully coupled flow deformation calculation seems to accumulate the anchor forces and displacements over time due to repetitive loading of the construction. The water level changes and corresponding anchor forces do get modelled properly, but accumulate over time making the results incorrect.

For the determination of the hidden capacity the corrected measurements and the static calculations have been used. It is assumed that when  $X_{\text{structural,measured}} < X_{\text{structural,calculated}}$  there is presence of hidden capacity. For the anchor forces, a hidden capacity of 14% during the average situation and 68% during the normative situation has been created. A hidden capacity of 80% on average and 79% has been created for the combi wall deformations. The deformations of the superstructure have an undercapacity of -105% in positive direction (landside) and an overcapacity of 446% in negative direction (water side). When the relative values are compared, the hidden capacities are 267% in positive direction and 110% in negative direction. It can be stated that hidden capacity or overcapacity has been created during the design process of the quay wall and the static results of the calculation match with the measured values.

Also, the ratio between the measured values and the design calculations has been determined to check how safe the construction is. The ratio between measurements and design calculation of the anchor forces is approximately 4. For the deformations of the combi wall there is a ratio of approximately 9. The horizontal displacements of the top of the construction have a ratio of approximately 33. The quay wall is therefore considered safe.

The most important recommendations made for follow-up research are: the use of the Hardening Soil small strain model instead of the Hardening Soil model. The Hardening Soil small strain is commonly used when performing dynamic earthquake calculations and could result in more realistic results. Also, an extreme load could be applied in order to eliminate the hardening points that might cause the incrementing anchor forces. The geometry of the calculation also should be updated after the site visit at the EMO quay. The update of the geometry will give more realistic results, but the adaption will cause a deviation of the usual design procedures.

# TABLE OF CONTENTS

<b>PREFACE</b>	<b>I</b>
<b>SUMMARY</b>	<b>III</b>
<b>1 INTRODUCTION</b>	<b>1</b>
1.1 Context	1
1.2 Purpose	1
1.3 Method	2
1.4 Report structure	3
1.5 Target audience	3
<b>2 LITERATURE STUDY</b>	<b>4</b>
2.1 A brief history on quay walls	4
2.2 The Port of Rotterdam and EMO B.V.	4
2.3 The Mississippi Harbour	5
2.4 Definition of the “hidden capacity”	7
2.5 Safety check according to the CUR211	8
2.6 Modelling software: PLAXIS 2D	9
2.6.1 The principle of the Finite Elements Method used by Plaxis	9
2.6.2 The Hardening Soil model	10
2.6.3 Fully coupled flow-deformation	10
2.6.4 On the use of the finite element method to design quay walls	11
2.6.5 Plaxis vs. D-Sheet Piling	11
2.7 Previous studies on the behaviour of quay walls	12
2.8 Data processing	12
2.8.1 Matching date and time	13
2.8.2 Excluding thermal effects in anchor force measurements	13
2.8.3 Corrupted data	14
<b>3 MODELLING IN PLAXIS 2D</b>	<b>15</b>
3.1 Structural geometry	15
3.2 Geotechnical properties of the soil	15
3.2.1 Expectation, characteristic and design values	17
3.3 Hydrologic conditions	17
3.4 Loading sequence	17

3.5	Plaxis results	18
<b>4</b>	<b>DATA ANALYSIS</b>	<b>20</b>
4.1	Corrected anchor forces	20
4.2	Anchor forces	20
4.3	Combination wall position	21
4.4	Displacements of the superstructure	22
<b>5</b>	<b>COMPARISON BETWEEN MEASURED AND CALCULATED VALUES</b>	<b>23</b>
5.1	Anchor Forces	23
5.2	Combi Wall Position	24
5.3	Displacement of the superstructure	24
<b>6</b>	<b>HIDDEN CAPACITIES OF THE QUAY WALL</b>	<b>26</b>
6.1	Hidden capacities	26
6.1.1	Anchor forces	26
6.1.2	Combi wall position	26
6.1.3	Deformations of the superstructure	27
6.2	Proven safety according to CUR211	27
<b>7</b>	<b>SENSITIVITY ANALYSES</b>	<b>28</b>
7.1	Sensitivity of the Plaxis model	28
7.1.1	Flow conditions	28
7.1.2	Stiffness parameters	28
7.2	Sensitivity data analyses	29
7.2.1	Data analyses	29
7.2.2	Displacement measurements	29
<b>8</b>	<b>SITE VISIT EMO B.V.</b>	<b>30</b>
<b>9</b>	<b>CONCLUSIONS</b>	<b>31</b>
9.1	Discussion	31
9.2	Conclusions	32
9.3	Recommendations	34
<b>10</b>	<b>BIBLIOGRAPHY</b>	<b>35</b>

Last page

36

**APPENDICES****Number of  
pages**

I. Fault Tree Quay Wall	1
II. Starting Points Memo	12
III. Expectation, Representative and Design Parameter Sets	1
IV. Graphs of the Measured Data	13
V. Static and Dynamic Calculation Results	5
VI. Statistics of Measured and Calculated Values	4
VII. As-built Drawing of the EMO Quay Wall	1
Digital: Measurement Data	-
Digital: Soil Interpretation Parameter Sheet	-
Digital: Determination of HSM Parameter Non-Cohesive	-
Digital: Soil Investigation	-



# 1 Introduction

The introduction of the project plan will provide a context of the problem that will be tackled with the thesis and a definition of the research questions, which will be the basis of the report. This chapter also addresses the set up and the target audience of the thesis.

## 1.1 Context

All around the world the demand for bigger, quicker and cheaper transportation costs has significantly increased over the last few decades. Transportation corporations have anticipated on these demands by creating enormous cargo ships and bulk carriers to carry as much as possible. Ports have to create an equally enormous infrastructural network to facilitate these huge vessels in order to distribute the goods and make profits.

The harbour of Rotterdam has created new loading docks in order to be able to compete with other harbours. The new quay wall has a soil retaining height of 23m, which gives the largest vessels of the world the possibility to dock in the harbour. The excavators, cranes and deposit sites that are needed to tranship all the bulk induce incredible forces that influence the quay wall. It is a priority that quay walls are more than secure in highly active areas, such as the Port of Rotterdam. Chances of accidents and the personal and economic consequences are disastrous when failure may occur.

An accurate as possible model of the environment has to be made to ensure that the designed structure will be both secure and economically favourable. The design in combination with the modelled subsoil will be the verification of the safety of the design. During the design of the structure the characteristics of the surrounding environment have been mapped using measurements and lab tests. The results of these studies will never be fully complete, but the aim is to create an image as complete as possible of reality. In this pursuit of completeness certain assumptions have to be made to close the gaps between the actual data. An engineer will have to analyse the certainties and take the uncertainties into consideration to ensure safety. When a project is similar to past projects experience is a backup to make these assumptions but when this is not the case conservative assumptions have to be made.

Several calculation methods and modelling software have been developed to complement the geotechnical knowledge of the engineer. Complex modelling software, such as Plaxis, is capable of performing complex FEM(Finite Elements Method) calculations which provides a very realistic representation of the reality. These model results are realistic representations but still are a product of the tests, assumptions and experiences of the engineer. Despite the uncertainties and assumptions the construction will be declared safe according to the current Dutch standards.

## 1.2 Purpose

The purpose of the research is to determine the actual behaviour of a complex quay wall and to compare this with the model that has been used for the design of the quay wall. The comparison should give an insight of the difference between the predicted and actual behaviour of the quay wall. By recalculating the design of the quay wall it is possible to determine whether or not the quay wall is secure according to current standards. Alongside with the safety of the quay wall, it will be possible to determine hidden capacities of the quay wall. Hypothetically, the amount of this hidden capacity will grow during the design process because of the conservative way the engineers build their models and designing their constructions.

The main research question of the research will be as follows:

- How does the (potential) hidden capacity of the quay wall relate to the comparison of the actual behaviour and the calculated models?

The next sub questions will lead to an answer of the main question:

- Which assumptions, which derive from uncertainties, will have to be made to create a model that is as realistic as possible to design the quay wall?
- What does the design of the quay wall look like?
- What is the actual behaviour of the quay wall as recorded by the sensors for the past 5 years?
- Does the measured data suggest that the quay wall is safe according to current Dutch standards?
- What is the amount of hidden capacity of the quay wall?
- To what extent is the model consistent with the measured behaviour of the quay wall?
- What are sensitive aspects of the analyses that influence the hidden capacity?

### 1.3 Method

As starting, a literature study has been conducted to gain basic knowledge of the different aspects of the research subject. Information about the Port of Rotterdam, the EMO quay wall and quay wall design processes have been looked up. A definition of the hidden capacity of the quay wall has been developed with the use of the literature. Also, the theory of FEM (Finite Element Modelling) and the soil models that are used by Plaxis have been studied to prevent black boxes during the modelling process. The final part of the literature study consists of analysing monitor reports and earlier researches on the measurement data of the quay wall. The exact values of the measurements have been introduced in a later stage of the research in order to prevent biases during the design process of the model.

The second part of the research consists of setting up the Plaxis model. A starting point memo has been set up to define the parameters that will be used in the model. Soil parameters have been derived from soil investigations that have been performed in the past. Hydrologic conditions have been provided by public data from the Port of Rotterdam. Structural parameters and properties have been adopted from the original design and as-built drawings as the research is focused on uncertainties rather than the structural design of the quay wall itself. With the use of Plaxis, three types of calculations have been set up: one model with expected soil parameters, one model with representative soil parameters and one model with design soil parameters and load combinations. The Plaxis model with the expected soil parameters is a model with values as realistic as possible. This calculation also contains measured harbour water levels to check the effect of real water levels in Plaxis. Plaxis has a module to perform a dynamic flow calculation with the use of a 'fully coupled flow deformation' analyses. Depending on the permeability of the soil layers and the boundary conditions it is possible to calculate the response of the groundwater level behind the quay wall dependent on the various input water levels. The dynamic flow calculation provides an option to calculate realistic results. All of the different models will be used to compare with the measured data.

The third part of the research focuses on the data analysis. The available data will be cleaned and corrected during this part of the research. A lot of different kinds of measurements are available. These different types of data are linked to each other with the use of an identical feature: time. It is possible to use a table merger that combines two, or more, tables with each other with the use of a matching feature. Analyses can be performed when the dataset has been combined, cleaned and corrected. This includes a temperature correction for the anchor forces.

The comparison between the measurements and the calculations can be performed with the information of the data analyses and the calculations of the Plaxis calculations available. This comparison will be performed to check the consistency of the calculated values.

The values of the Plaxis calculations and the corrected data will be used for the last analyses to determine the hidden capacity of the quay wall. The calculated values aren't verified, while the measured values serve as a sort of 'proven' capacities of the quay wall to determine the amount of 'extra' capacity that will be created in the design. A distinction has been made between the resistance of the construction and the acting forces of the construction. When the resilience factors of the construction are calculated larger than the measured values, there can be assumed that there is a presents of hidden capacity within the design.

A sensitivity analyses will be performed by screening the uncertainties of the models and the data analyses that are used. The sensitivity analyses will be used to indicate points of interest that are sensitive to changes. It is also possible to determine the safety of the quay wall by comparing the values of the design calculations with the measured values. The design calculation model will provide an insight in the effect of making conservative chooses and partial factors during the design of the construction.

At the end of the research time a site visit on the terrain of EMO has been planned. During this site visit reference material will be gathered concerning the construction and the loads that are working on the construction. It will also possible to speak to one of the employees of EMO. A small interview with the site manager of the EMO terrain will be held to gather information about the properties of the bulk and the site management of the terrain.

## 1.4 Report structure

Chapter 2 consists of a literature study to present the general knowledge of the topic. Chapter 3 contains the starting points that are used to build the Plaxis model. The data that has been provided by the Port of Rotterdam and the data analyses are presented in chapter 4. Chapter 5 gives the comparison between the measured values and the calculated values to check the consistency of the calculated values. Chapter 6 provides the amount of hidden capacity that has been created during the design process. Chapter 7 gives the sensitivity analyses to show the uncertainties of the model and the data analyses that are performed. Chapter 8 gives an overview the results of the site visit that has been planned on 15-12-2106. Chapter 9 will conclude and discuss the report and provide recommendations for further investigation. Chapter 10 contains the bibliography of the report. At the end of the report are the appendixes annexed.

## 1.5 Target audience

The thesis will be written for the geotechnical professionals of Witteveen+Bos Consulting Engineers B.V. and the lecturers and reviewers of Hogeschool Van Hall-Larenstein. In addition, students with an interest in geotechnical engineering are welcome to read the report as well.

# 2

## Literature study

In the literature study an introduction of the theoretical background of the subject will be provided. The chapter will go from a broad point of view of harbours towards the specific quay wall. The literature will also give an explanation of safety philosophies of the CUR standard. In addition to the safety philosophies, the definition of the term "hidden capacity" will be given. As third, a brief explanation of the modelling software PLAXIS and the models, which are going to be used, will be given. As last, a set-up of the data analyses will be provided.

### 2.1 A brief history on quay walls

Water, in both terms of the sea as rivers, has always had a strange attraction towards people. It has a reputation of killing numerous amounts of people but it also provides fertile lands, fresh water and a medium for transportation of goods and people. Where ships could land, villages would grow up and some of them would develop into ports and trading places. Mooring places would grow into quay walls and ports would flourish because of the trade and industries they attracted.

The first known functioning port lies in India near Lothal and it was functioning about 4.000 years ago. Along with the distribution of goods and people, knowledge and skills were spread. 300 years before Christ the city of Alexandria was the trade centre of the ancient world because of the facilities she had available for the entrance of ships. Stone quays are still to be found on the ancient island of Alexandria. Around 100 BC the Romans were already capable of creating concrete and using this in the construction of quay walls, even under water. During the Middle Ages quay walls were threatened by two major problems: siltation and poor equipment. Siltation has been known to put ports out of order, leaving only bigger ports left. The poor equipment of ports constructed from wood made it impossible to compete with other, stone constructed ports. Ports were already in a search to make their selves even more efficient. Wooden cranes operated by means of a treadmill were constructed to increase efficiency. The wooden cranes needed a solid foundation and a vertical quay wall, created an enormous advantage for the ports with stone walls. Alongside the technological developments, economic cooperatives enhanced the development of trading. A large amount of European cities began to set up a Hanse. This unique cooperation resulted in a shipping volume of 60,000 ton at the end of the fifteenth century. With the decline of power over the trading in Europe, Amsterdam knew to wrestle its way up. Amsterdam with its cooperating ports in the Netherlands was the centre of the trade industry till the end of the seventieth. After that it had to hand over its ruling position to England. Sailing ships were gradually scraped and replaced by steam ships by the nineteenth century and a following consequence in the twentieth is the continual increase in tonnage and draught. For various reasons, many ports weren't capable to maintain a competitive position and remaining ports evolved into what is currently known as 'Hubs'.

### 2.2 The Port of Rotterdam and EMO B.V.

The Port of Rotterdam is one of these ports that grew into a hub. It has made an incredible increase in water depth and retaining height in the past two centuries. In the ninetieth century, the water depth was 'only' 10,0m deep, the Botlek harbours that have been constructed around the 1960's have a depth of NAP -16,0m. During the most recent constructions of port infrastructure the water depths of the waterways and berths are at a depth of NAP-23,0m. Outside the port of Rotterdam a canal with the same depth and a length of 30,0km has been dredged in order to keep up with the demand of the transportation industries. Parallel with the development of the retaining heights of the quay wall, the type of quay wall has changed. In the 17<sup>th</sup> century the masonry quay walls were built on shallow foundations. Through bitter experience the quay walls developed from their shallow foundations to pile foundations. The material that was used evolved from masonry to concrete to steel sheet piles. By means of pile trestle systems and soil improvements, retaining heights of 18,0m could be achieved in 1963. Several different shapes have been used to construct the quay walls. They vary from L-shaped beams to delta-shaped beams or boxes. Summarizing, it can be said that the simple masonry quay wall has evolved into a complex combination of different quay wall elements to

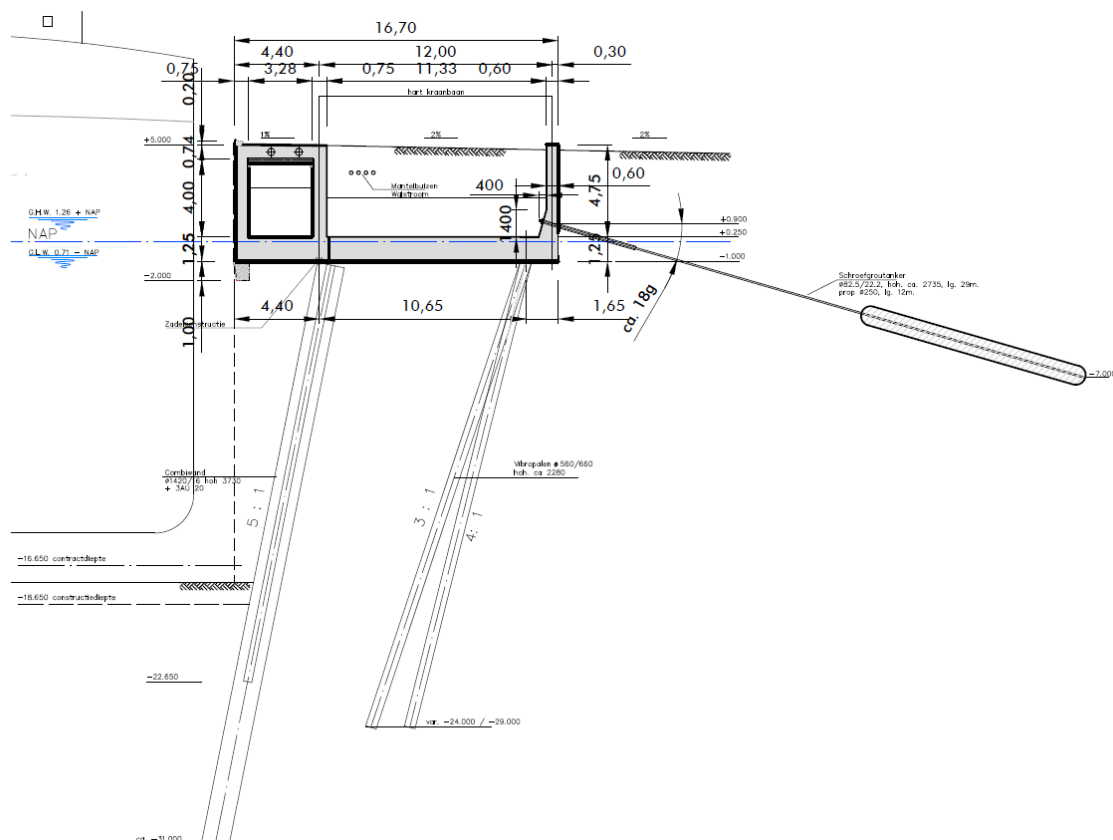
achieve a maximal amount of draught for ships. In the Mississippi harbour the quay wall construction consists of a combination wall of steel tubular piles and intermediate sheet piles with a superstructure that rests on a pile foundation consisting of bearing and tension piles. The piles and the combined wall are constructed at an angle of about 12° to reduce soil pressure and anchor tension that are working on the wall and anchors.

This combined wall gives the largest bulk carriers of the world the opportunity to berth in the Mississippi Harbour at EMO B.V., Europees Massagoed-Overslagbedrijf B.V. (EMO). EMO is the largest dry bulk terminal of Europe that processes coal and iron ores. The state-of-the-art terminal is largely automated to store, process and tranship the coal and iron ores to whole of Europe. Costumers of EMO are mainly companies in the steel- and energy sector. In 2015, EMO has distributed 20 million tonnes of coal and 13 million tonnes of iron ores (EMO B.V., 2015). These amounts of coal and ores are supplied by the deep-draught ore carriers or Very Large Ore Carriers (VLOC). Vessels like the Vale Italia belong to this category, and have been built in or after 2011 and have a loading capacity of 400,000 tonnage deadweight (DWT). Smaller vessels, such Panamax and inland vessels, berth at the quay wall that is subject to the research.

## 2.3 The Mississippi Harbour

Within the Mississippi harbour lays the EMO quay wall, see Figure 2.1. This quay wall is a structure with a relieving platform, consisting of 6 different elements designed for heavy duty. These 6 elements all have a contribution in the quay wall's function. The main functions of a quay wall are: providing berthing facilities for ships, soil retaining, providing a bearing capacity to carry loads imposed by the transshipment of bulk and also serve as a water retaining wall during high water.

Figure 2.1 The EMO quay wall, appendix VII presents the full as-built drawing

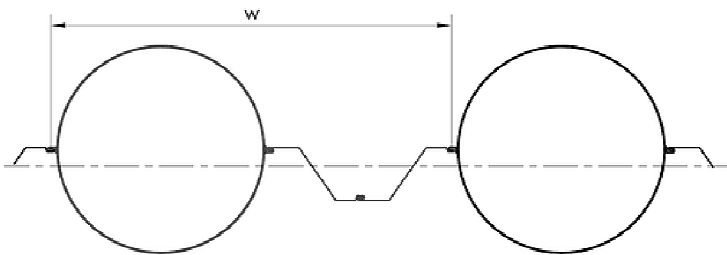


The elements to fulfil these functions are:

- Combined wall: the combined elements of the wall consist out of steel tubular piles and (shorter) sheet piles. This combination is often used in areas with high retaining heights in combination with heavy structures and loads. The sheet piles are allowed to be shorter because the pressure is transformed to

the primary, tubular piles due to arch action. The combined wall has both a retaining function as a foundation function. In the EMO quay wall construction, the combined wall has been placed with a inclination of 5:1.

Figure 2.2 Schematic representation of a combination wall



- Screw injection anchors: anchors support the earth retaining structures. The anchors used in the EMO quay wall consist of a hollow, perforated stem auger. A grout mixture will be inserted into the soil when the anchor is been drilled in. The anchor is capable of absorbing tensile stresses due to the friction between the soil and the grout body that has been inserted. The maximum design value of the tensile strength lays around 300 to 3,000 kN.
- Bearing pile: bearing piles, along with the anchors, are part of the foundation of the superstructure of the quay wall. They ensure both horizontal as vertical stability of the quay wall. The bearing piles absorb the compression forces coming from the loads on top of the quay wall. Bearing piles usually consist out of prefabricated concrete piles.
- Superstructure with relieving platform: The relieving platform provides the capacity to spread loads and distribute bearing capacity. The horizontal load on the quay wall will be significantly reduced due to the relieving platform because of the pile foundation. The pile foundation causes discharge of pressure on the quay wall which allows the combined wall to be thinner.
- Connection: a cast iron saddle is used to connect the superstructure with its foundation. The eccentric support reduces the bending moment of the sheet pile wall.
- Steel Fibre Reinforced High Performance Concrete (SFRHPC) facing: This facing is used because it resilience to the destructive forces of coal barges. It has fenders and ladders build in, reducing the gap between the ship and the quay wall. The structure reduces construction and maintains costs and less bulk is spilled during transhipment because of the smaller gap.

### Ship types

As been stated in chapter 1.2., in the Mississippi Harbour there is a berthing spot for a large number of vessels. The quay walls that is subject to the investigation (sections M6, M5 and M4) are designed for Panamax vessels(M6 and M5) and inland vessels (M4). Table 2.1 shows the specifications for the Panamax tanker.

Table 2.1 Characteristics VLOC \*Draught of an empty vessel with ballast, not the maximum draught

Vessel type	Displacement [tonnes]	Length x Beam x Draught* [m]
Panamax tanker	10.000	246 x 32 x 6,6

### Bulk loads

The bulk that will be stored behind the quay has the following properties:

Table 2.2 Bulk properties

Material	Specific gravity [ $\text{kNm}^3$ ]	Angle internal friction [°]
Iron ore	22,4-32	35-40,9
Rough coal	10	45

### Machinery

Cranes are necessary to transport these bulk goods from the ship towards their storage depots. The following table contains an indication of the parameters of the cranes that are used on the quay wall.

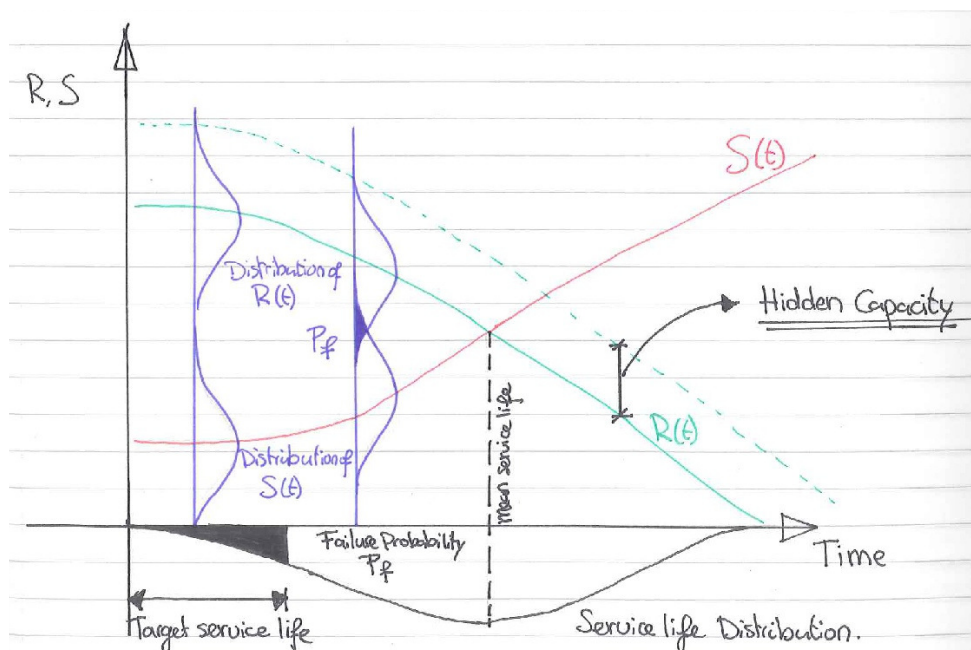
Table 2.3 Crane properties

Type of crane	Lifting capacity [kN]	Outreach waterside [m]	Rail gauge [m]	Max. vertical load [kN]	Max. wheel load [kN]	Number of wheels [-]	Wheel distance [m]
Grab gantry crane	850	45,5	70 (4 rails)	30.000 (tot. weight)	625	56	1,35 2,15 6,8

## 2.4 Definition of the "hidden capacity"

Figure 2.3 gives a schematic representation of the term "hidden capacity". The black section of the figure represents the service life of the quay wall. On the left side of the service life distribution is the target service life projected, which is often 50 years. The continuous, red line represents the increase of loads that are applied on the construction over time,  $S(t)$ . The continuous, green line represents the resistance of the construction over time,  $R(t)$ . Because of degradation of the construction the resistance will decline. Whenever  $R(t) > S(t)$ , the construction will be capable to fulfil its functions, but when  $R(t) \leq S(t)$  the construction will fail. In blue, the distribution of both  $R(t)$  and  $S(t)$  are presented. Whenever the distributions of  $R(t)$  and  $S(t)$  overlap there is a probability of failure. This failure probability,  $P_f$ , is the acceptance criterion and usually given by the index  $\beta$  (further explanation in chapter 2.5). The acceptance criterion has to be larger than the target service life to ensure a safe construction (Siemes, 1999).

Figure 2.3 Schematic representation of the failure probability and the hidden capacity



In the design of the construction several margins, through partial factors, have been adopted during the process to enclose the distributions of  $R(t)$  and  $S(t)$ . The dotted line represents the hypothetical excess capacity of the construction or hidden capacity (Walraven, 2010).

This hidden capacity is created by making conservative assumptions on the uncertain factors of the design of the construction. An accumulation of capacity in the design is created by making conservative assumption after conservative assumption, resulting in an actual  $R(t)$  represented by the dotted line in Figure 2.3. An example: using the unfavourable section in combination with the lower limits of the strength parameters of the soil.

## 2.5 Safety check according to the CUR211

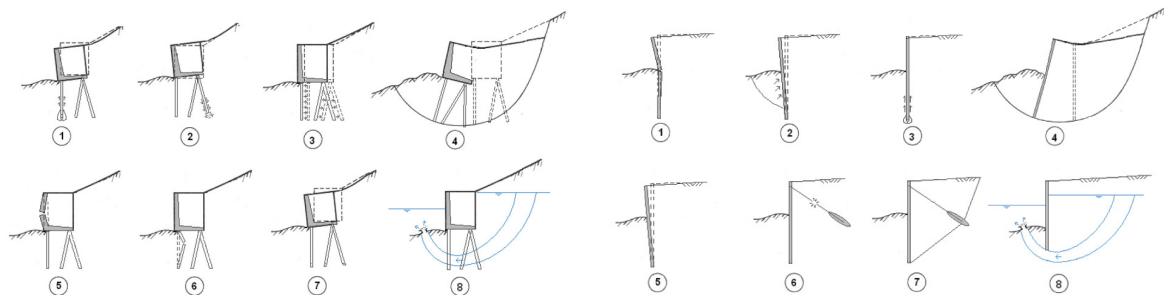
A quay wall-like structure is considered failed when one of the following functions cannot be fulfilled anymore:

- Earth retaining;
- Load bearing when the quay is in use;
- Resistance against scouring, due to river discharge, tide and ship manoeuvres.

Failure of one of these functions can be a direct consequence of a failure mechanism of the sheet pile wall construction. It is possible that one of the following events occur:

- Loss of stability, due to trespassing of maximal passive soil resistance, rupture of the front wall and rupture of the anchor;
- Failure of the stud/anchor system, including 'Kranz';
- Uplifting;
- General loss of stability;
- Exceeding of deformation.

Figure 2.4 Failure mechanisms of retaining walls founded on piles and sheet pile walls



In order to minimise the chance of failure, a well calculated design has to be made. The eventual design has to be able to fulfil its minimal lifespan. Possible threatening events have been determined with the use of a fault tree, starting from the bottom up (see appendix I). Probabilistic calculations have been made to calculate the allowable probability of failure of the failure events. The individual events have an occurrence probability of e.g.  $0,2 p$  of a total failure probability of  $p$ . All the probabilities of failure of all the individual events combined give a failure probability of  $2,4 p$  to  $3,6 p$ . This is the failure probability of one of the three main failure mechanisms of a sheet pile construction. These failure probabilities lead to safety classes, with each their failure probability and allowable repetition time and damage. The risk classes according CUR 211:

- Class I:  $\beta_{\text{constrction}} \approx 2,5$  (failure probability  $0,62 \cdot 10^{-2}$ );
- Class II:  $\beta_{\text{constrction}} \approx 3,4$  (failure probability  $0,34 \cdot 10^{-3}$ );
- Class III:  $\beta_{\text{constrction}} \approx 4,2$  (failure probability  $0,13 \cdot 10^{-4}$ ).

The failure probabilities/risk classes are linked with the partial factors that are used for the design of the sheet pile constructions. The amount of personal and economical damage increases with the classes. Class I has almost no economic damage and negligible life risk, class II does have economic damage but the life risk is negligible again and class III has a high life danger and high economic damages. So, a higher risk means higher partial factors and will result in a more robust design to reduce these risks. These partial factors and the design check for the CUR 211 has been annexed in the starting points memo, in appendix II.

Table 2.4 gives an indication of the failure probability,  $P_f$ , linked to several reliability indexes.  $P_f$  gives the probability that a system will fail to perform its intended function for a specific period of time under certain conditions. Thus, the reliability index  $\beta$  is related to the design working life of a structure.  $\beta$  is determined according to the following equation, where  $-\Phi_U^{-1}(P_f)$  indicates the inverse standardised normal distribution function:

$$\beta = -\Phi_U^{-1}(P_f)$$

Table 2.4 Relationship between the failure probability and the reliability index, source: (Holický & Vrouwenvelder, 2005)

$P_f$	$10^{-1}$	$10^{-2}$	$10^{-3}$	$10^{-4}$	$10^{-5}$	$10^{-6}$	$10^{-7}$
$\beta$	1,3	2,3	3,1	3,7	4,2	4,7	5,2

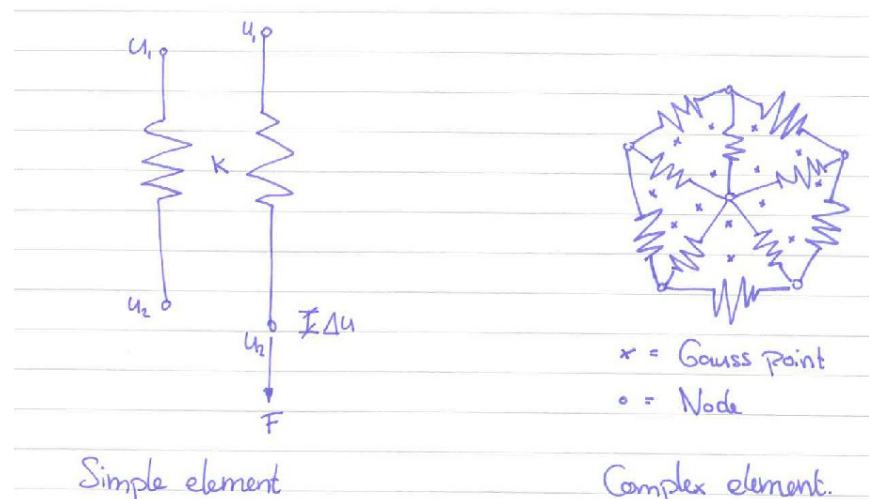
## 2.6 Modelling software: PLAXIS 2D

The modelling software of Plaxis will be used to perform the calculations of the quay wall. Plaxis is a finite element method, which is specially developed for analysis of deformations, stability and groundwater flow in geotechnical engineering. The following chapter will explain the general principle on which Plaxis is based and the soil model that is going to be used in the calculation.

### 2.6.1 The principle of the Finite Elements Method used by Plaxis

The elements of the model are described as a continuum and divided into large amount of smaller elements. These divided, smaller elements, or a mesh, have a far less complex geometry than the original situation and thus it is possible to use these shapes for analysis. Each of these elements has a number of nodes that correspond to the degree of freedom. The degree of freedom corresponds to the discrete values of the unknowns in the boundary value problem to be solved. In the case of deformation, the degrees of freedom are the same as the displacement components (x,y,z-coordinates). It is possible to calculate the deformation of the nodes with the use of stiffness parameters of the interconnections between the nodes and the forces that are acting on the nodes. The simplest example of this theory is a simple spring, see Figure 2.5.

Figure 2.5 Schematisation of a simple and a complex finite element. In the complex element, the Gauss points and nodes are shown as well



The properties of the spring will determine the amount of deformation that is caused by a certain force. This principle is used over the entire mesh that has been created for the geometry. Within an element the displacement  $\underline{u}$  is obtained by using the interpolation functions from matrix  $\underline{N}$  from the discrete nodal values in a vector  $\underline{v}$ . This is described by:

$$\underline{u} = \underline{Nv}$$

With the use of this equation and strain interpolation matrix  $\underline{B}$ , it is possible to calculate the strain increments. A stress increment is formed in order to create equilibrium between the external force vector and the internal reaction vector. Most relations between stress and strain increments are non-linear. The strain calculations usually cannot be calculated directly, and thus, iterative procedures are required in order to create the equilibrium condition. The equilibrium equation, with a substitution of the relationship between the increments of stress and strain, is written as:

$$\underline{K}^i \Delta v^i = \underline{f}_{ex}^i - \underline{f}_{in}^{i-1}$$

In the equation  $K$  is a stiffness matrix,  $\Delta v$  is the incremental displacement vector,  $f_{ex}$  is the external force vector and  $f_{in}$  is the internal force vector. The stiffness matrix  $K$  represents the material behaviour. This includes the elastic material matrix and strain interpolation matrices. More information on the stiffness matrixes and corresponding soil models will be given in chapter 2.6.2.

Plaxis also includes a groundwater flow theory and a consolidation theory in the finite element formulation. By means of interpolation, between gauss points in the mesh elements, it is possible to combine all of the defined properties of the materials and derive a second order of material properties like stresses, strains, (excess) pore pressures in soils and deformations, moments, shear forces and axial forces in structural elements (Plaxis bv, 2016).

## 2.6.2 The Hardening Soil model

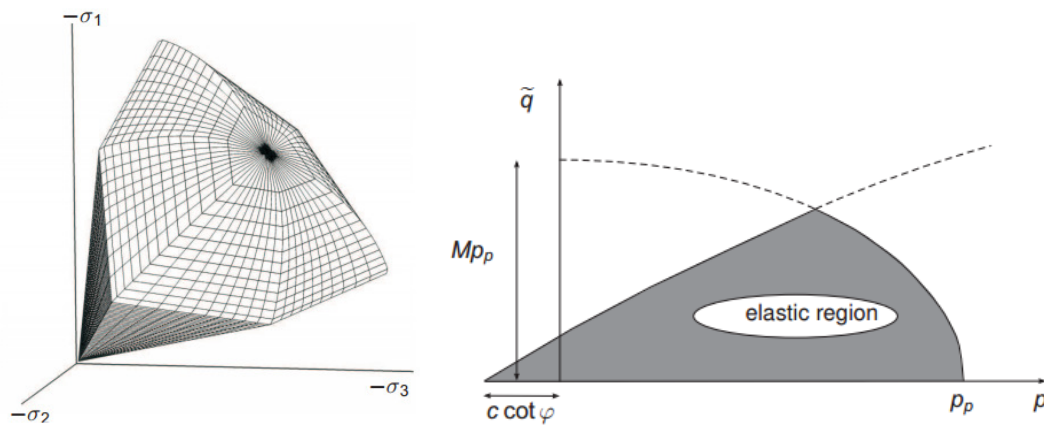
The Hardening Soil model (HS) is an advanced soil model that describes behaviour of the development of axial strain and deviatoric (variable) stress. A basic feature of the model is the stress dependency of soil stiffness. The HS model is capable of modelling this behaviour more accurately than the Mohr-Coulomb model by using the theory of plasticity (instead of the theory of elasticity) along with the addition of soil dilatancy and a yield cap. Elastic solids' state of strain is only depended on the final state of stress. In a plastic solid, the complete history of loading is responsible for the deformations. The plasticity problem is therefore incremental in nature (Chakrabarty, 2006). In a hardening plasticity model the principal stress space is not fixed, like in an elastic perfectly-plastic model, but can expand due to plastic straining (like in the plasticity problem). Shear and compression hardening due to loading cause irreversible strains in the soil, which result in an increase of strength. Shear strain also causes mobilisation of the dilatancy angle. This is described by Rowe in the stress-dilatancy theory and states that dilatancy only occurs for high stress ratios  $\phi_{mobilised} > \phi_{critical}$ . The shear hardening process mobilizes shear strength until the maximum shear strength has been reached according to the Mohr-Coulomb model failure criterion. The last characteristic of the HS model is the use of a yield cap. The  $E_{50}^{ref}$  largely controls the magnitude of the plastic strains associated with the shear yield surface and the  $E_{oed}^{ref}$  controls the magnitude of the plastic strains from the yield cap. The  $E_{50}^{ref}$  and  $E_{oed}^{ref}$  are used as input parameters to determine the yield surface and the yield cap. When the stresses remain inside of the principal stress space (see Figure 2.6), they will remain in the elastic region of the material. Outside, the material will behave plastic and increase in strength as mentioned above (Plaxis bv, 2016). For explanation of the standard parameters that are used by Plaxis see the Material Models Manual 2016.

## 2.6.3 Fully coupled flow-deformation

The fully coupled flow-deformation is a calculation mode to model both deformations and groundwater flow calculation simultaneously. It integrates deformation, pore pressure and flow calculations into one time dependent calculation. The fully coupled flow deformation calculation also allows inserting a dynamic flow

function in the calculation. These features make this calculation option useful to make time dependent calculations.

Figure 2.6 3D and 2D representation of the principal stress space of the Soil Hardening Model



## 2.6.4 On the use of the finite element method to design quay walls

Ho, et al. questions the reliability of FE modelling because of the 'black-box' nature of the powerful software. FE software contains lots of different options. Lack of knowledge of the calculation methods, principles of the geotechnical problems and lack of experience in conducting numerical analysis could result in so called 'computer-aided-disasters' (Ho, Donohoo, Boyes, & Lock, 2003). Therefore, they have made a few validation calculations to test the reliability of the FEM method. The results were positive, but the quay wall was modelled as a simple sheet pile wall.

Wolters, Bakker and de Gijt (2014) (Wolters, Bakker, & de Gijt, 2014) have performed a probabilistic calculation to validate the usability of Plaxis in comparison to the CUR 211 method. This has been done for a much more complex quay wall, including a relieving platform. The reliability indexes and the corresponding partial safety factors have been compared between Plaxis and CUR 211. The paper has found that the obtained safety indexes for quay walls with relieving platforms are too low. The design of this kind of structure is more complicated than a simple sheet pile wall, and thus, the partial factors should be modified to design a structure with an acceptable failure probability.

## 2.6.5 Plaxis vs. D-Sheet Piling

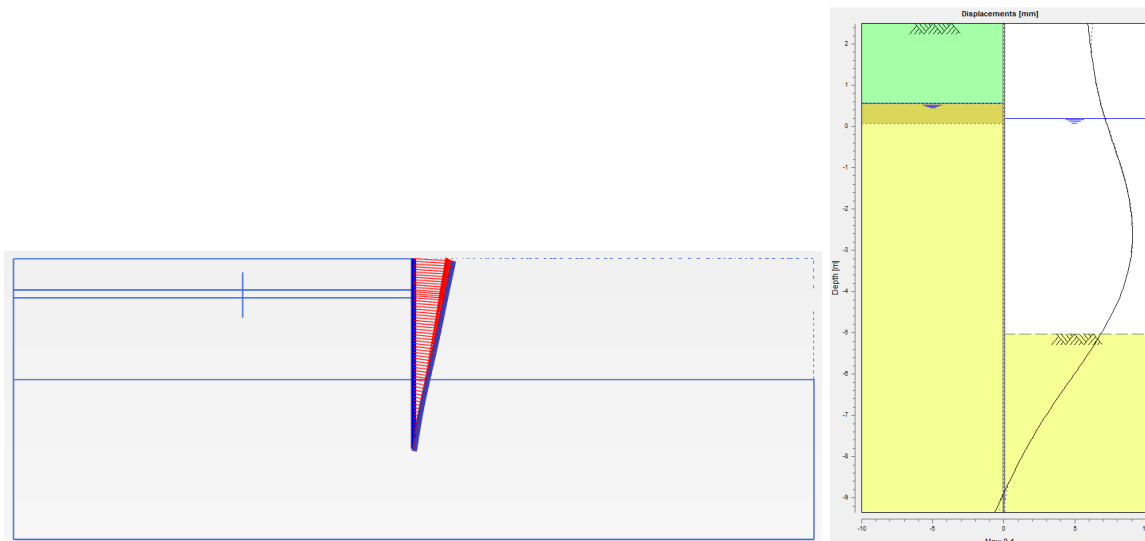
A simple comparison has been made to check the results that are going to be presented by Plaxis. A simple model with a very simple geometry has been set up in both Plaxis and D-Sheet Piling. The model contains a sheet pile wall with an anchor behind it, combined with different combinations of loads. All of the parameters are equal to each other in order to make a clean comparison. The construction sequence corresponds to each other. Figure 2.7 shows the results of the deformations in the sheet pile wall of both Plaxis and D-Sheet Piling. Table 2.1 shows the rest of the corresponding results.

Table 2.5 Comparison of results from Plaxis 2D and D-Sheet Piling

	Plaxis 2D	D-Sheet Piling
Bending moments [kNm]	Max: -54,37 Min: -156,7	Max: 92,1 Min: -60,2
Shear forces [kN]	Max: 88,97 Min: -81,45	Max: 74,3 Min: -61,6
Displacement [m]	Max: 0,1248	Max: 0,091

	Plaxis 2D	D-Sheet Piling
Anchor forces [kN/anchor]	344,195	330,4

Figure 2.7 Deformation results from Plaxis 2D and D-Sheet Piling



The bending moments and shear forces have a similar shape, but the displacements have a different shape. Plaxis shows a movement of the wall, whilst D-Sheet Piling shows a rotation of the sheet pile wall. The biggest differences of values are within the bending moments of the sheet pile wall. Plaxis has the advantage that it's capable of defining the construction sequences very precise and the possibility to model complex geometries and structures apart from a simple sheet pile wall.

## 2.7 Previous studies on the behaviour of quay walls

A new container terminal has been built in Lomé, West Africa in 2014. In Plaxis, an extensive analysis has been conducted to predict both horizontal as vertical displacements. The monitoring program contains both horizontal and vertical displacements as well as inclinometer records. The records show that the both of the displacements are significantly smaller than the displacements that have been calculated (Jorgens & Hansen, 2016). The measured data shows less than 30 percent of the predicted movement of the quay wall in Plaxis. Plaxis also calculated the crane rail displacement caused by crane loads at the seaside of the rail. The lateral displacements were less than 50 percent of the calculated amounts.

## 2.8 Data processing

The Port of Rotterdam has provided measurement data of the EMO quay wall. The locations of the sensors are given in Figure 2.8 and are placed by Inventec b.v. commissioned by the Port of Rotterdam. All of the sensors use optic measurement principals, which mean that all the sensors contain fibreglass for measurements. The data of the following sensors<sup>1</sup> have been collected:

- Air pressure;
- Temperature;
  - Air;
  - Harbour water;
  - Ground water;
- Water level;

<sup>1</sup> More information about the different of sensors, individual specifications and measurement methods is available on: <https://www.livesense.com>.



$$F_{total} = \varepsilon_{total} * A_{anchor} * E_{anchor} \quad (1)$$

With:

- F = force [kN];
- $\varepsilon$  = strain [-];
- A = area of the anchor [mm<sup>2</sup>], 4181 mm<sup>2</sup>;
- E = modulus of elasticity [kN/mm<sup>2</sup>], 210 kN/mm<sup>2</sup>.

$\varepsilon_{total}$  consists of two components, namely the anchor strain and the thermal strain. Equation (2) shows how the strains that applies on the anchor.

$$\varepsilon_{total} = \varepsilon_{anchor} + \varepsilon_{thermal} \quad (2)$$

$\varepsilon_{thermal}$  can be calculated with the use of equation (3).  $T_0$  is the reference temperature to calculate the temperature differences during the measurements. It will be assumed that the soil water temperature corresponds with the first temperature measurement because the exact temperature of the ground water during installation is unknown.

$$\frac{\Delta L}{L} = \alpha * (T_x - T_0) \quad (3)$$

With:

- $\Delta L$  = length change of the sensor [mm];
- L = sensor length [mm];
- $\alpha$  = coefficient of thermal expansion [m/m],  $12 * 10^{-6}$  m/m °C<sup>-1</sup>;
- $T_x$  = Temperature [°C];
- $T_0$  = Reference temperature [°C].

When the thermal strains have been calculated, it is possible to recalculate the corrected anchor forces using equation (1) again. For the correction it is important to note that the dates have been changed arbitrary to match the seasonal temperature to the anchor force changes. Besides that, the reference temperature also has been assumed due to absence of a measurement during installation.

### 2.8.3 Corrupted data

As noticed in the report by the Port of Rotterdam, there is data that does not behave according to the expectations. Inspection routines are executed every 3 to 4 months by Inventec b.v. to check the validity of the measured data and to check the measurement equipment. The maintenance reports of Inventec b.v. present the following results:

- The DSS, anchor force and temperature sensor data is recorded according to expectations and the available measurements are considered true. This also applies for groundwater piezometer 1;
- Groundwater piezometer 2 does not work according to expectations until March 2013. Values until and upon this date are considered corrupted and will not be taken into account in the data analysis;
- Groundwater piezometer 3 does not work according to expectations from May 2013 until 15 July 2014. Values between these dates are considered corrupted and will not be taken into account in the data analysis;
- Groundwater piezometer 4 does not work according to expectations from 19 December 2012 until June 2015. Values between these dates are considered corrupted and will not be taken into account in the data analysis.

# 3

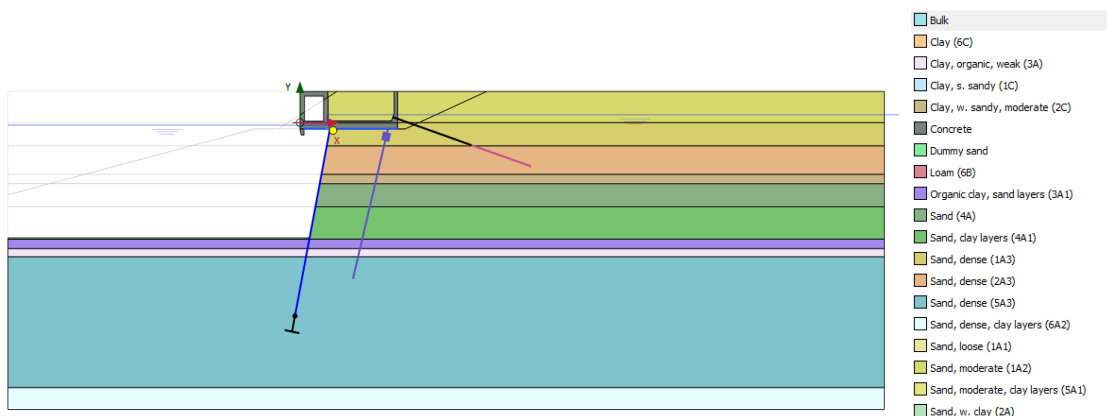
## Modelling in Plaxis 2D

This chapter will explain how the model in Plaxis has been set up and how the soil/structural parameters have been determined. These parameters will be used for the two models that will be produced. A distinction has been made between the model that is used to design the quay wall and the model to compare the measured data and the calculated values. The design model follows the methods that are normally used to design a quay wall, including the pre-defined loads provided by the client. The model to compare the measured data and the calculated values will use the same structural and geotechnical parameters but different loads. The loads will agree with the recorded loads by the user of the quay wall, EMO B.V.

### 3.1 Structural geometry

Figure 3.1 shows the geometry of the EMO quay wall. The structure consists out of a concrete superstructure on a combination wall and vibro pile as described in chapter 2.3. The dimensions of the structure have been taken from a design, with drawing number 2016-072A1L\_1, made by the Port of Rotterdam. The construction depth in front of the combi wall is -18,65 m+NAP. The super structure itself is 7,0 m high, 16,7 m wide and approximately 400 m long. The remaining dimensions of the quay wall and the hydrological conditions are presented in appendix II. Appendix II contains all the information that is required for the Plaxis calculations.

Figure 3.1 Geometry of the EMO quay wall



### 3.2 Geotechnical properties of the soil

In the past, soil investigation has been conducted for the purpose of designing the quay wall (Gemeentewerken Rotterdam, 6 april 2010). This soil investigation has been used to set up a soil investigation report in order to determine the soil characteristics in the project area. The following tests have been conducted:

- 72 CPTs (cone penetration test);
- 4 deep borings;
- 9 CD triaxial tests;
- 35 sieve analyses;
- 16 permeability tests;
- 51 determinations of unit weights and water contents;
- 6 determinations of the Atterberg limits.

Based on the CPTs and borings a geotechnical soil profile has been set up along the longitudinal side of the quay wall. One CPT has been selected as normative situations for the Plaxis calculation. The properties of the corresponding soil layers have been determined with the rest of the test results. All the information that had

been gathered during the investigation is collected into one file. The samples, including the results, have been linked to the depth from where they have been gathered. Distinction between soil layers has been made through the interpretation of CPTs and borings, including the provided soil descriptions. Due to the presence of soil profiles, it is possible to assign the unit weights to the corresponding soil layers. The unit weights and the soil profiles are the basis towards further parameter determination. The values of the results are all averages of the properties they represent. Averages are used to in order to create a realistic representation of the soil parameters instead of a set with safety in mind.

During the processing of the test results it became clear that only 1 of the CD triaxial tests was useful for interpretation. Correlations have been used to assign strength and stiffness properties to the soil layers. The general soil parameters have been derived from table 2.b Characteristic values of soil properties from NEN 9997-1+C1:2012, using the unit weights and the average cone resistance ( $q_c$ ) of the soil layers. For the HS model, there aren't any tables with correlations between characteristic values of the required parameters. The following correlations are used for the HS parameter determination:

- For non-cohesive soils:
  - Relative density according to Lunne et al. (1997),  $Re = \ln \left( \frac{q_c}{61(\sigma'_v)^{0,71}} \right) \frac{100\%}{2,91}$
  - $E_{50} = 60 * Re$ ;
  - $E_{50} = E_{oed}$ ;
  - $E_{ur} = 4 * E_{50}$ .
  - Dilatancy angle,  $\Psi = \phi' - 30^\circ$  ( $\phi' > 30^\circ$ )
  - $\Psi = 0^\circ$  ( $\phi' < 30^\circ$ )
- For cohesive soils:
  - HS model parameters have been derived from correlations described by Kulhawy, Muir-Wood, Lambe-Whitman, EPRI and Wroth;
  - $\Psi = 0^\circ$

The stiffness, strength and unit weight parameters of the soils are presented in appendix II. Also, there is additional information about the soil parameters and the conducted soil tests.

Table 3.1 Normative soil profile used for the calculation

CPT EN384, top profile = +4,76 mNAP		
Bottom soil layer [mNAP]	Layer id [-]	Soil type [-]
3,6	1A1	Sand, loose
2,8	1C	Clay
2,4	1A1	Sand, loose
-5,2	1A3	Sand, dense
-7,2	2A3	Sand, dense
-8,3	2A	Sand, thin clay layers
-12,2	4A	Sand
-21,2	4A1	Sand, clay layers
-22,6	3A	Organic clay
-39,2	5A3	Sand, dense
-40,0	6B	Loam
-42,5	6C	Clay
-50,0	6A2	Sand, dense, clay layers

### 3.2.1 Expectation, characteristic and design values

In order to get the right answers to the research questions, the right model including the right parameter set has to be compared with the measurement data. There are three possible datasets within the process of creating a design: the expected values, characteristic values and design values. The implementations of the parameters of each specific parameter set are presented in appendix III.

The *expected values* are average parametric values that are expected. These are properties that have been investigated and assigned to soil layers by performing (soil) tests. No safety factors have been used in order to cover possible variations.

The *characteristic values* are determined by calculating the 5% lower limit of the parameters. This can be done by using the Student-T distribution to calculate this limit, or can be adopted from the NEN 9997-1+C1:2012 table (lower limit). The Student-t method to calculate the lower limits of the soil parameters is only useable when a number of soil tests have been performed. For the research, the lower limits of the NEN table have been used. The lower limits of the parameters are used in order to create a safety margin.

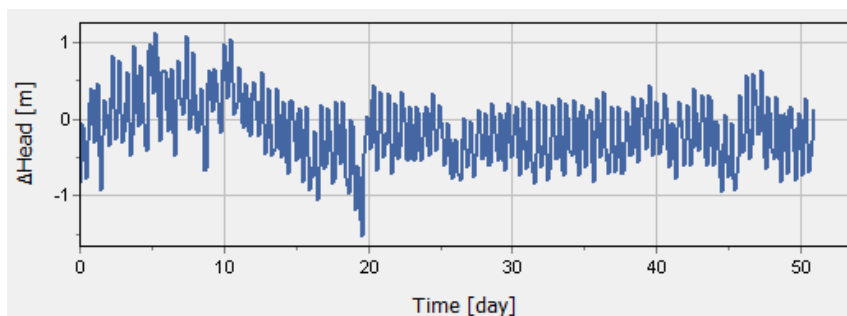
The *design parameters* can be calculated by applying partial factors over the characteristic values of the parameters. These partial factors are depended on the risk classes as described in chapter 2.5. The design parameters are used to design the construction and check the resistance during normative situations.  $\varphi'$  has a partial factor of 1,2 that applies on  $\tan(\varphi')$  and  $c'$  has a partial factor of 1,5 according to CUR211. The value of the parameter has to be divided by the partial factor in order to apply the factor.

### 3.3 Hydrologic conditions

Appendix II contains the water levels that are used during the static calculations in Plaxis. The Port of Rotterdam provides the water levels. There has been made a distinction between spring, average and dead tide for the calculations. During the load combinations, the average tide will be used as standard.

Figure 3.2 shows the signal that has been used as an input for the dynamic flow calculation. The signal contains an average water level shifting over a time span of 50 days, causing both loading and unloading of the quay wall. The signal will be applied on the harbour water level. The fully coupled flow calculation will be used to calculate the responses of the groundwater behind the quay wall. Assumed is that the water head of the soil layers will be completed up to a head of 0,00 m+NAP as a result of the water management of the land. It is assumed that the water signal has no influence on the Pleistocene soil layers.

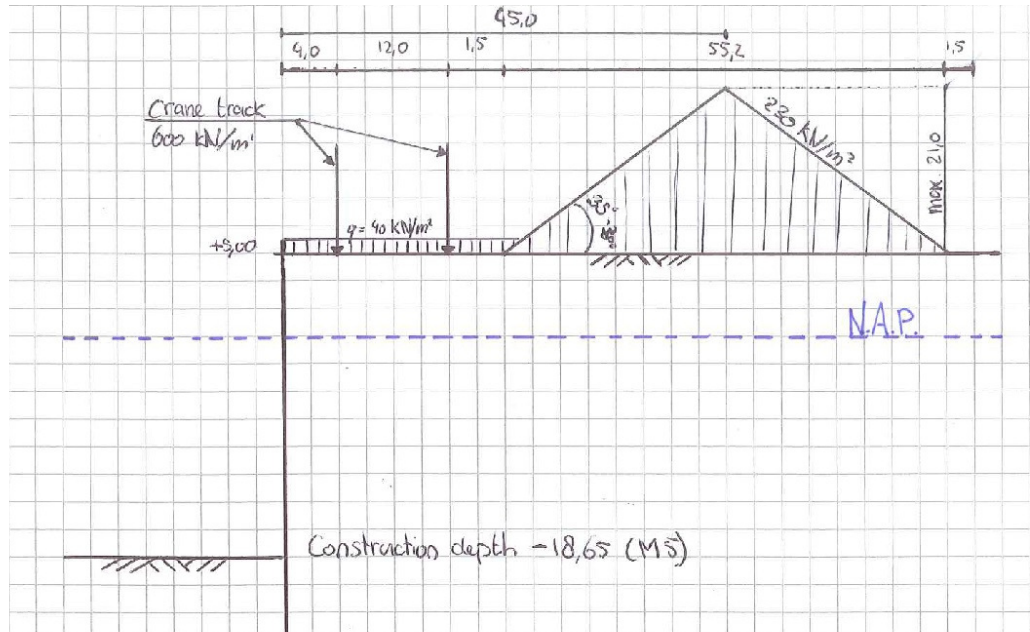
Figure 3.2 Dynamic water signal, harbour water level



### 3.4 Loading sequence

Plaxis has the option to define different phases in combination with different influences to model the effects on the structure. These phases are divided into two major parts, namely the construction phases and the load phases. The construction phases are specified in appendix II. In the contract documents provided by the Port of Rotterdam are the loads given that are to be used for the calculation. Figure 3.3 shows the loads as the Port of Rotterdam has given them.

Figure 3.3 Principal sketch of the loads on the EMO quay wall



During the design calculation one of the loads will be dominant over another. The dominant load will be applied with a factor of 1, whilst the minor load will be applied with a factor of 0,7 (according to the Eurocode 7 (CEN, 2010)). The load combinations are given in Table 3.2. For the expectation calculations, a load factor of 1,0 will be used because in reality all of the forces work during a load. Less load combinations will be used for the expectation calculations because there are fewer combinations possible.

Table 3.2 Load combinations

Load combination / LC	Dominant load (Load factor = 1,0)	Minor load(s) (Load factors = 0,7)
1	Water, neap tide	-
2	Water, average tide	-
3	Water, spring tide	-
4	Water, maximum water level difference	Surface load including bulk load, vertical loads crane, horizontal loads seawards crane, bolder load
5	Surface load incl. bulk load	Vertical loads crane, horizontal load seawards crane, bolder load, water <sup>1</sup>
6	Surface load incl. bulk load	Vertical loads crane, horizontal load landwards crane, water <sup>1</sup>
7	Bolder load	Surface load incl. bulk load, vertical loads crane, horizontal load seawards crane, water <sup>1</sup>
8	Crane vertical and seawards	Surface load incl. bulk load, bolder load, water <sup>1</sup>
9	Crane vertical and landwards	Surface load incl. bulk load, water <sup>1</sup>
10	Bulk load excl. surface	Water <sup>1</sup>
11	Exceptional load	Surface load including bulk load, vertical loads crane, horizontal load seawards, water <sup>1</sup>

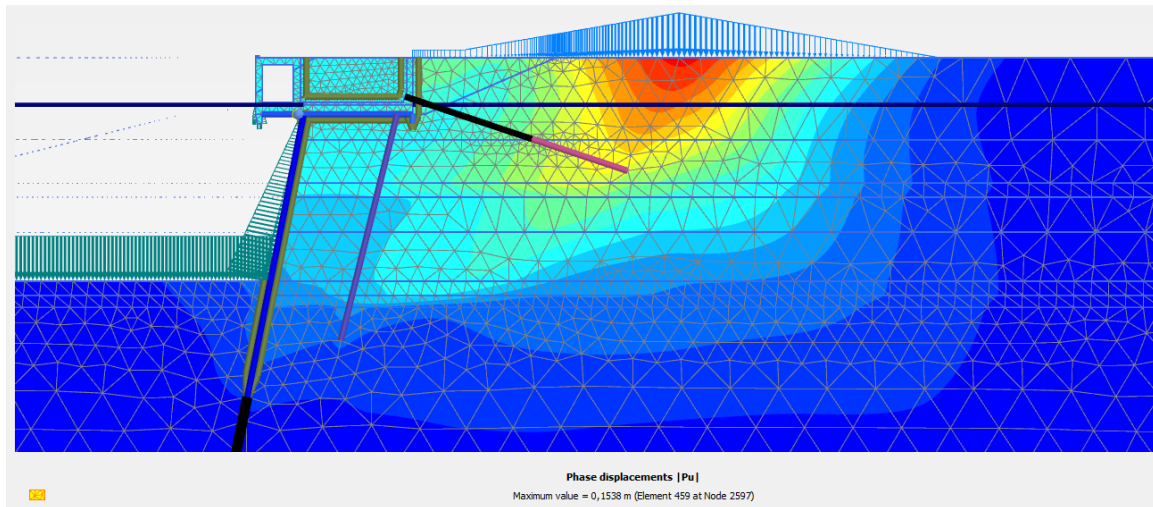
<sup>1</sup>) Average tide water level difference

### 3.5 Plaxis results

Plaxis gives a various amount of results with give a realistic impression. These have been annexed in appendix V. Figure 3.4 shows the phase displacements of load combination 10. Load combination 10 gives

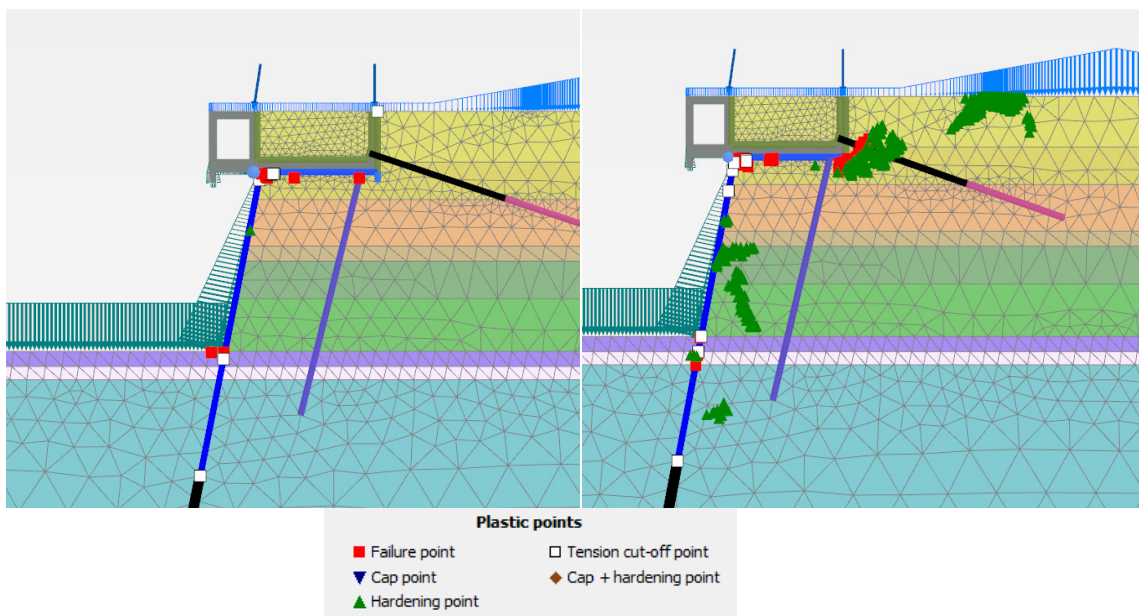
the highest amount of anchor forces during the static calculations. The amount of anchor forces created in the anchor during the presents of only bulk load is 847 kN. The maximum displacements during this phase are -0.1538 m.

Figure 3.4 Phase displacements of LC10



However, the results of the dynamic flow calculation aren't according to the expectations. The calculated anchor forces increment over time. The graphs of the anchor forces and the displacements of the top of the quay wall are also presented in the appendix V. Plaxis Support has been consulted to investigate why the anchor forces and displacements increment over time. After some research done by Plaxis, it turned out that the repetitive loading / unloading caused by the variation of water level causes some of the soil's stress paths in some of the stress points to reach the shear hardening yield or failure line in some of the calculation steps, see Figure 3.5.

Figure 3.5 Two phases during the fully coupled flow deformation calculation



On the right image of Figure 3.5, there is a presents of a lot of hardening and failure points. In these regions the soil doesn't behave fully elastic as it does in the left image. The variation causes the plastic points to be both absent and present during certain calculation phases, maybe causing the accumulation of the anchor forces and movement over time.

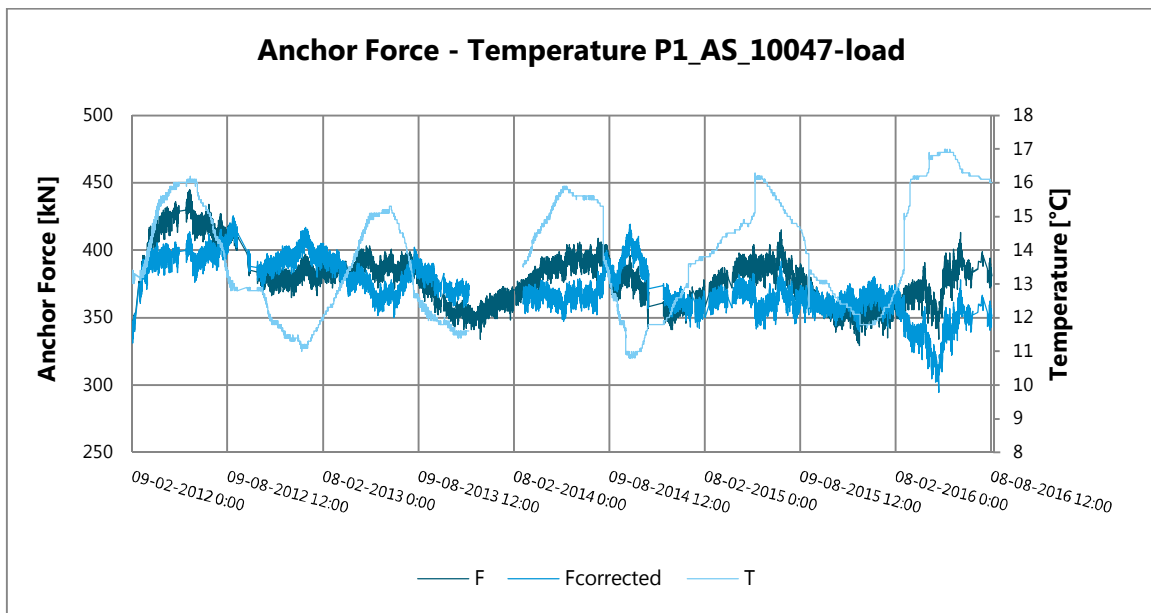
# 4 Data analysis

This chapter will give the results and the conclusions of the analyses that have been performed on the available data. The graphs of the remaining sensors are attached in appendix IV.

## 4.1 Corrected anchor forces

Figure 4.1 displays the anchor forces against the temperature. The dark blue line, labelled F, represents the original anchor forces as provided by Livesense®. The middle blue line, labelled Fcorrected, represents the anchor forces after the correction has been performed to exclude the thermal influences on the anchor forces. The higher temperatures during the summers cause the steel of the anchors to expand, increasing strains in the steel parts. The influence of the temperature has to be eliminated to get a clear view of the external forces that act on the anchors. Standing out is the fact that the anchor forces don't follow the temperature changes anymore, assuming that external forces acting on the quay wall cause the visible forces. The corrected anchor forces vary between 294,4 kN and 505,0 kN with an average value of 395,5 kN for anchors 1, 2 and 3. Anchor 4 has significant lower values, varying between 148,1 kN and 275,6 kN with an average value of 220,8 kN. The normative cross section for anchor 4 has a different geometry than the other anchors. The ground level of the harbour is shallower than the rest of the ground levels in front of the quay wall.

Figure 4.1 Anchor Force correction in sensor P1\_AS\_10047-load



## 4.2 Anchor forces

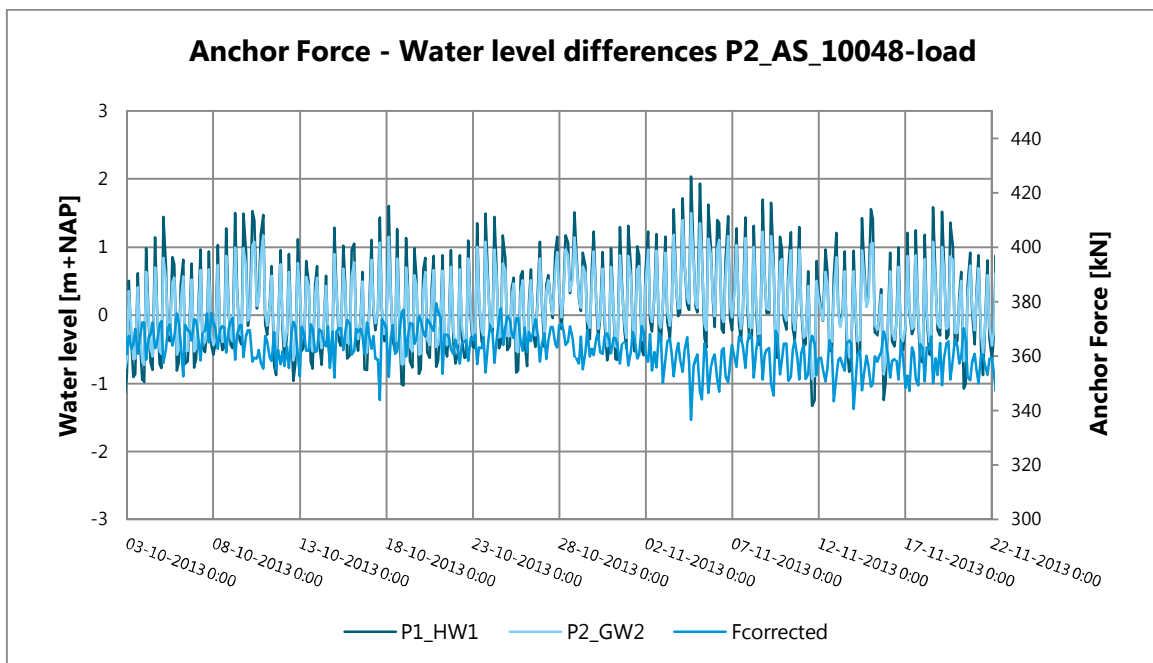
When zoomed into the anchor force and temperature of a random section of the graph presented in Figure 4.1 little variations are present in the anchor force. These are visible when zoomed into a time span of approximately two months. The number of anchor force peaks results in roughly 9 when the amounts of peaks are counted. It is assumed that the influence of the tide is the cause of the variations in anchor forces. This assumption has been crosschecked with the theory that has been collected for the starting points for the model in appendix II and the measured water levels inside of the harbour. The public data from the Port of Rotterdam shows that the effects of tidal fluctuation have a time span of about 14 hours. The number of peaks corresponds with the tidal fluctuations over time. A time span of 14 hours results in 8,6 peaks. On average, the tide differs between 1,26 m+NAP and -0,42 m+NAP. These values can differ because of the

variation in time of the tide and because the water level difference varies between neap, average and spring tide.

The measurement data of sensor P1\_HW1 confirm the assumptions based on the theory. Figure 4.2 shows an inverted fluctuation between anchor force and water level when both data points are plotted. The data also shows the variation in water level change in both duration and intensity. A connection becomes visible when the anchor force and the water levels. The amount of anchor force increases when the values of the harbour and ground water levels decrease, and vice versa. This effect becomes visible when zoomed into a time span of approximately 2 months. If the water level rises with about 0,50 m, the anchor forces drop with approximately 5 kN. This is visible in Figure 4.2. The forces in the other anchors show similar behaviour when the water level changes over time. The impact of the daily water level difference varies between  $9,8 \Delta\text{kN/m}^1$  and almost  $11,4 \Delta\text{kN/m}^1$  ( $\Delta\text{kN/m}^1 = \text{positive/negative change in kN per m global water level change}$ ).

Anchor forces also follow the global changes of the water levels. When the overall water levels rise, the amount of anchor forces drops. Major changes of water levels over time are capable of changing the anchor forces with a change of force varying between  $40 \Delta\text{kN/m}^1$  and  $70 \Delta\text{kN/m}^1$ . However, the water level changes do not always explain the major differences in the anchor forces. Other external influences act on the anchor forces, such as horizontal and vertical loads on the outside of the construction.

Figure 4.2 Anchor force and water level fluctuations



### 4.3 Combination wall position

The Shape Accel Array / Field sensor (SAAF) has been used to collect momentary recordings of the position of the tubular piles of the combination wall. The individual inclinometers have been measured 14 times each, between 20-01-2012 and 03-04-2016. The sensors make measurements from 0 m until -35 m, which is the bottom level of the tubular piles. Assumed is that the top of the inclinometer is attached to the top of the tubular piles, resulting in an overview of the displacements over the entire length of the pile.

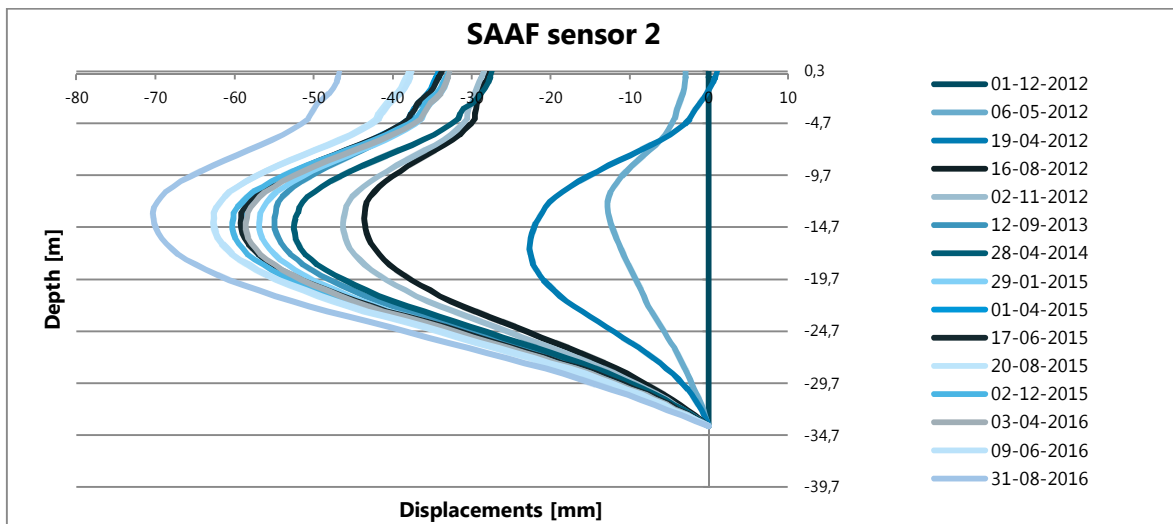
There is a large difference present between the first three measurement sets, both in deformation shape and in maximum deflection. At the time of set 2 on 06-03-2012, the amount of deformation is at its smallest and the shape of the deformation is different from the rest of the measurements. This can be seen in Figure 4.3. Before 06-03-2012, the maximum deflection has a higher point of engagement. Afterwards, the dredging activities probably have taken place and have cleared all the soil in front of the wall. The reduction of soil height of the passive side of the quay wall results in a different deformation shape of the sheet pile wall and an increase of amount of deformation. Table 4.1 shows the dates when the maximum amount of

deformation was reached. The maximum amount of deformation often is accompanied with a low harbour water level and a high anchor force. The maximum amount of deformation in sensor 1 is larger than in sensor 3, even though the amount of anchor force is higher and the water levels are lower. It is possible that a bolder load inflicted by a mooring ship has caused the accidental extra deformation.

Table 4.1 Measured conditions during maximum deformation sheet pile wall

Sensor	Date	Soil water level	Harbour water level	Water level difference	Anchor force	Maximum deformation
[-]	[d-m-y]	[m+NAP]	[m+NAP]	[m]	[kN]	[mm]
1	13-10-13		0,47		364,7	59
2	20-08-15	-0,612	-0,784	-0,1722	439,3	64
3	20-08-15		-0,784		413,5	47
4	20-08-15	0,342	-0,784	-1,1264	210,6	34

Figure 4.3 Results of SAAF sensor 2



#### 4.4 Displacements of the superstructure

Fugro GeoServices B.V. has performed displacement measurement of the superstructure several times in the past 5 years. A small summary of the measurements has been presented in Table 4.2. The last report states that there have been measured significant deformations in the quay wall relative to the reference measurement. This applies to both the horizontal as the vertical displacements of the measuring bolts. The maximum vertical displacement is +22,8 mm relative to the reference measurement and the maximum horizontal displacement is -14,0 mm.

Table 4.2 Statistics of the displacements on top of the construction after 5 years

	Max	Min	Median	Average
$\Delta x$ [mm]	10,00	-10,60	0,00	-0,10
$\Delta y$ [mm]	12,50	-14,00	0,00	0,03
$\Delta z$ [mm]	22,80	-5,00	6,00	7,82

The results of the horizontal displacements show that the quay wall moves both back and forward over time, but hasn't past the maximum deformation relative to the last measurement. Appendix IV also gives all of the results of the measurements taken by Fugro.

# 5 Comparison between measured and calculated values

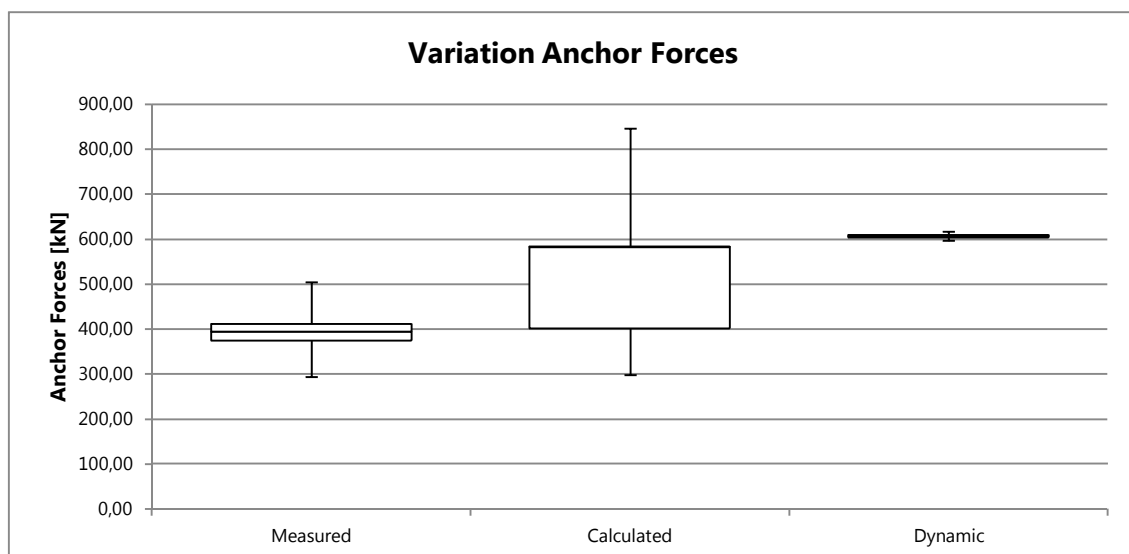
This chapter will compare the results of the Plaxis calculation with the measurements that have been taken. The goal of the chapter is to determine the degree of similarity between the values. The Port of Rotterdam has provided measurements of the anchor forces, deformations of the sheet pile wall and the measuring bolts on top of the superstructure as shown in the Data analyses. Both the trend and the exact values of the anchor forces will be compared, because of the corrections that has been applied over the results. Exact values and the directions of the displacements will be compared because the displacements are linked to the environmental conditions around the quay wall. No further corrections have been made for the displacement measurements. The values of both the static calculations (staged construction) and the dynamic flow calculation (fully coupled flow deformation) have been presented. The exact results are annexed in appendices V and VI.

## 5.1 Anchor Forces

The four anchor forces sensors have measured forces for the past 5 years, every 3 hours. This resulted in 40.561 measurements that have been taken into account. Anchor sensors 1, 2 and 3 are located into a similar geometry, while sensor 4 has a different profile and will be ignored. The sensors have measured anchor forces varying between 505,0 kN and 294,4 kN over time on a large scale. It seems that the anchor sensors started measuring after the completion of the dredging activities, because there are no sudden increases of anchor forces in the measurements. So it will be assumed that the measurements have taken place during the usage phase of the quay wall. The increases and decreases of the anchor forces are visible over time. An important feature of the measured anchor forces is the trend of the measurements. The anchor forces both increase and decrease but don't increment over time, which means that there is a response to loading and unloading.

The calculated values differ between the 846,3 kN and the 60,0 kN during the static calculations in Plaxis, and the dynamic calculations have a variation between 616,9 kN and 596,8 kN (LC4, result of the static calculation of LC4 = 587,1 kN). The values of the static calculations have some overlap with the measured values, but most of the values don't match with the measured ones. The results of the dynamic calculations don't show the same trends as the measured values. The calculated anchor forces increment over time and don't show the same reaction as the measured values when the anchor is unloaded. The repetitive loading sequence during the fully coupled flow deformation calculation seems to accumulate in the anchor forces, and causes it to not decrease over time.

Figure 5.1 Measured and calculated variation in anchor force sensors 1, 2 and 3



The amount of variation in the anchor forces created by tidal influences is also lower in the measured forces compared to the calculated values. A water level difference of 0,25 m between soil water level and the harbour water level creates an anchor force increase of approximately 8,2 kN in the measured values. Result of the calculated values show an increase of 25 kN when the water level difference between soil water and harbour water level is 0,25 m.

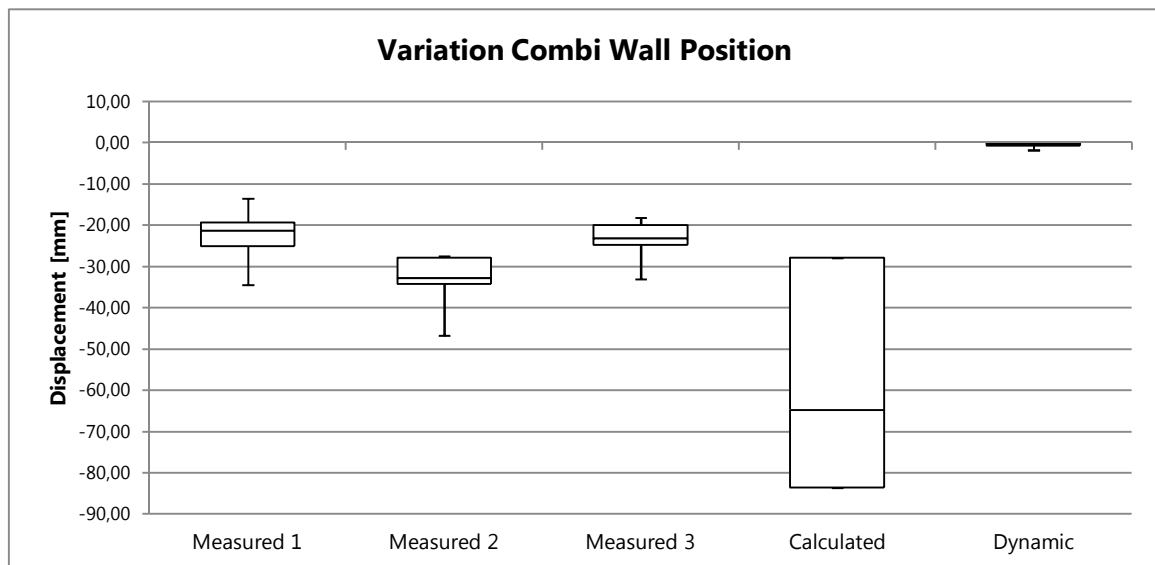
## 5.2 Combi Wall Position

The SAAF sensors have registered the position of the combi wall over a period of 5 years. Over these 5 years, there have been performed 13 measurements in each of the 4 piles. The top of the combi wall will be used as a reference point to compare the calculated and measured values. All of the deformation measurements suggest the same shape of deformation, but the quantity of the deformations varies. During the analyses of the data 4 benchmarks have been identified over time: a reference measurement, a measurement after finishing the dredging activities and the range of deformation during the users phase. The measurement data shows a deformation varying between the 25mm and 33 mm towards the water next to a calculated value of 27,8 mm towards the water, after the dredging activities have been completed.

After completing the dredging activities, the users phase starts. The measurements show a variation between the 15 mm and the 36 mm, and move in both positive and negative direction. The calculated values show a variation between the 27,9 mm and 83,6 mm. The position of the top of the sheet pile wall also moves in both positive as negative direction.

A small amount of values of the measured and the calculated values overlap, but the majority of the values aren't in the same region. The dispersion of the calculated values is larger than the measured values.

Figure 5.2 Measured and calculated variation of the top of the combi wall

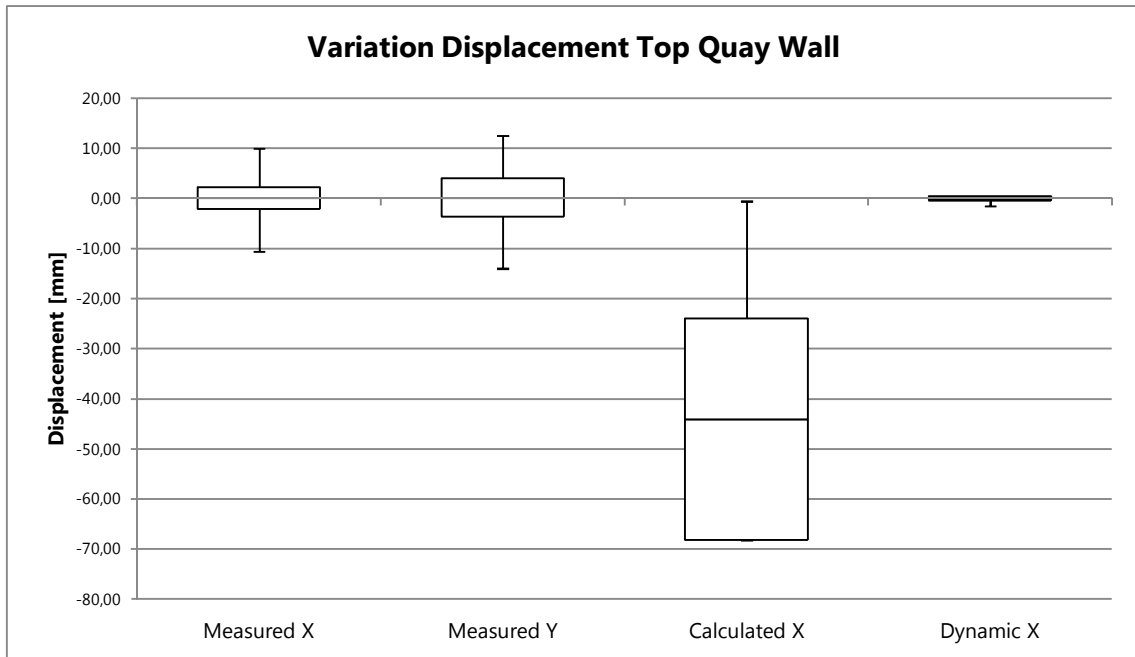


## 5.3 Displacement of the superstructure

Measuring bolts have been placed on top of the concrete superstructure. Over the past 5 years of monitoring of the quay wall, the measurement bolts have been measured 5 times. Only the front bolts of the relieving platform that have been marked on the design have been measured in X,Y,Z-directions. The report that Fugro has composed, commissioned by the Port of Rotterdam, states that there is an 80% guarantee that the measurements are correctly measured. The measurements of the displacements of the measuring bolts also indicate the complement of the dredging activities. The largest displacements have taken place after the dredging activities have completed. Horizontal displacements vary between the 10 mm and -10,6 mm in X-direction (perpendicular to the quay wall) and between 12,5 mm and -14,0 mm in Y-direction (longitudinal). Plaxis 2D has been used for the calculations, so only 1 direction has been calculated instead of

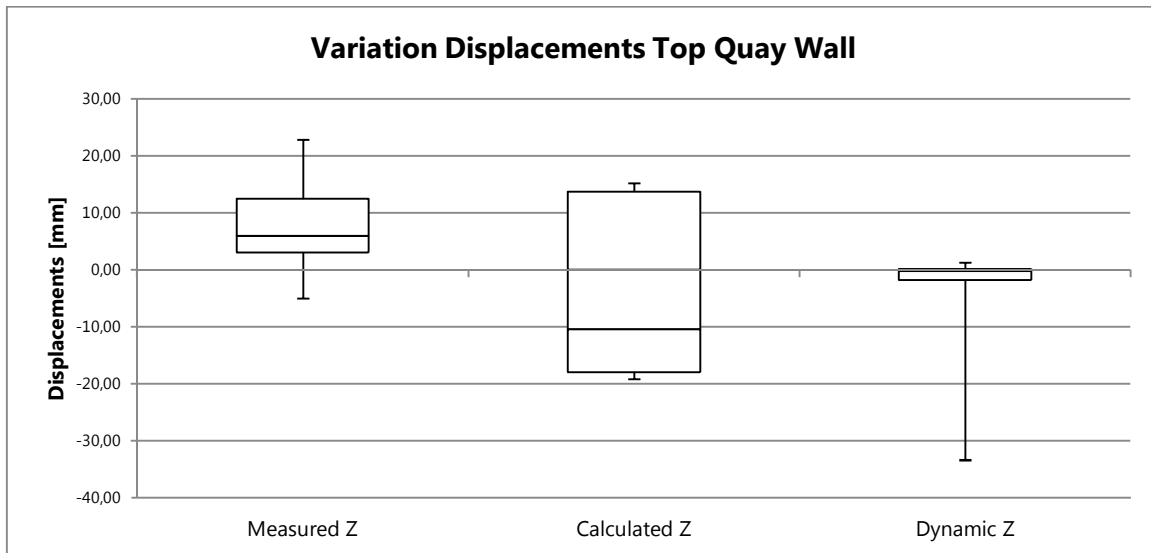
2. These X values vary between the -0,59 mm and the -91,58 mm, showing movement towards the waterside only.

Figure 5.3 Measured and calculated variation of the horizontal displacement of the top of the quay wall



The measurements of the vertical movements, Z-direction, vary between the 22,8 mm and the -5 mm. The calculated vertical values vary between the 15,2 mm and the -17,9 mm. The horizontal displacements show a small overlap in values, but the majority of the calculated measurements are outside of the measured ranges. The vertical displacements show greater similarities between the calculated and measured values.

Figure 5.4 Measured and calculated variation of the vertical displacements of the top of the quay wall



# 6

## Hidden Capacities of the quay wall

Chapter 2.4 gives an explanation of the concept of hidden capacity. In this explanation there has been made a distinction between the forces acting on the construction and the resistance of the construction. The resistance of the construction will be based on the response of the constructive elements that are part of the construction, i.e. the grout anchor, combi wall and the concrete superstructure. Measured values of the induced anchor forces and the displacements of the superstructure and the combi wall will clarify how much force they process and how stiff the structural elements react to actual environmental influences. The presence of hidden capacity within the structure will present when:

$$X_{structural,measured} < X_{structural,calculated} = \text{presents of hidden capacity}$$

Chapter 2.4 explains the hidden capacity as a concept that takes place during time. For the determination of the quantity of the hidden capacity a moment during the service life span of the construction will be used and further time dependency will be ignored.

### 6.1 Hidden capacities

The “expected” parameter set and corresponding calculation will be used for the determination of the hidden capacity, because this parameter set has no safety implementations and thus should present the realistic results of the calculations. If there is a hidden capacity present, an overcapacity has been created during the design process of the construction.

#### 6.1.1 Anchor forces

The anchor forces are calculated at the front of the embedded beam that has been modelled in Plaxis. Unfavourable influences on the construction will result in higher forces in the anchors. The normative situation calculated in Plaxis will be used to compare with the values that have been measured for the determination of the hidden capacity. The normative situation according to the results of the calculations is LC10 (= only bulk loads behind the superstructure). Table 6.1 shows the normative and average values for the anchor forces. For the normative situation it is assumed that both of the values are extreme results.

Table 6.1 Normative and average anchor forces

	Measured anchor forces [kN]	Calculated anchor forces [kN]
Max/normative	505,0	846,6
Average	395,5	471,2

The calculated anchor force is greater than the measured anchor force, thus for the anchors there a hidden capacity has been modelled. The amount of this overcapacity that has been calculated is 67,6% more than the measured values during the normative situation.

The calculated anchor forces also exceed the measured forces when analysing the average values. The average values have an overcapacity of 13,7%.

#### 6.1.2 Combi wall position

The SAAF sensors will be read-out on the top of combi wall, because here the largest displacements will take place. The deformations are relative to the directions they move to. So, negative values suggest that the wall is moving towards the waterside according to the measurements. Unfavourable conditions will result in larger displacements of the combi wall toward the waterside. The normative situation according to the results of the calculation is LC5 (= all loads applied, horizontal crane load towards the waterside). Table 6.2

shows the normative and average values for the combi wall displacements. It is assumed that the normative values are extremes.

Table 6.2 Normative and average values of the combi wall displacements

	Measured displacements [mm]	Calculated displacements [mm]
Min/normative	-46,7	-83,6
Average	-29,2	-52,6

The calculated displacements are greater than the measured displacements, thus a hidden capacity is present that has been modelled. The amount of overcapacity has been calculated is 79,0% larger than the measured displacements during the normative situation. During the average situation, there is an overcapacity of 80,2% compared to the measured combi wall displacements.

### 6.1.3 Deformations of the superstructure

The front of the concrete superstructure has been measured. The measured values of the movement vary between positive (land side) and negative values (water side). Even though the exact values of the calculated displacements are all negative; the relative values vary both towards the water as landside. Table 6.3 shows the values of the displacements of the top of the quay wall.

Table 6.3 Deformations of the superstructure

	Measured displacements X [mm]	Measured displacements Y [mm]	Calculated displacements X [mm]	Relative displacements X [mm]
Max	10,0	12,5	-0,6	41,3
Average	0,0	0,0	-41,9	0,0
Min	-11,0	-14,0	-68,2	-26,3

When the absolute values of the calculated and measured displacements are compared there is an under capacity of approximately -105,3% in positive direction (land side). In negative direction (water side) there is an overcapacity of 445,5%.

The same values could also be applied relatively to the average value of the calculated displacements. In positive direction there is an overcapacity of 267,2%. In negative direction there is an overcapacity of 110,3%.

## 6.2 Proven safety according to CUR211

A calculation with partial factors has been performed in order to provide an inside on the safety of the quay wall. For this calculation the design parameter set has been used. The design parameter set is based on risk class 2 of the CUR211, manual quay walls. The risk class applies partial factors of 1,2 on the angle of internal friction and 1,5 on the cohesion of the soils. The risk class also makes a distinction between dominant and minor loads. Dominant loads have to be applied with a factor of 1, whilst the minor loads have to be applied with a factor of 0,7.

The ratio between the measured values and the calculated values with risk class 2 will provide an inside on the amount of safety that is present compared to the reality. The normative values will be used for the comparison. The normative values for the anchor force occur during load combination 5 with a force of 1757,7 kN. The maximum measured anchor force is 505,0 kN. The safety ratio compared to the CUR211 factors is 3,5.

The normative value of the measured displacement of the combi wall is -46,7 mm, compared to a displacement of -410,0 mm. This gives a safety ratio of 8,8. The top of the superstructure has a maximum deformation -360,0 mm during load combination 7 in the X-direction. The measured deformation of the top of the superstructure has a deformation of -14 mm in the same direction. This gives a ratio of 32,7.

# 7 Sensitivity Analyses

The results of both of the data analyses and the calculated values by Plaxis are easy to manipulate. Chapter 7 will point out a few of the found sensitivities of the results.

## 7.1 Sensitivity of the Plaxis model

Plaxis has a lot of options to make geotechnical calculations. Due to the high amount of variation possible, it is easy to get different values. A few boundary conditions have been altered to check the influence of the condition.

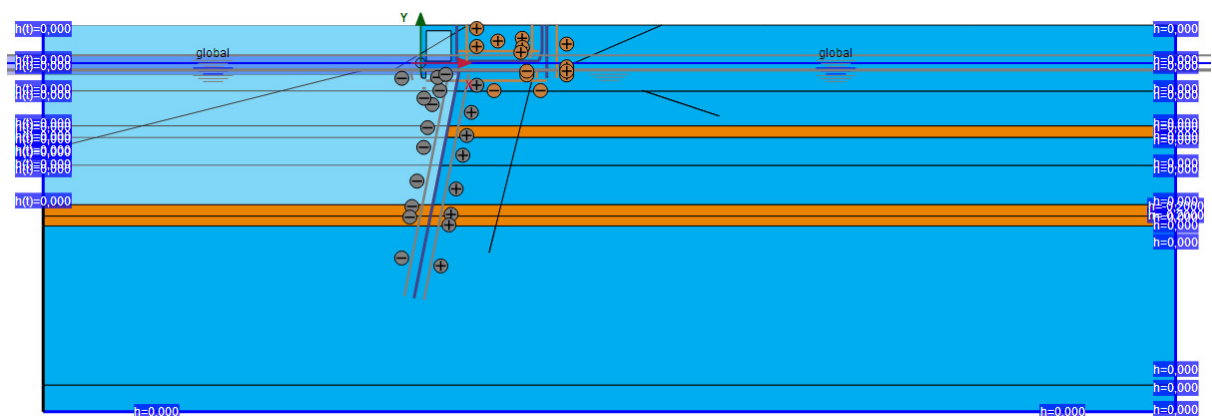
### 7.1.1 Flow conditions

Plaxis enables their users to specify their flow conditions up to a great amount of detail. At the interest of the report, it has been investigated what the most realistic conditions are to model the groundwater flow. It is possible to either use static or dynamic water level signals. Figure 7.1 gives the eventual flow conditions that have been used for the dynamic calculation.

The groundwater level behind the quay wall is assumable higher than the harbour water level when the static flow conditions are used. This is an unfavourable assumption and will create a high amount of deformation and anchor forces. The water level behind the quay wall will 'follow' the harbour level when dynamic conditions are used. The fully coupled flow-deformation calculation uses the permeability of the soil to determine the response of the soil behind the quay wall, and uses this flow condition to calculate the remaining results. Default permeability values have been used to calculate the flow responses in the soil. Another flow condition that has an impact on the flow calculation is the head of the groundwater behind the quay wall. The water head assigned to both the Holocene as Pleistocene layers is set to 0 m+NAP, but the actual drainage level on the terrain of EMO isn't known.

The permeability of the sheet pile is also an uncertainty. Plaxis has two options for the wall: fully closed (impermeable) or fully open (permeable). A fully permeable sheet pile wall gives results that are closer to the reality, while in reality a sheet pile wall will never be fully permeable. The permeable parts of the sheet pile walls are the spaces in between the locks of the individual sheet piles.

Figure 7.1 Model flow conditions



### 7.1.2 Stiffness parameters

The stiffness parameters  $E_{oed}$ ,  $E_{50}$  and  $E_{ur}$  are very determinative for the results calculated by Plaxis. The stiffness parameters have been determined with the use of correlations and have been reviewed to check the validity of the chosen parameters. In some cases, the differences between the stiffness parameters of

cohesive and non-cohesive soils are large. Assigned parameters of very weak cohesive soils are overruled because Plaxis considers the differences too big.

The dynamic flow calculation causes loading and unloading upon the quay wall over time. This gives changes in stresses and strains in a relatively short amount of time. Along with the large amount of differences, Plaxis has issues with the dynamic flow calculations and causes the results to increment. The results level off with a longer calculation time.

## 7.2 Sensitivity data analyses

The data that has been collected and the analyses that have been performed also have a few considerations. The data analysis that is performed is variable and thus easy to manipulate.

### 7.2.1 Data analyses

At the interest of the research, the anchor forces have been corrected in order to use the values for the comparison between the calculated values and the measured values. The anchor forces have been subjected to a temperature correction, but as noted before: the temperature during the installation wasn't measured and thus not ascertainable. For the current correction, the first temperature measurement available will be used as the reference temperature. It would seem that this first measurement was during the installation of the anchors, but a cross check suggests otherwise. Correcting the temperature with  $-1\text{ }^{\circ}\text{C}$  will change the corresponding anchor force with  $-10\text{ kN}$ , and proportional in the positive direction.

Also the seasonal temperature did not match the variation in anchor forces, perhaps because of malfunctioning of the sensors or recording system. Therefore, the measurements of the temperature have been moved in time to match their corresponding anchor forces. The transpose of the temperature causes the measurements to overlap.

### 7.2.2 Displacement measurements

Measurement data of the displacements of the combi wall and the deformation bolts on top of the quay wall have been supplied for the research. The displacement measurements are, in contrary to the anchor force measurements, not continuously. The measurement give the exact position in time, but aren't capable of portraying a trend over time. The measurements have been taken during various times in the year, resulting in different conditions that will influence the results of the measurements. The interval between the measurements also creates an uncertainty about the measurement series, because it's unclear if the measurement is an extreme value or an average measurement.



Figure 8.1 Sea vessel loader (left) and compacted coal pile (right), approximate height: 12m



On December 15, a site visit at the quay wall took place. Employees of Inventec were measuring in the inclinometers and cleaning the rest of the sensors that are part of their responsibility. These activities take place every 3 months. During the visit, there also have been taken a few photos as reference material for the research, see figure Figure 8.1. At the end of the site visit there was a possibility to interview one of the employees of EMO, Ben Gillebaard. Mister Gillebaard is responsible for the location management and planning of the bulk storages. Thereby, he also takes care of the administration of the information of the bulk that is / will be stored on the terrain of EMO. The interview with Ben results in a few interesting conclusions about the information of the bulk.

- The overall type of bulk that is typically stored on the quay wall is coal. Variation between different types of coal is possible but typically the weight of the bulk is the same. It is possible to store piles of coals with different degrees of compaction. The weight of the coals vary usually between the 0,8 tonnes/m<sup>3</sup> (loose coal) and 1,2 tonnes/m<sup>3</sup> (compacted coal). There is a small cone of iron ore present on the terrain behind the quay wall, but this is a very small pile. Thereby, it is only used as dumping spot to collect left overs and spread them over other iron ore pile on the rest of the terrain. Ben told that the maximum capacity was approximately 100.000 tonnes (coal and the singular cone of iron ore).
- The maximum height of the coals pile is approximately 17m high instead of the assumed 21m, provided by the Port of Rotterdam. It is possible to stack the coals higher, but a height of 17m gives the open sea vessel loader the possibility to easily manage the coal piles.
- With the optimum height of the piles, EMO is capable of fully loading/unloading complete vessels in approximately 24 hours, depending on the circumstances. This is linked to the mooring time of the vessels, but also tells that the layout of the terrain can change a lot within 24 hours. Even though there is a possibility that the layout of the terrain can change very fast, the bulk is stored at a fixed position. The quay wall subject to the research is used for loading of ships only. This will result in slower loading of the quay wall compared to the unloading of the quay wall during the filling process of the ships.
- The information provided by the Port of Rotterdam suggests that the space between the crane track on the landside and the toe of the coal pile is approximately 1,5m. The open sea vessel loader has a protruding element on the construction. Along with the protruding elements of the machine, there has to be space between the loader and the coal pile in order to be capable to move along the quay wall. The combined space of the protruding element and workspace results in a distance of approximately 10m, measured from the landside rails to the toe of the quay wall.

# 9

## Conclusions

Chapter 9 will serve as a closing chapter to both discuss the report and answer the research questions to conclude the thesis. Recommendations for further investigation on the subject will be presented as well to give potential direction.

### 9.1 Discussion

A lot of information has been looked up in order to set up the report. The original analysis that has been done to investigate the boundary conditions is absent, creating the need for a second interpretation / implementation of the boundary conditions that apply on the construction. Soil investigation with lots of different experiments has been made available during the tender phase of the quay wall. So, the same soil investigation that has been used during the design of the actual construction has been reused to make a new soil interpretation report. The soil interpretation is based on characteristic values, and converted to expectation and design values. There are no exact calculation rules to converted characteristic values to expectation values, but the average values between the upper and lower expectation values have been used. The new soil interpretation has been checked, but never fully reviewed by peer assessment. Structural characteristics of the quay wall were available from earlier research, and have been verified to check the correctness of the specified values. The results of the Plaxis static calculations are within the range of the expected values, making it possible to assume that the input parameters are correct. It was expected that the results of the calculations should be bigger than the measured calculations.

The dynamic calculations are also within the range of expected values, but the results over time give a not-expected output. The results of the dynamic calculation give a cumulative result over time, whilst the results should vary both in positive and negative directions over time when the construction gets loaded and unloaded. The increase of the anchor forces may fixed by applying a very large load in order to fully mobilise the soil, allowing the soil to stay within the elastic region of the soil model. Another possible solution is to increase the strength of the soil directly surrounding the anchor, forcing the soil to stay within its elastic region. The flow calculation that is integrated within the model also gives divergent results. In order to get results that matched with the measured water levels, the porosity of the sheet pile wall has to be set to completely permeable. In reality, the maximum permeability of a sheet pile wall / combi wall is a permeability of  $1 \cdot 10^{-6}$  m/s, which is approximately the same as silty sands.

The results of the data analyses are hard to verify, mainly the measurements of the anchor forces. According to the maintenance report of Inventec, the anchor forces measure realistic forces and the sensors work according expectations. It also has been said that the effect on the anchor force measurement have been eliminated from the presented results. Yet, there is a very clear variation visible in the measurements of the anchor forces that follow the seasonal variation of the groundwater temperature. Also, the groundwater temperature during installation isn't known, resulting in an estimated reference temperature for the correction. The deformation measurements are expected to be correct, but aren't measured continuously. Therefore, the deformation measurements only give an insight of momentary conditions of the quay wall.

The results of the comparison between the measured values and the calculated values show an overlap in results in all of the compared measurements. The measured values fall within the lower half of the calculated values, causing the values of the calculated values to be higher on average. Also, the distribution of the calculated values is larger than the distribution of the measured values. A remark on this is the amount of samples there are available and the load combinations that have been used during the calculations.

The determination of the hidden capacity gives a good view on the amount of overcapacity that has been created during the design process of the construction. But a clear distinction should be made between the types of hidden capacity that has been determined. The differences between the maximum/minimum of the values and the averages can be quite large as seen in the anchor forces. The hidden capacity could be dependent on the most common situation that applies to the construction, which is probably LC10 (only

bulk storage) as the influence of the crane only applies on a limited amount of space on the quay wall. The second part of the hidden capacity determination consists out of a factor determination of the safety of the quay wall with the use of partial factors. This isn't an actual safety calculation because the failure mechanisms that apply aren't assessed on the structural and geotechnical elements of the construction. The design calculation gives the results when the partial factors are applied on the materials and forces that act on the construction.

## 9.2 Conclusions

To conclude the thesis, answers to the research questions will be given. The main research question of the thesis is:

- *How does the (potential) hidden capacity of the quay wall relate to the comparison of the actual behaviour and the calculated models?*

Hidden capacity has been created during the process of designing the EMO quay wall. The results of the static calculated models are close to the measured values, but with greater variation. The dynamic calculation does not replicate the measured behaviour as well as expected. During the dynamic calculation, the model does calculate the tidal influences on the construction but lets the overall anchor forces increment over time instead of increasing and decreasing. During the design process, an overcapacity of 14% on average and 68% during extremes has been created for the anchor forces. Plaxis calculates a bigger amount of hidden capacity for the displacements. The combi wall has an overcapacity of approximately 80% on average and extreme. The deformation of the superstructure has an even bigger overcapacity, 267% (landside) and 110% (water side).

The next sub questions have lead to better understanding of the subject.

- *Which assumptions, which derive from uncertainties, will have to be made to create a model that is as realistic as possible to design the quay wall?*

Several assumptions have been made to frame the boundary conditions of the model. For the construction of the model the following boundary conditions have been assumed:

- The structural parameters don't have a wide distribution of variation, resulting in quite certain values. The soil parameters on the other hand are very uncertain due to high amount of variation.
- The amount of variation and the lack of possibility to knowledge of the entire subsoil make the soil parameters the most uncertain of the entire model. The composition of the soil profile varies over the entire length of the quay wall. In order to create a safe design of the construction it is assumed that the most unfavourable cross-section decisive is. The soil parameters have been estimated based on the soil investigation. Unit weights could be assigned based on the investigation, but strength and stiffness parameters are based on table 2.b from NEN 9997-1+C1:2012 and correlations.
- Hydrological conditions are also based on measurement data and interpretation, but are also unclear because return times of water levels are uncertain.
- The geo-hydrological conditions are as uncertain as the soil mechanical parameters. Parameters relating to the modelling of a geotechnical construction are very indistinct, but are always interpreted to gain safety.
- The loads and load combinations that act on the quay wall are given by the Port of Rotterdam and contain information about the machines operating on the quay wall and the bulk. The Port of Rotterdam assumed that the load combinations are unfavourable moments and extreme situations.

- *How does the design of the quay wall look like?*

The construction is based on frequently used heavy-duty design. The relieving platform relieves stress from the front wall, making the steel less thick. The combi wall has been placed at an inclination of 12° forcing the construction to move towards the land when the relieving platform gets loaded. Grout anchors and vibropiles ensure that the construction stays at its place. The innovative part of the construction is the front of the quay wall. It consists out of SFRHPC (high strength concrete), causing the fender construction to be unnecessary. The exact measurements of the construction have been included in appendix VII. The scope of the project didn't include the exact dimensioning and specification of the

structure but did comprehend the following design checks to make sure that the specified values are reliable. All of these elements are combined in the Plaxis model, and are specified in appendix II:

- Composing a soil interpretation report in order to specify the soil conditions for the model (stiffness, strength and HSM parameters).
  - Recalculation of the structural elements.
  - End bearing capacity determination for the combi wall and vibropiles.
  - Skin resistance determination for the vibropiles and grout anchors.
  - Construction phasing.
  - Load (combination) determination.
- *What is the actual behaviour of the quay wall as recorded by the sensors for the past 5 years?*  
During the thesis, access to the following measurements has been provided: anchor forces, displacements of the measuring bolts and the combi wall position. The data analyses clear the following behavioural aspects of the quay wall:
- The anchor forces in sensors 1, 2 and 3 varied between the 294,4 kN and 505,0 kN, after correction. Anchor 4 was much lower than the rest due to a deviating geometry, resulting in a variation between 148,1 kN and 257,6 kN. The anchor forces both increase and decrease over time, assuming that the anchors respond to loading and unloading of the quay wall. The completion of the dredging activities can't be traced back in the anchor sensor data, assuming that the measurements only take place during the users phase. The variation is caused by tidal differences and external (un)loading of the quay wall.
  - The inclinometer enables to pinpoint the dredging activities and the users' phases. The measurement of 06-03-2012 shows a large deflection caused by the dredging activities. After that, the combi wall moves back and forth over time, varying between the 64 mm and approximately 25 mm.
  - The measurement bolts show the same behaviour over time as the inclinometers. The horizontal displacements vary between the 10 mm and -14 mm and the vertical displacements vary between the 22,8 mm and -5,0 mm.
  - The water level, temperature and anchor force measurements are all continues, giving a clear view of the variation in time and the trends of the measurements. The displacements are all momentary recordings, making trends between two measurements unclear.
- *Does the measured data suggest that the quay wall is safe according to current Dutch standards?*  
A design calculation with partial factors on the materials and loads has been made to compare the safety calculation with the measured values. The ratio between the measured and calculated values that have been calculated show that the construction can be considered safe by the following results:
- The safety ratio of the anchor force results in 3,5 ( $F_{\text{measured}} = 505 \text{ kN}$ ,  $F_{\text{calculated}} = 1758 \text{ kN}$ ).
  - The combi wall displacements have a ratio of 8,8 ( $x_{\text{measured}} = -47 \text{ mm}$ ,  $x_{\text{calculated}} = -410 \text{ mm}$ ).
  - The horizontal displacements at the top of the construction even have a ratio of 32,7 ( $x_{\text{measured}} = -14 \text{ mm}$ ,  $x_{\text{calculated}} = -360 \text{ mm}$ ).
- *What is the amount of hidden capacity of the quay wall?*  
During the design process, hidden capacity has been created due to the uncertainties that are present. For the purpose of the determination of the hidden capacity are the expectations and measured values of the construction used. The amount of hidden capacity is:
- There is an amount of 68% hidden capacity within the anchor forces when the extremes of the measured and calculated values are used ( $F_{\text{measured}} = 505 \text{ kN}$ ,  $F_{\text{calculated}} = 847 \text{ kN}$ ). When based on the average situations, a hidden capacity of 14% has been determined ( $F_{\text{measured}} = 396 \text{ kN}$ ,  $F_{\text{calculated}} = 471 \text{ kN}$ ).
  - A hidden capacity of 79% has been created in the combi wall for the normative situation ( $x_{\text{measured}} = -47 \text{ mm}$ ,  $x_{\text{calculated}} = -84 \text{ mm}$ ). On average, the hidden capacity is 80% ( $x_{\text{measured}} = -29 \text{ mm}$ ,  $x_{\text{calculated}} = -53 \text{ mm}$ ).
  - The deformations of the superstructure have an undercapacity of -105% in positive direction (landside,  $x_{\text{measured}} = -11 \text{ mm}$ ,  $x_{\text{calculated}} = -1 \text{ mm}$ ) and an overcapacity of 446% in negative direction (water side,  $x_{\text{measured}} = -13 \text{ mm}$ ,  $x_{\text{calculated}} = -68 \text{ mm}$ ). When the relative values are compared, the hidden capacities are 268% in positive direction ( $x_{\text{measured}} = -11 \text{ mm}$ ,  $x_{\text{calculated}} = -41 \text{ mm}$ ) and 110% in negative direction ( $x_{\text{measured}} = -13 \text{ mm}$ ,  $x_{\text{calculated}} = -26 \text{ mm}$ ).

- *What is the extent to which the model is consistent with the measured behaviour of the quay wall?*  
In general, the parameters have been underestimated in the design of the quay wall resulting in overestimation of the anchor forces and displacements. The calculated values are within the same ranges as the measured values, despite the fact that the majority of the calculated results are larger than the measured values. Distinction has been made between:
  - The static calculation result in a bigger range of variation compared to the measured values, mainly in the horizontal displacements of the construction.
  - The dynamic calculations don't match with the measured values. The results of the calculations don't have the same anchor force development over time. In reality, the anchor forces increase and decrease depending on the situation. But, the fully coupled flow deformation calculation calculates incremental forces due to repetitive loading of the construction.
  
- *What are sensitive aspects of the analyses that influence the hidden capacity?*  
There are several aspects that are manipulative and are capable of influencing the hidden capacity. The most important aspects are:
  - The flow conditions of the model that are used to perform the dynamic calculation are very influential on the results. The flow conditions are the variable factor in the model, inducing anchor forces and deformations.
  - The stiffness parameters of the model are also a very sensitive part of the model. The parameters have been determinate with correlations, but Plaxis sometimes overrules proposed values.
  - The data analyse also has a few flaws. The first is the absence of the reference temperature for the temperature correction.
  - The second is the time correction to match the trends of temperature and forces. Due to these corrections are the results questionable and are the absolute values not always applicable.
  - As last, the displacements are momentary recordings. Therefore, no trends can be investigated for the displacements.

### 9.3 Recommendations

The following recommendations are made for follow-up research:

- The use of the Hardening Soil small strain model (HSss) instead of the Hardening Soil model. The HSss could be more suitable to modelling loading-unloading situations. Usually this kind of model is used for dynamic earthquake calculations.
- To avoid hardening point, a very large load (almost to failure) could be applied before performing the fully coupled flow deformation calculation in order to allow the stress point to be retained within the elastic region. After this, hardening point might not occur no more and might take away the incrementing anchor forces and front displacements. Another possible solution is to increase the strength of the soil directly surrounding the anchor, forcing the soil to stay within its elastic region.
- Updating the geometry of the load combinations of the model. The site visit and the interview with the site manager have provided a clear view on the usage of the quay wall. The update of the geometry will give more realistic results, but the adaption will cause a deviation of the usual design procedures.
- Introduction of a parameter to vary the permeability of the sheet pile wall. The permeability is dependent on the soil that is directly behind the sheet pile wall. Currently, the sheet pile wall is fully permeable or fully impermeable.
- Performing a full sensitivity analyse. Due to lack of time, there was no possibility to check the effect of certain parameters on the amount of hidden capacity. The sensitivity analyse should make clear which parameters have more effect on the results.

# 10

## Bibliography

- Arcadia, D. H. (2009). Mohr-Coulomb Parameters For Modelling Of Concrete Structures. *Plaxis Bulletin, Spring Issue 2009*, Delft.
- Cabal, R. a. (2014). *Guide to Cone Penetration Testing for Geotechnical Engineering, 6th Edition*.
- CEN. (2010). *Eurocode 7: Geotechnical design*.
- Chakrabarty, J. (2006). *Theory of Plasticity*. Oxford: Elsevier Butterworth-Heinemann.
- CUR. (oktober 2003). *CUR-rapport 2003-7 'Bepaling geotechnische parameters'*. Gouda: Stichting CUR.
- de Gijt, J., & Broeken, M. (2014). *Quay Walls, Second Edition*. Rotterdam, the Netherlands: CRC Press/Balkema.
- EMO B.V. (2015). *Wie zijn wij*. Retrieved 2016 йил 6-Septembe from EMO: <http://www.emo.nl/wie-zijn-wij/>
- Frölke, G. (2016). *Oriëntatie data uit 'slimme' kademuren*. Rotterdam.
- Gemeentewerken Rotterdam. (6 april 2010). *Rapport EMO kade M5+ M6 Rapportage geotechnisch grondonderzoek*. Rotterdam: Gemeentewerken Rotterdam.
- Het Nederlands Normalisatie Instituut. (2012). *NEN 9997-1+C1 (nl)*. Delft: Stichting Reprorecht.
- Ho, D., Donohoo, S., Boyes, K., & Lock, C. (2003). Numerical Analysis and the Real World - It Looks Pretty But Is It Right? *In Proceedings of the NAFEMS World Congress*.
- Holický, M., & Vrouwenvelder, T. (2005). Basic concepts of structural reliability. In *Implementation of Eurocodes, Handbook 2, Reliability Backgrounds* (pp. I-1 to I-10). Prague.
- Jorgens, M., & Hansen, A. (2016). Geotechnical Engineering for a new container terminal in Lomé, Togo, West Africa. *Nordic Geotechnical Meeting 2016 Reykjavik*, (pp. 879-888). Reykjavik.
- Lunne, Robertson, & Powel. (1997). *Cone Penetration Testing in Geotechnical Practice*.
- Lunne, T., Robertson, P., & Powell, J. (1997). *Cone Penetration Testing in Geotechnical Practice*. London: Blackie Academic and Professional.
- Mayne, P. (2014). Interpretation of Geotechnical Parameters from Seismic Piezocone Tests. *3rd International Symposium on Cone Penetration Testing*. Las Vegas.
- Plaxis bv. (2016). *Material Models Manual*. Delft: Plaxis bv.
- Plaxis bv. (2016). *Scientific Manual*. Delft: Plaxis bv.
- Port of Rotterdam. (2012). *HydroMeteobundel nr. 4*. Rotterdam: Port of Rotterdam N.V.
- Schanz, T., Vermeer, P., & Bonnier, P. (1999). The hardening soil model: Formulation and verification. *Beyond 2000 in Computational Geotechnics - 10 Years of Plaxis* (pp. 281 - 297). Rotterdam: Balkema.
- Siemes, T. (1999). DURACRETE: SERVICE LIFE DESIGN FOR CONCRETE STRUCTURES. *Durability of Building Materials and Components 8*, 1343-1356.
- Stichting CURNET. (2008). *CUR-publicatie 166 (vijfde druk) Damwandconstructies*. Gouda: Stichting CURNET.
- Walraven, J. (2010). OLD BRIDGES IN NEW TIMES. Searching for hidden quality. *Structure and Environment No. 4*, 10-15.
- *Wikimedia Foundation, Inc.* (2016, August 26). Retrieved September 2, 2016, from Wikipedia: [https://en.wikipedia.org/wiki/Data\\_analysis](https://en.wikipedia.org/wiki/Data_analysis)
- Wolters, H., Bakker, K., & de Gijt, J. (2014). Reliability of Quay Walls Using Finite Element Analysis. *Plaxis Bulletin*, 12-15.

# 11

## Reflection

For the past 4 months I've been individually working on my bachelor thesis for Witteveen+Bos. The acquisition of the assignment was arranged fairly quickly as I was working as an intern before the start of the thesis. At the start of the assignment the exact goals of the thesis weren't completely clear, because some of the concepts weren't specified yet. Writing the research plan resulted in clarification of these concepts as it was possible to specify them. The research plan contained the research questions and a planning that have been drafted. As the research plan contains several subjects that I've never worked with before, a global assumption of the amount of time that will be spent on the subjects has been made. During the discussion of the research plan it has been stated that the amount of research activities was high, but the plan was mostly been kept the same. At this time of the research it wasn't clear which quay wall would be the eventual subject to the research but activities were started.

Starting up the project went quite smooth. Witteveen+Bos made a workspace with PC available at their office as I was going to work with geotechnical software. During the thesis a lot of co-workers were available to ask questions about various amounts of subjects. Because of this, everything went according to the project plan up to the start of the modelling in Plaxis. Setting up a running model was harder than expected because I was unfamiliar with the software (no experience) and the complex nature of the programme. Getting a working (dynamic flow) model took more time than expected, causing a slight delay in the planning. Acquiring the measurement data also took quite some time as the thesis wasn't accepted as assignment yet. It took a lot of effort and emails to get the data in the correct format that we needed for the data analyses.

The final part of the research emerged with the results of the models and data analyses ready. The hardest about this part of the research is the lack of possibility to discuss the report with someone that has been working on it as well. Discussions with my supervisor or co-workers are possible but they were not as directly involved as I was, making the quick discussion difficult. Overall, I think that doing the research and writing the thesis has been going good, and I am satisfied with the produced results.

A lot of subjects have been addressed, but geotechnics always interesting me during the Land- and Water Management study. Choosing a geotechnical subject at an engineering and consulting company for my thesis gave the possibility to gain a lot of technical knowledge of an interesting subject. Over the past 4 months I've learned lots about the technical side of the subject, e.g. modelling of geotechnical models, determination of relative parameters and performing data analyses en interpretations. In addition to the technical part of the thesis, I learned about the communicative / management side of the project as well, e.g. professional external communication between client and contractor and project management of a long-term project such as the monitoring of the project boundaries and project planning. I've enjoyed my time at the company by spending time learning about an interesting topic and expanding my professional network by meeting new colleagues.

# Appendices



# I

## Appendix: Fault Tree Quay Wall



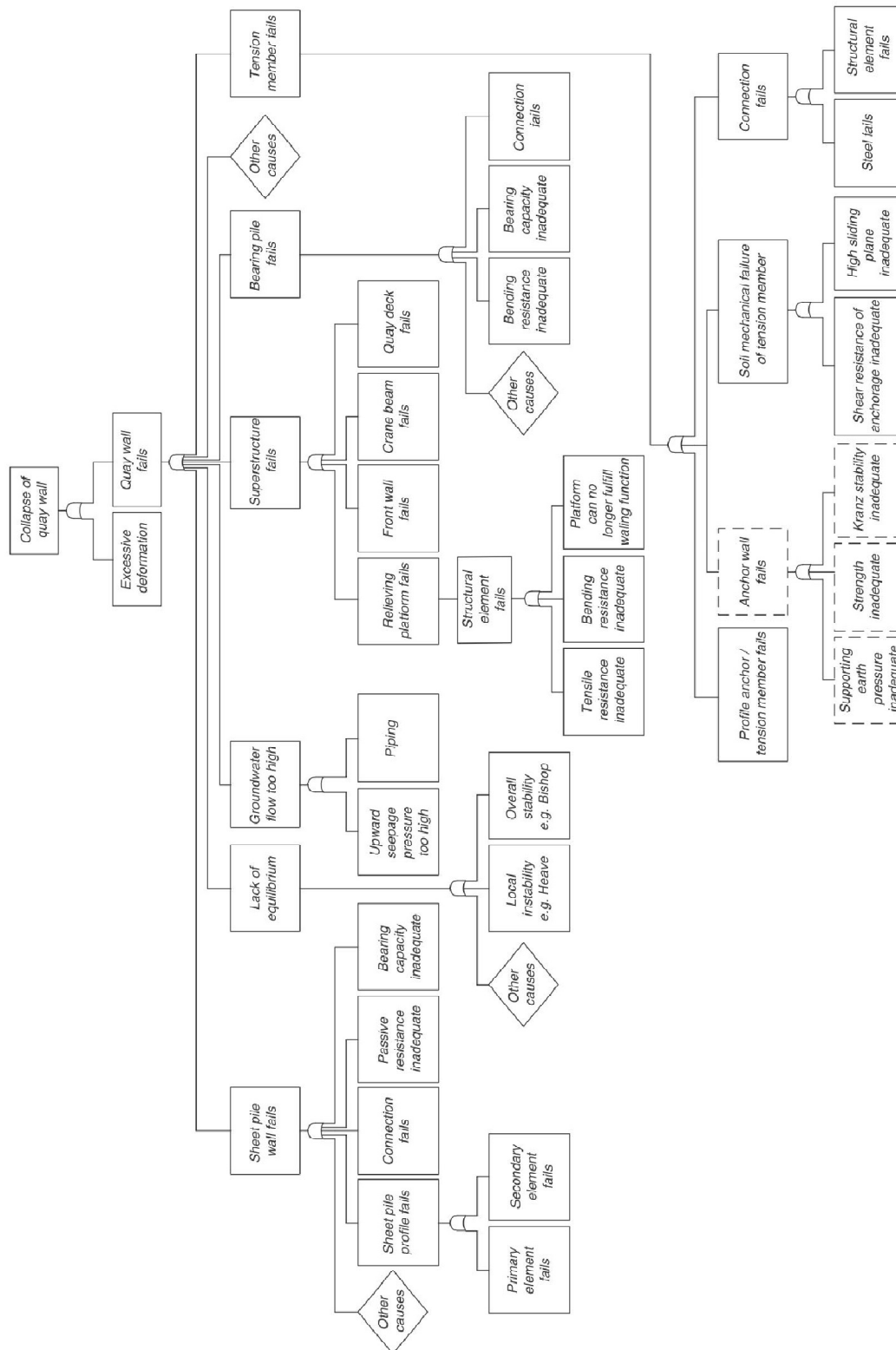


Fig. 6.11 An example of a fault tree for a quay wall with a relieving structure.



# II

## Appendix: Starting Points Memo



## Memorandum

---

<b>Subject</b>	Starting points EMO quay wall
<b>Project code</b>	-
<b>Date</b>	13 October 2016
<b>Reference</b>	-
<b>Author(s)</b>	J.M. Verstijnen
<b>Appendices</b>	I. Parametersheet_EMOquay.xls II. Determination HSM parameter non-cohesive.xls III. Expected, characteristic and design parameters
<b>To</b>	-
<b>Copy</b>	-

---

# 1 INTRODUCTION

This appendix has been set up to provide an overview of the parameters that are necessary to construct the geotechnical model in Plaxis. These include: an interpretation of the soil tests that have been conducted by Gemeentewerken Rotterdam, properties of the quay wall, hydrologic conditions, load combinations and an explanation of the applied safety philosophy. The structure of the report will be as follows:

- 1 Introduction;
- 2 Geotechnical;
- 3 Hydrology;
- 4 Structure;
- 5 Building sequences;
- 6 Loads;
- 7 Safety philosophy;
- 8 References.

# 2 GEOTECHNICAL

This chapter will provide the determination of the soil parameters that will be used for the Plaxis calculation.

## 2.1 Soil investigation

In order to set up a soil interpretation report, a soil investigation has been set up and executed. Gemeentewerken Rotterdam has commissioned a soil investigation with the following specifications:

- 72 CPTs (cone penetration test);
- 4 deep borings;
- 9 CD triaxial tests;
- 35 sieve analyses;
- 16 permeability tests;
- 51 determinations of unit weights and water contents;
- 6 determinations of the Atterberg limits.

### **CPTs / borings**

CPTs and borings are used to determine the composition of the subsoil. The tests give the possibility to recognise the different soils and at which depths a certain layer appears. It is also useable to assign mechanical properties to the different soil layers.

### **Triaxial tests**

During a triaxial test, the soil sample will be compressed in the  $\sigma_1$ ,  $\sigma_2$  and  $\sigma_3$  directions. This happens either in a single stage, or multistage. For the soil investigation single stage CD (Consolidated Drained) tests have been preformed. The triaxial tests will result in a number of different results. These include: development of the deviatoric stresses, stress path, mobilisation curve and the volume strain. With these test results it is possible to construct the circles of Mohr. The strength parameters  $\phi'$  and  $c'$  can be derived from the circles. The parameters will be determined by a strain level of 2%, which is a typical amount for sheet pile and quay wall calculations.

With a triaxial test it is also possible to determine the stiffness parameters. The stiffness parameter E50 has been defined as deviatoric stress divided through the vertical strain. The value of E50 differs in the different load stages and is dependent on the stress and strain levels. The modulus of elasticity has been specified as 50% of the value with a maximum deviatoric stress. The dilatancy angle  $\Psi$  and Poisson's coefficient  $\nu$  are to be determined through the triaxial test.

### **Sieve analysis**

Sieve analyses are preformed to classify the soil samples according to the grain distribution. The test is preformed with the aid of several sieves. This will result in a number of fractions that allows assigning both a sand and gravelling median. Dry sieving is used to determine the sand and gravel fraction, wet sieving is used to determine the amount of particles smaller than 63  $\mu\text{m}$ . Only dry sievings have been preformed for the EMO quay wall design.

### **Permeability tests**

Permeability tests provide an insight in the permeability of a soil sample. This has been done using the constant head method. The potential difference has been kept constant during the test. The amount of water that flows through the sample is measured in both quantity and time.

### **Determination of unit weights and water contents**

The unit weights of soil samples and its water contents are determined by drying the samples. For the 24 hours the samples are put into an oven, at a temperature of 105 °C. The weight differences between before drying and after drying allows determining of: dry unit weight, saturated unit weight, water content, pore volume, pore number, degree of saturation.

### **Plasticity limits according to Atterberg**

There are 3 phases in which clay behaves, depending on the moisture content. These 3 phases are: solid, plastic and liquid. It is possible to classify the soil samples using the international classification according Casagrande by determining the plastic limit, liquid limit and plasticity index. The A-line (continuous line) separates clay (above) and silt (below) soils from each other. Samples plotted above the B-line (dotted line) have a higher compressibility than soils below the B-line. Both of the samples are considered clay samples.

## **2.2 Soil interpretation**

All the information that had been gathered during the investigation is collected into one file. The samples, including the results, have been linked to the depth from where they have been gathered. Distinction between soil layers has been made through the interpretation of CPTs and borings, including the provided soil descriptions. Due to the presence of soil profiles, it is possible to assign the unit weights to the corresponding soil layers. The unit weights and the soil profiles are the basis towards further parameter determination. The values of the results are all averages of the properties they represent. Averages are used to in order to create a realistic representation of the soil parameters instead of a set with safety in mind.

During the processing of the test results it became clear that only 1 of the CD triaxial tests was useful for interpretation. Correlations have been used to assign strength and stiffness properties to the soil layers. The general soil parameters have been derived from table 2.b Characteristic values of soil properties from NEN 9997-1+C1:2012, using the unit weights and the average cone resistance ( $q_c$ ) of the soil layers. For the HS model, there aren't any tables with correlations between characteristic values of the required parameters. The following correlations are used for the HS parameter determination:

- For non-cohesive soils:
  - Relative density according to Lunne et al. (1997),  $Re = \ln \left( \frac{q_c}{61(\sigma'_v)^{0,71}} \right) \frac{100\%}{2,91}$
  - $E_{50} = 60 * Re$ ;
  - $E_{50} = E_{oed}$ ;
  - $E_{ur} = 4 * E_{50}$ .
  
  - $\Psi = \phi' - 30^\circ$  ( $\phi' > 30^\circ$ )
  - $\Psi = 0^\circ$  ( $\phi' < 30^\circ$ )
  
- For cohesive soils:
  - HS model parameters have been derived from correlations described by Kulhawy, Muir-Wood, Lambe-Whitman, EPRI and Wroth;
  - $\Psi = 0^\circ$

### 2.3 Normative soil profiles

A geological profile has been set up based on the CPTs that have been performed by Gemeentewerken Rotterdam. One CPT has been selected that will serve as normative CPT for the calculations. **Error! Reference source not found.** gives the normative soil profile of the CPTs.

Table 2.1 soil profile CPT EN384, top soil profile = +4,76 mNAP

Bottom soil layer [mNAP]	Layer id [-]	Soil type [-]	Lithostratigraphy [-]
3,6	1A1	Sand, loose	Anthropogenic
2,8	1C	Clay	Anthropogenic
2,4	1A1	Sand, loose	Anthropogenic
-5,2	1A3	Sand, dense	Anthropogenic
-7,2	2A3	Sand, dense	"Duinkerke II/III"- formation
-8,3	2A	Sand, thin clay layers	"Duinkerke II/III"- formation
-12,2	4A	Sand	"Calais"- formation
-21,2	4A1	Sand, clay layers	"Calais"- formation
-22,6	3A	Organic clay	Holland peat
-39,2	5A3	Sand, dense	"Kreftenheye"- formation
-40,0	6B	Loam	"Kedichem"- formation
-42,5	6C	Clay	"Kedichem"- formation
-50,0	6A2	Sand, dense, clay layers	"Kedichem"- formation

## 2.4 General soil parameters

Table 2.2 gives the general soil parameters for the different layers. These are applicable to the non-hardening Mohr-Coulomb model.

Table 2.2 General soil parameters

Layer id [-]		$q_c$ [MPa]	$\gamma_{unsaturated}$ [kN/m <sup>3</sup> ]	$\gamma_{saturated}$ [kN/m <sup>3</sup> ]	$\phi'$ [°]	$c'$ [kN/m <sup>2</sup> ]
1A1	Sand loose	2	17,0	19,0	30,0	0
1A2	Sand, moderate	10	18,0	20,0	32,5	0
1A3	Sand, dense	25	19,0	21,0	35,0	0
1C	Clay, s. sandy	2	18,0	18,0	32,5	1,0
2A	Sand, w. clay	5	16,9	17,4	27,0	0
2A3	Sand, dense	20	17,5	19,0	35,0	0
2C	Clay, w. sandy, moderate	2	17,1	18,2	22,5	5,0
3A	Clay, organic, weak	2	15,4	16,6	15,0	1,0
3A1	Clay, organic, sandy	5	18,1	18,5	15,0	1,0
4A	Sand	22	18,9	19	32,5	0
4A1	Sand, clay layers	21	18,1	18,7	27,0	0
5A1	Sand, moderate, clay layers	8	18,0	20,0	30,0	0
5A3	Sand, dense	40	19,0	21,0	35,0	0
6A2	Sand, dense, clay layers	25	18,0	20,0	32,5	0
6B	Loam	6	19,5	19,7	27,5	2,5
6C	Clay	4	20,1	20,3	25,0	15,0

## 2.5 Plaxis Hardening Soil model parameters

Table 2.3 gives the soil parameters that are specifically necessary for the Plaxis model. The  $E_x^{ref}$  and  $m$  parameters give the stiffness properties of the soil layer.  $\Psi$  is an additional strength parameter for non-cohesive soils. For the advanced parameters of the Plaxis model the default values will be used.

Table 2.3 Plaxis HSM parameters

Layer id [-]	$R_e$ [%]	$E_{50}^{ref}$ [MN/m <sup>2</sup> ]	$E_{oed}^{ref}$ [MN/m <sup>2</sup> ]	$E_{ur}^{ref}$ [MN/m <sup>2</sup> ]	$m$ [-]	$\Psi$ [°]	$R_{inter}$ [-]
1A1	45,6	27,35	27,35	109,40	0,5	0	0,8
1A2	78,7	47,20	47,20	188,79	0,5	2,5	0,8
1A3	97,4	58,47	58,47	233,87	0,5	5,0	0,8
1C	-	8,48	4,24	24,48	1	0	0,8
2A	27,2	16,35	16,35	65,39	0,5	0	0,8
2A3	77,5	46,48	46,48	185,93	0,5	5,0	0,8
2C	-	3,14	1,57	11,07	0,9	0	0,8
3A	-	4,01	2,32	17,57	1	0	0,8
3A1	-	8,17	4,80	33,31	1	0	0,8
4A	74,2	44,53	44,53	178,10	0,5	2,5	0,8

Layer id [-]	Re [%]	$E_{50}^{ref}$ [MN/m <sup>2</sup> ]	$E_{oed}^{ref}$ [MN/m <sup>2</sup> ]	$E_{ur}^{ref}$ [MN/m <sup>2</sup> ]	m [-]	$\Psi$ [°]	$R_{inter}$ [-]
4A1	67,9	40,72	40,72	162,88	0,5	0	0,8
5A1	17,9	10,74	10,74	42,95	0,5	0	0,8
5A3	78,1	46,84	46,84	187,34	0,5	5,0	0,8
6A2	53,8	32,26	32,26	129,04	0,5	2,5	0,8
6B	-	8,26	13,51	54,80	0,7	0	0,8
6C	-	19,37	11,97	76,73	0,7	0	0,8

## 3 HYDROLOGY

Port of Rotterdam has assembled hydrological and meteorological data of the harbour into a public file, the HydroMeteoBundel (Port of Rotterdam, 2012). The data has been compiled from data gathered from the operating measurement network. The measurement station that is useful for the quay wall calculations is stationed at the Suurhoffbrug, as shown in Figure 3.1. In Table 3.1 the data from the HydroMeteoBundel has been presented. The values are the extremes for the high and low water levels that vary over a time period of 14 hours.

Figure 3.1 Graph of the water levels at the measurement station Suurhoffbrug

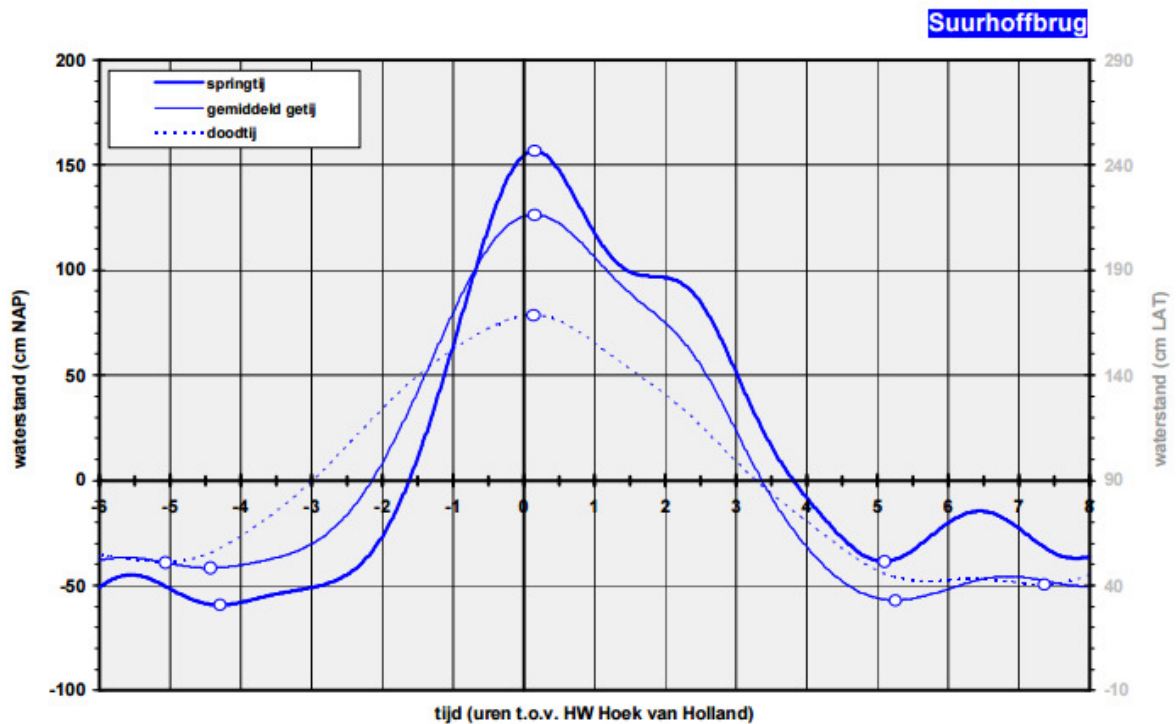


Table 3.1 Extreme values of the water levels

	Neap tide (= doodtij)	Average tide (= gemiddeld getij)	Spring tide (= springtij)
High water level [mNAP]	0,78	1,26	1,57
Low water level	-0,39	-0,42	-0,59

Neap tide (= doortij)

Average tide (= gemiddeld getij)

Spring tide (= springtij)

[mNAP]

# 4 STRUCTURE

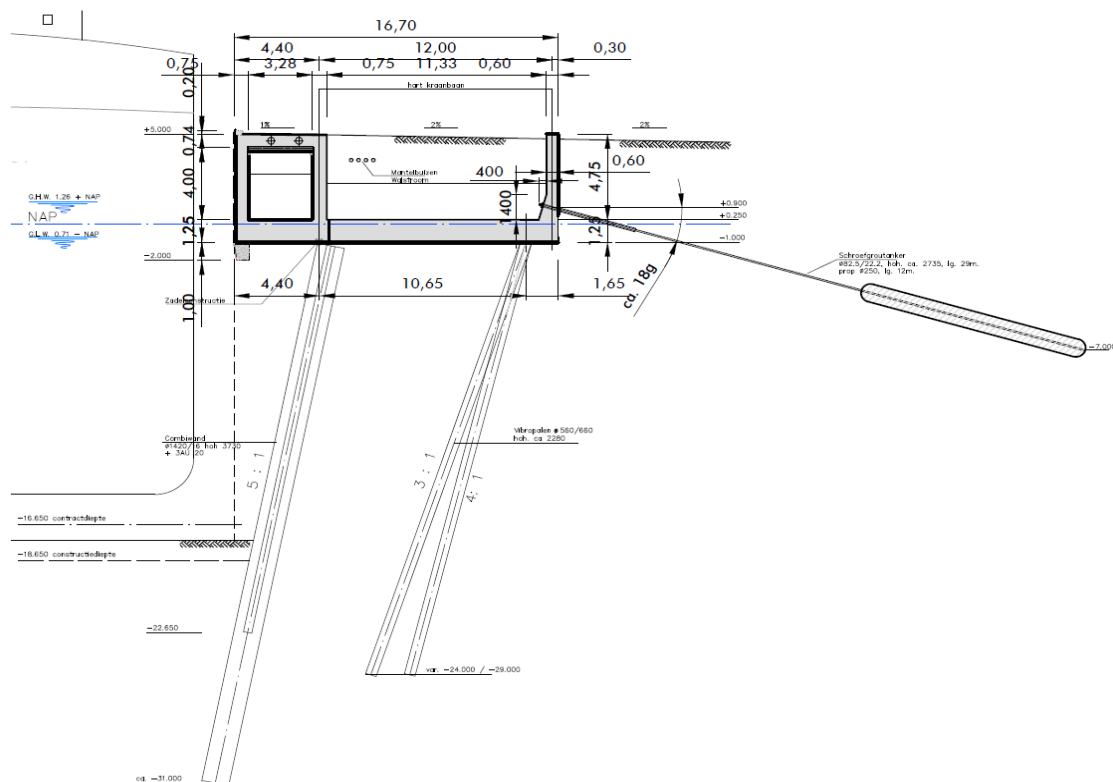
The EMO quay wall consists of concrete relieving platform which is mounted on a combi wall. Also, the relieving platform has been founded on vibro piles and stabilized by pre-stressed anchors. Table 4.1 gives the properties of the structural properties of the construction. The vibro pile has a bearing capacity of  $F_{\max} = 535,0$  kN/m. The bearing capacity of the pile and the skin resistance has been calculated by using D-Foundations v15.1.

Table 4.1 Structural properties of the EMO quay wall

Construction element [-]	EA [kN/m]	Stiffness EI [kNm <sup>2</sup> /m]	w [kN/m/m]	Pre-tension [kN/m]	$T_{\text{skin, start, max}}$ [kN/m]	$T_{\text{skin, end, max}}$ [kN/m]
Combi wall 1420/16 + AU20	6,058E+06	1,031E+06	2,265	-	-	-
Vibro pile	1,08E+06	21,17E+03	2,75	-	100	900
Pre-stressed anchor	301,5E+03	-	-	150	-	-
Grout body	210E+06	-	-	-	330	330

Figure 4.1 gives the dimensions of the quay wall.

Figure 4.1 As-built drawing of the EMO quay wall, including dimensions



The concrete with which the construction has been constructed is modelled as an elastic-perfectly plastic material with the linear-elastic model in Plaxis. The parameters that have been used are given in Table 4.2.

Table 4.2 Concrete properties of the EMO quay wall, source: (Arcadia, 2009)

Material [-]	$\gamma$ [kN/m <sup>3</sup> ]	E [kN/m <sup>2</sup> ]	$\nu$ [-]	c [kN/m <sup>2</sup> ]	$\phi$ [°]	Tensile strength for tension cut off [kN/m <sup>2</sup> ]
Concrete	24,0	24,0E6	0,2	365,0	35,0	450,0

## 5 BUILDING SEQUENCES

The building sequence that has been executed will be used in the Plaxis calculation in order to gain an accurate representation of the behaviour of the quay wall. The construction phases succeeded as presented in Table 5.1. The total amount of time that the construction of the quay wall consumes is 206 days.

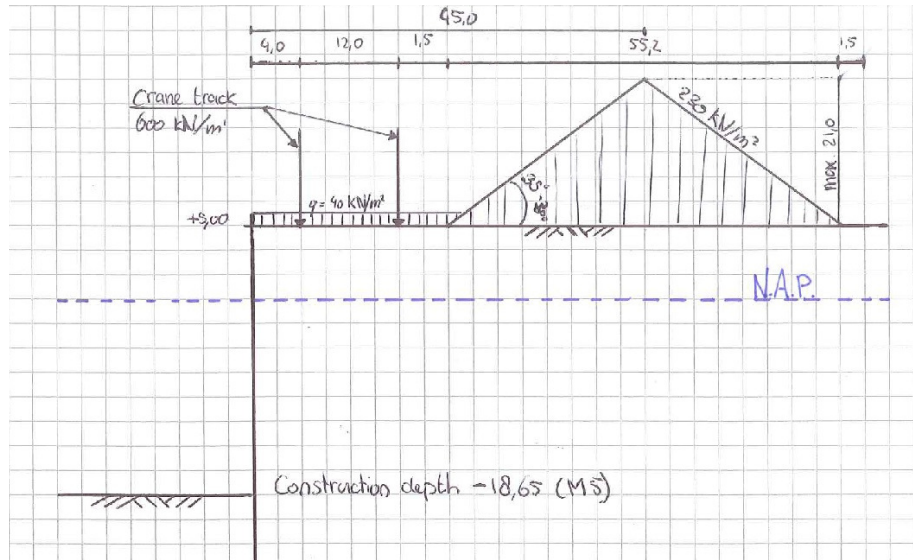
Table 5.1 Construction phases of the EMO quay wall

#	Construction phase [-]	Duration phase [days]
1	Creation of a building pit by enclosure of water/tidal influences	7
2	Shallow excavation to create a construction pit wherein the quay wall will be build. Excavation until a depth of -1,0 mNAP	30
3	Pile driving of the combi wall. This includes the placement of the sheet piles between the tubular piles	30
4	Vibro pile driving for the foundation of the relieving platform	30
5	Placement/casting of the relieving platform	21
6	Installing the pre-stressed anchor in the relieving platform	14
7	Backfilling behind and in the relieving platform	14
8	Dredging of the berthing channel in front of the quay wall	60

## 6 LOADS

Several forces affect the quay wall. In this chapter, all of the loads will be specified and described. Figure 6.1 gives a principal sketch of the loads that will be taken into account during the Plaxis calculation.

Figure 6.1 Principal sketch of the loads on the EMO quay wall



The individual scenarios for the calculation that will inflict loads on the construction consist out of:

- Own weight, water level difference according to neap tide situation;
- Own weight, water level difference according to average tide situation;
- Own weight, water level difference according to spring tide situation;
- Failure of drainage (maximum water level difference);
- Surface load on the superstructure including bulk load behind the superstructure;
- Boulder load;
- Vertical force on both legs of the crane;
- Horizontal load on the front leg of the crane;
- Horizontal load on the back leg of the crane;
- Exceptional load case/fender load.

## 6.1 Properties of the different loads

This sub-chapter will provide the properties of the various loads that have been distinguished and will be taken into account during the calculation.

### Bulk load

Table 6.1 presents the properties of the bulk that will be stored behind the quay, source: (de Gijt & Broeken, 2014). For the calculation, it will be assumed that the bulk will be stored 17,5 m behind the beginning of the quay wall. The load will increase from 0,0 kN/m<sup>2</sup> to 230,0 kN/m<sup>2</sup> at 45 m behind the quay wall and then decline to 0,0 kN/m<sup>2</sup>.

Table 6.1 Theoretic properties of the bulk

Material	Specific gravity [kN/m <sup>3</sup> ]	Angle internal friction [°]
Iron ore	22,4-32	35-40,9
Rough coal	10,9	45

### Surface loads on the quay wall

Cranes are necessary to transport these bulk goods from the ship towards their storage depots. The quay wall should be suitable for a surface load of 40 kN/m<sup>2</sup> as visualised in Figure 6.1. This load represents the vehicles that move around on the quay wall. As normative loads caused by the cranes, a load of 600 kN/m' will be assigned on both of the cranes legs. Table 6.2 contains an indication of the parameters of the cranes

that are used on the quay wall, source: (de Gijt & Broeken, 2014). In the contract documents a few horizontal loads caused by the cranes are provided. Normative horizontal crane loads are:

- 1 90 kN/m' on the waterside of the crane rails;
- 2 90 kN/m' on the landside of the crane rails;

Table 6.2 Properties of the transportation equipment

Type of crane	Lifting capacity [kN]	Outreach waterside [m]	Rail gauge [m]	Max. vertical load [kN]	Max. wheel load [kN]	Number of wheels [-]	Wheel distance [m]
Grab gantry crane	850	45,5	70 (4 rails)	30.000 (tot. weight)	625	56	1,35 2,15 6,8

### Bolder loads

Bolders are placed on top of the quay wall in order to keep the berthed ships into place. The maximum bolder loads are specified by the client in the contract documents. These are the maximum loads that the bolders can manage and will be used as representative values for the calculation. The representative values of the loads are: 1500 kN. A bolder will be set every 17,5 m resulting in a force of 85.7 kN/m<sup>1</sup>. This force has a point of engagement 0,5 m above the quay wall.

### Exceptional load / Fender load

The contract documents also describe an exceptional load that applies to the quay wall. This is a horizontal impact load that is caused by the berthing of a ship. The impact caused by the mooring ship leads to a load of 10.000 kN distributed over a surface of 5,0m x 5,0m on a level of +5,0 mNAP until -2,0 mNAP. This load will be distributed over 3 tubular piles including intermediate sheet piles resulting in a line load of 10.000 / (3 \* 3,73) = 894 kN/m<sup>1</sup>. This is an exceptional load case.

## 6.2 Load combinations

Considering the amount of different possible loads on the quay wall, a lot of different load combinations are possible. It is possible that not all of the loads are applicable during the same time. The only static load that works on the quay wall is its own weight. The rest of the identified loads are temporal loads on the quay wall. The cranes move over the wall and the bulk will be temporally stored and then transhipped. During the calculation one of the loads will be dominant over another. The dominant load will be applied with a factor of 1, whilst the minor load will be applied with a factor of 0,7 (according to the Eurocode 7(CEN, 2010)). The load combinations are given in Table 6.3.

Table 6.3 Load combinations

Load combination	Dominant load (Load factor = 1,0)	Minor load(s) (Load factors = 0,7)
1	Water, neap tide	-
2	Water, average tide	-
3	Water, spring tide	-
4	Water, maximum water level difference	Surface load including bulk load, vertical loads crane, horizontal loads seawards crane, bolder load
5	Surface load incl. bulk load	Vertical loads crane, horizontal load seawards crane, bolder load, water <sup>1</sup>
6	Surface load incl. bulk load	Vertical loads crane, horizontal load landwards crane, water <sup>1</sup>
7	Bolder load	Surface load incl. bulk load, vertical loads crane, horizontal load seawards crane, water <sup>1</sup>
8	Crane vertical and seawards	Surface load incl. bulk load, bolder load, water <sup>1</sup>

Load combination	Dominant load (Load factor = 1,0)	Minor load(s) (Load factors = 0,7)
9	Crane vertical and landwards	Surface load incl. bulk load, water <sup>1</sup>
10	Bulk load excl. surface	Water <sup>1</sup>
11	Exceptional load	Surface load including bulk load, vertical loads crane, horizontal load seawards, water <sup>1</sup>

<sup>1</sup>) Average tide water level difference

More load combinations can be defined but the amount of scenarios that have to be calculated will be minimised by using given scenarios. The chosen scenarios will give a representative view of what the loads of the quay wall are in reality.

## 7 SAFETY PHILOSOPHY

Usually, a safety philosophy with corresponding safety factors has to be used to ensure a safe design. No safety factors will be used during the calculation that will be performed for the purpose of the thesis. This will be done because the design of the construction is adopted from earlier calculations, where a safety check already has been performed. In the original design a risk class 2 has been taken into account to ensure a safe construction.

Table 7.1 Partial factors for soil parameters ( $\gamma_M$ )

Parameter	Risk class 2
Friction angle $\gamma_{\varphi}$ <sup>1</sup>	1,175
Effective cohesion $\gamma_c$	1,25
Undrained shear strength $\gamma_{cu}$	1,6
Volume weight $\gamma_y$	1,0
Unfavourable loads	1,0

<sup>1</sup> This factor applies on  $\tan \varphi'$

## 8 REFERENCES

The following standards and works have been used/cited.

Arcadia, D. H. (2009). Mohr-Coulomb Parameters For Modelling Of Concrete Structures. *Plaxis Bulletin, Spring Issue 2009*, Delft.

Cabal, R. a. (2014). *Guide to Cone Penetration Testing for Geotechnical Engineering, 6th Edition*.

CEN. (2010). *Eurocode 7: Geotechnical design*.

CUR. (oktober 2003). *CUR-rapport 2003-7 'Bepaling geotechnische parameters'*. Gouda: Stichting CUR.

de Gijt, J., & Broeken, M. (2014). *Quay Walls, Second Edition*. Rotterdam, the Netherlands: CRC Press/Balkema.

Gemeentewerken Rotterdam. (6 april 2010). *Rapport EMO kade M5+ M6 Rapportage geotechnisch grondonderzoek*. Rotterdam: Gemeentewerken Rotterdam.

Het Nederlands Normalisatie Instituut. (2012). *NEN 9997-1+C1 (nl)*. Delft: Stichting Reprorecht.

- Jorgens, M., & Hansen, A. (2016). Geotechnical Engineering for a new container terminal in Lomé, Togo, West Africa. *Nordic Geotechnical Meeting 2016 Reykjavik*, (pp. 879-888). Reykjavik.
- Lunne, Robertson, & Powel. (1997). *Cone Penetration Testing in Geotechnical Practice*.
- Lunne, T., Robertson, P., & Powell, J. (1997). *Cone Penetration Testing in Geotechnical Practice*. London: Blackie Academic and Professional.
- Mayne, P. (2014). Interpretation of Geotechnical Parameters from Seismic Piezocone Tests. *3rd International Symposium on Cone Penetration Testing*. Las Vegas.
- Port of Rotterdam. (2012). *HydroMeteobundel nr. 4*. Rotterdam: Port of Rotterdam N.V.



# III

APPENDIX: PARAMETERSHEET\_EMOQUAY.XLS

# IV

APPENDIX: DETERMINATION HSM PARAMETER NON-COHESIVE.XLS

# V

## APPENDIX: CHARACTERISTIC AND DESIGN PARAMETERS



# III

## APPENDIX: EXPECTATION, REPRESENTATIVE AND DESIGN PARAMETER SETS



Expected values

Layer id		$q_c$	$Y_{unconsolid}$	$Y_{consolid}$	$\phi'$	$c'$	$R_e$	$E_{50}^{ref}$	$E_{ed}^{ref}$	$E_{ur}^{ref}$	$m$	$\psi$	$R_{base}$
[-]		[MPa]	[kN/m <sup>2</sup> ]	[kN/m <sup>2</sup> ]	[°]	[kN/m <sup>2</sup> ]	[%]	[MN/m <sup>2</sup> ]	[MN/m <sup>2</sup> ]	[MN/m <sup>2</sup> ]	[-]	[°]	[-]
1A1	Sand loose	2,0	17,0	19,0	32,5	0,0	45,6	27,4	27,4	109,4	0,5	0,0	0,8
1A2	Sand, moderate	10,0	18,0	20,0	35,0	0,0	78,7	47,2	47,2	188,8	0,5	2,5	0,8
1A3	Sand, dense	25,0	19,0	21,0	37,5	0,0	97,4	58,5	58,5	233,9	0,5	5,0	0,8
1C	Clay, s. sandy	2,0	18,0	18,0	30,0	0,5 -		8,5	4,2	24,5	1,0	0,0	0,8
2A	Sand, w. clay	5,0	16,9	17,4	29,8	0,0	27,2	16,4	16,4	65,4	0,5	0,0	0,8
2A3	Sand, dense	20,0	17,5	19,0	37,5	0,0	77,5	46,5	46,5	185,9	0,5	5,0	0,8
2C	Clay, w. sandy, moderate	2,0	17,1	18,2	25,0	7,5 -		3,1	1,6	11,1	0,9	0,0	0,8
3A	Clay, organic, weak	2,0	15,4	16,6	17,0	0,5 -		4,0	2,3	17,6	1,0	0,0	0,8
3A1	Clay, organic, sandy	5,0	18,1	18,5	17,0	0,5 -		8,2	4,8	33,3	1,0	0,0	0,8
4A	Sand	22,0	18,9	19,0	35,0	0,0	74,2	44,5	44,5	178,1	0,5	2,5	0,8
4A1	Sand, clay layers	21,0	18,1	18,7	29,8	0,0	67,9	40,7	40,7	162,9	0,5	0,0	0,8
5A1	Sand, moderate, clay layers	8,0	18,0	20,0	32,5	0,0	17,9	10,7	10,7	43,0	0,5	0,0	0,8
5A3	Sand, dense	40,0	19,0	21,0	37,5	0,0	78,1	46,8	46,8	187,3	0,5	5,0	0,8
6A2	Sand, dense, clay layers	25,0	18,0	20,0	35,0	0,0	53,8	32,3	32,3	129,0	0,5	2,5	0,8
6B	Loam	6,0	19,5	19,7	31,3	6,3 -		8,3	13,5	54,8	0,7	0,0	0,8
6C	Clay	4,0	20,1	20,3	25,0	14,0 -		19,4	12,0	76,7	0,7	0,0	0,8

Representative values

Layer id		$q_c$	$Y_{unconsolid}$	$Y_{consolid}$	$\phi'$	$c'$	$R_e$	$E_{50}^{ref}$	$E_{ed}^{ref}$	$E_{ur}^{ref}$	$m$	$\psi$	$R_{base}$
[-]		[MPa]	[kN/m <sup>2</sup> ]	[kN/m <sup>2</sup> ]	[°]	[kN/m <sup>2</sup> ]	[%]	[MN/m <sup>2</sup> ]	[MN/m <sup>2</sup> ]	[MN/m <sup>2</sup> ]	[-]	[°]	[-]
1A1	Sand loose	2,0	17,0	19,0	30,0	0,0	45,6	27,4	27,4	109,4	0,5	0,0	0,8
1A2	Sand, moderate	10,0	18,0	20,0	32,5	0,0	78,7	47,2	47,2	188,8	0,5	2,5	0,8
1A3	Sand, dense	25,0	19,0	21,0	35,0	0,0	97,4	58,5	58,5	233,9	0,5	5,0	0,8
1C	Clay, s. sandy	2,0	18,0	18,0	27,5	0,0 -		8,5	4,2	24,5	1,0	0,0	0,8
2A	Sand, w. clay	5,0	16,9	17,4	27,0	0,0	27,2	16,4	16,4	65,4	0,5	0,0	0,8
2A3	Sand, dense	20,0	17,5	19,0	35,0	0,0	77,5	46,5	46,5	185,9	0,5	5,0	0,8
2C	Clay, w. sandy, moderate	2,0	17,1	18,2	22,5	5,0 -		3,1	1,6	11,1	0,9	0,0	0,8
3A	Clay, organic, weak	2,0	15,4	16,6	15,0	0,0 -		4,0	2,3	17,6	1,0	0,0	0,8
3A1	Clay, organic, sandy	5,0	18,1	18,5	15,0	0,0 -		8,2	4,8	33,3	1,0	0,0	0,8
4A	Sand	22,0	18,9	19,0	32,5	0,0	74,2	44,5	44,5	178,1	0,5	2,5	0,8
4A1	Sand, clay layers	21,0	18,1	18,7	27,0	0,0	67,9	40,7	40,7	162,9	0,5	0,0	0,8
5A1	Sand, moderate, clay layers	8,0	18,0	20,0	30,0	0,0	17,9	10,7	10,7	43,0	0,5	0,0	0,8
5A3	Sand, dense	40,0	19,0	21,0	35,0	0,0	78,1	46,8	46,8	187,3	0,5	5,0	0,8
6A2	Sand, dense, clay layers	25,0	18,0	20,0	32,5	0,0	53,8	32,3	32,3	129,0	0,5	2,5	0,8
6B	Loam	6,0	19,5	19,7	27,5	2,5 -		8,3	13,5	54,8	0,7	0,0	0,8
6C	Clay	4,0	20,1	20,3	22,5	13,0 -		19,4	12,0	76,7	0,7	0,0	0,8

Design values

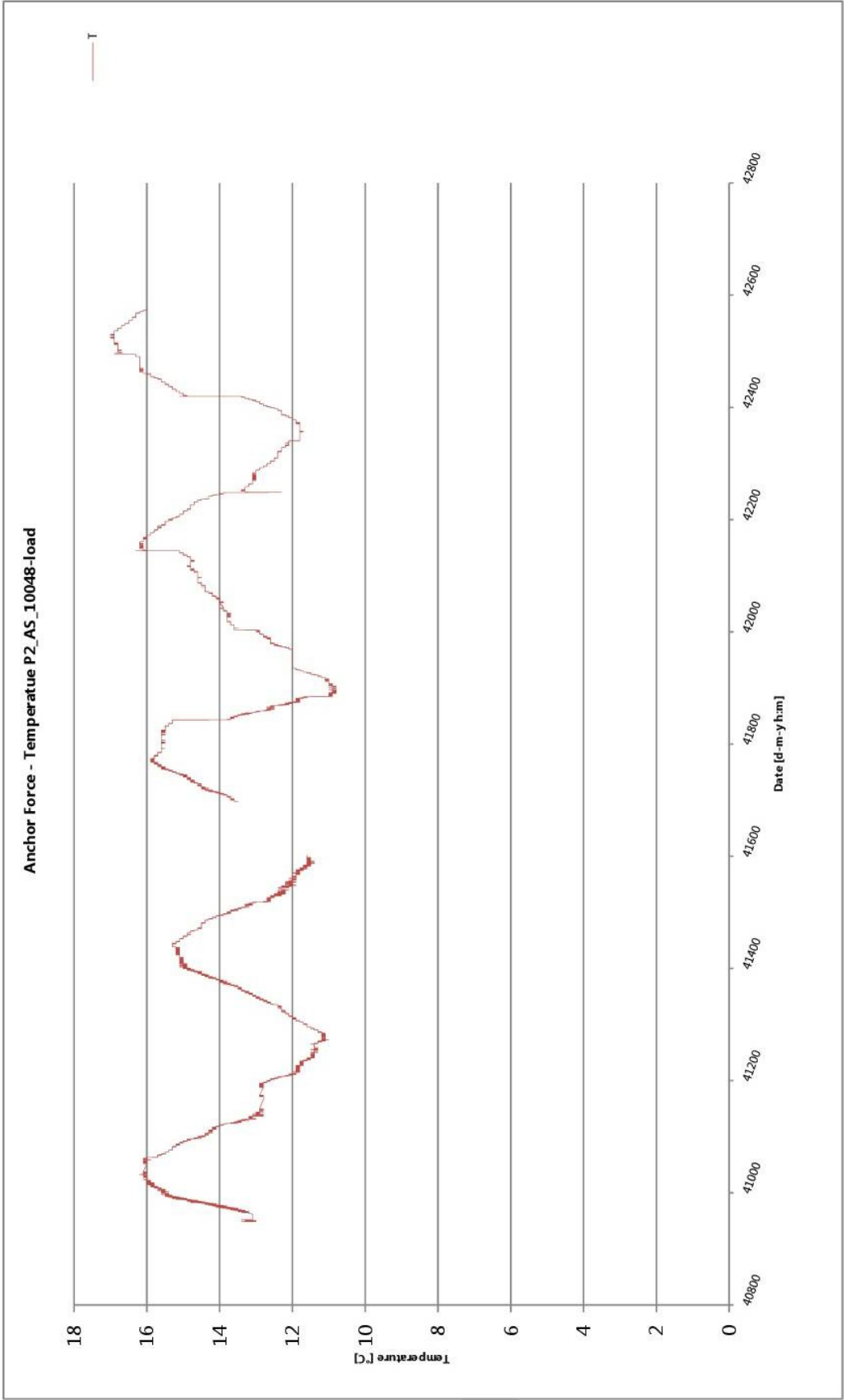
Layer id		$q_c$	$Y_{unconsolid}$	$Y_{consolid}$	$\phi'$	$c'$	$R_e$	$E_{50}^{ref}$	$E_{ed}^{ref}$	$E_{ur}^{ref}$	$m$	$\psi$	$R_{base}$
[-]		[MPa]	[kN/m <sup>2</sup> ]	[kN/m <sup>2</sup> ]	[°]	[kN/m <sup>2</sup> ]	[%]	[MN/m <sup>2</sup> ]	[MN/m <sup>2</sup> ]	[MN/m <sup>2</sup> ]	[-]	[°]	[-]
1A1	Sand loose	2,0	17,0	19,0	25,7	0,0	45,6	27,4	27,4	109,4	0,5	0,0	0,8
1A2	Sand, moderate	10,0	18,0	20,0	28,0	0,0	78,7	47,2	47,2	188,8	0,5	2,5	0,8
1A3	Sand, dense	25,0	19,0	21,0	30,3	0,0	97,4	58,5	58,5	233,9	0,5	5,0	0,8
1C	Clay, s. sandy	2,0	18,0	18,0	23,5	0,0 -		8,5	4,2	24,5	1,0	0,0	0,8
2A	Sand, w. clay	5,0	16,9	17,4	23,0	0,0	27,2	16,4	16,4	65,4	0,5	0,0	0,8
2A3	Sand, dense	20,0	17,5	19,0	30,3	0,0	77,5	46,5	46,5	185,9	0,5	5,0	0,8
2C	Clay, w. sandy, moderate	2,0	17,1	18,2	19,0	3,3 -		3,1	1,6	11,1	0,9	0,0	0,8
3A	Clay, organic, weak	2,0	15,4	16,6	12,6	0,0 -		4,0	2,3	17,6	1,0	0,0	0,8
3A1	Clay, organic, sandy	5,0	18,1	18,5	12,6	0,0 -		8,2	4,8	33,3	1,0	0,0	0,8
4A	Sand	22,0	18,9	19,0	28,0	0,0	74,2	44,5	44,5	178,1	0,5	2,5	0,8
4A1	Sand, clay layers	21,0	18,1	18,7	23,0	0,0	67,9	40,7	40,7	162,9	0,5	0,0	0,8
5A1	Sand, moderate, clay layers	8,0	18,0	20,0	25,7	0,0	17,9	10,7	10,7	43,0	0,5	0,0	0,8
5A3	Sand, dense	40,0	19,0	21,0	30,3	0,0	78,1	46,8	46,8	187,3	0,5	5,0	0,8
6A2	Sand, dense, clay layers	25,0	18,0	20,0	28,0	0,0	53,8	32,3	32,3	129,0	0,5	2,5	0,8
6B	Loam	6,0	19,5	19,7	23,5	1,7 -		8,3	13,5	54,8	0,7	0,0	0,8
6C	Clay	4,0	20,1	20,3	19,0	8,7 -		19,4	12,0	76,7	0,7	0,0	0,8



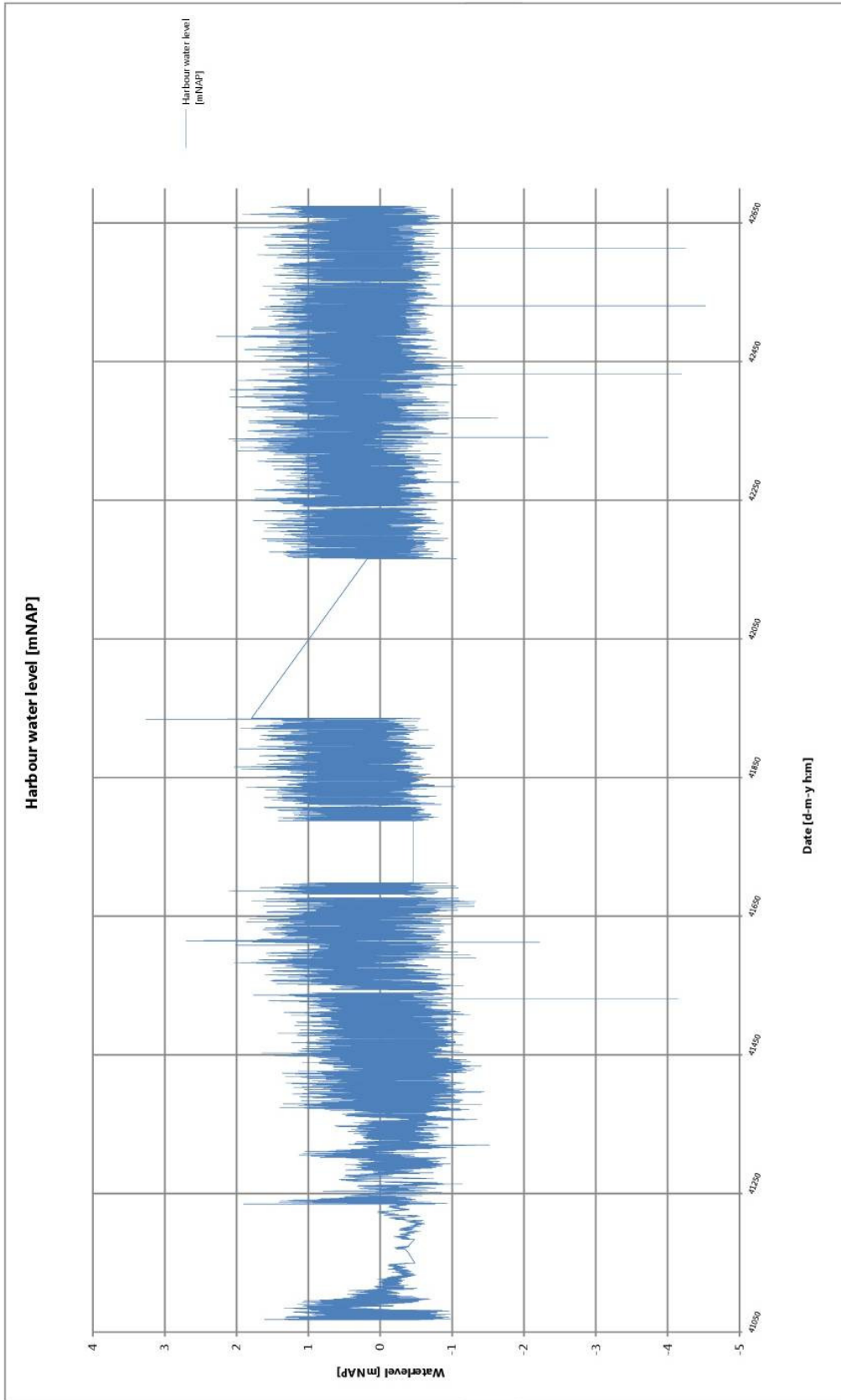
# IV

## Appendix: Graphs of the Measured Data

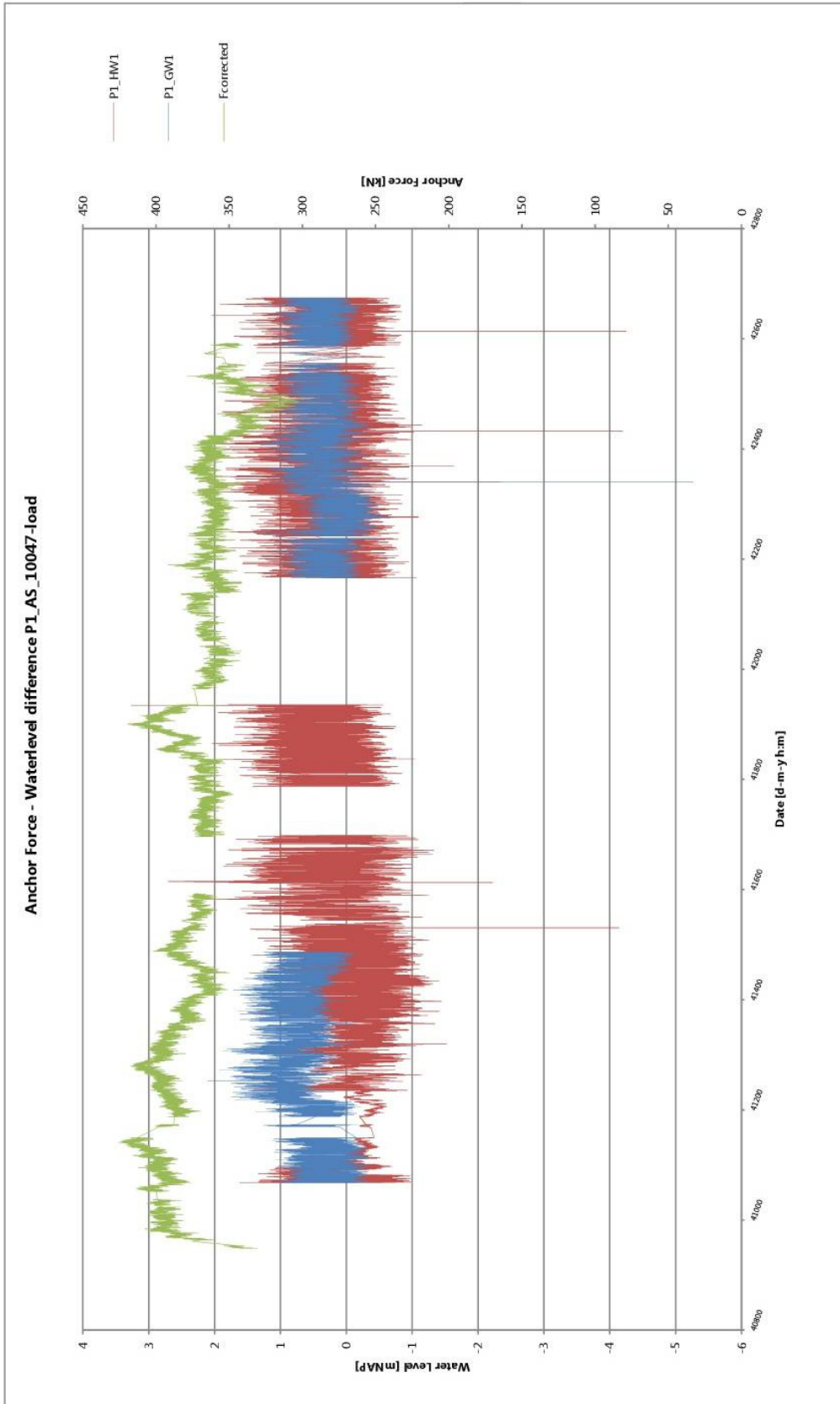




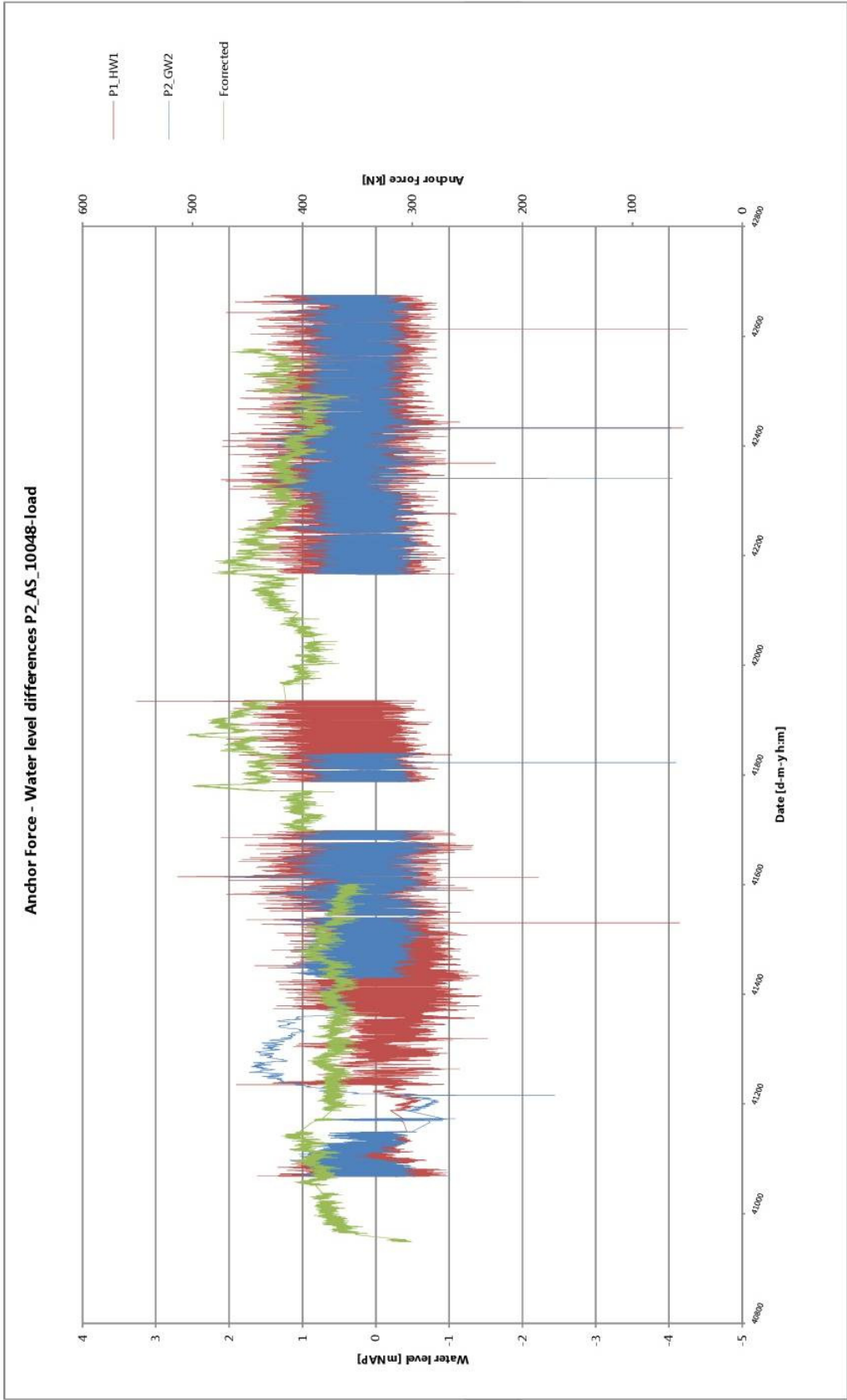
The tables with the exact values of the measurements have been annexed in the digital appendixes.



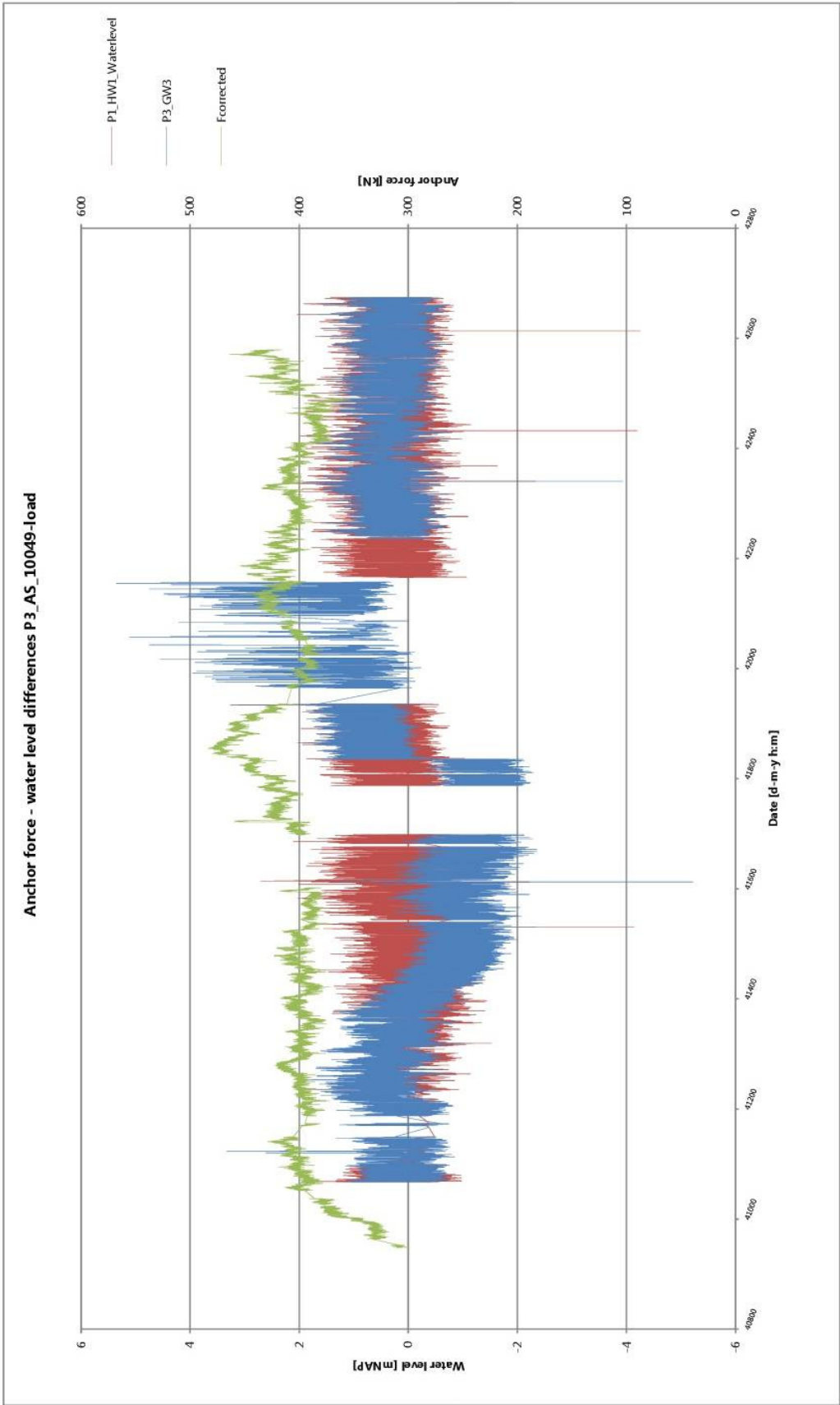
The tables with the exact values of the measurements have been annexed in the digital appendixes.



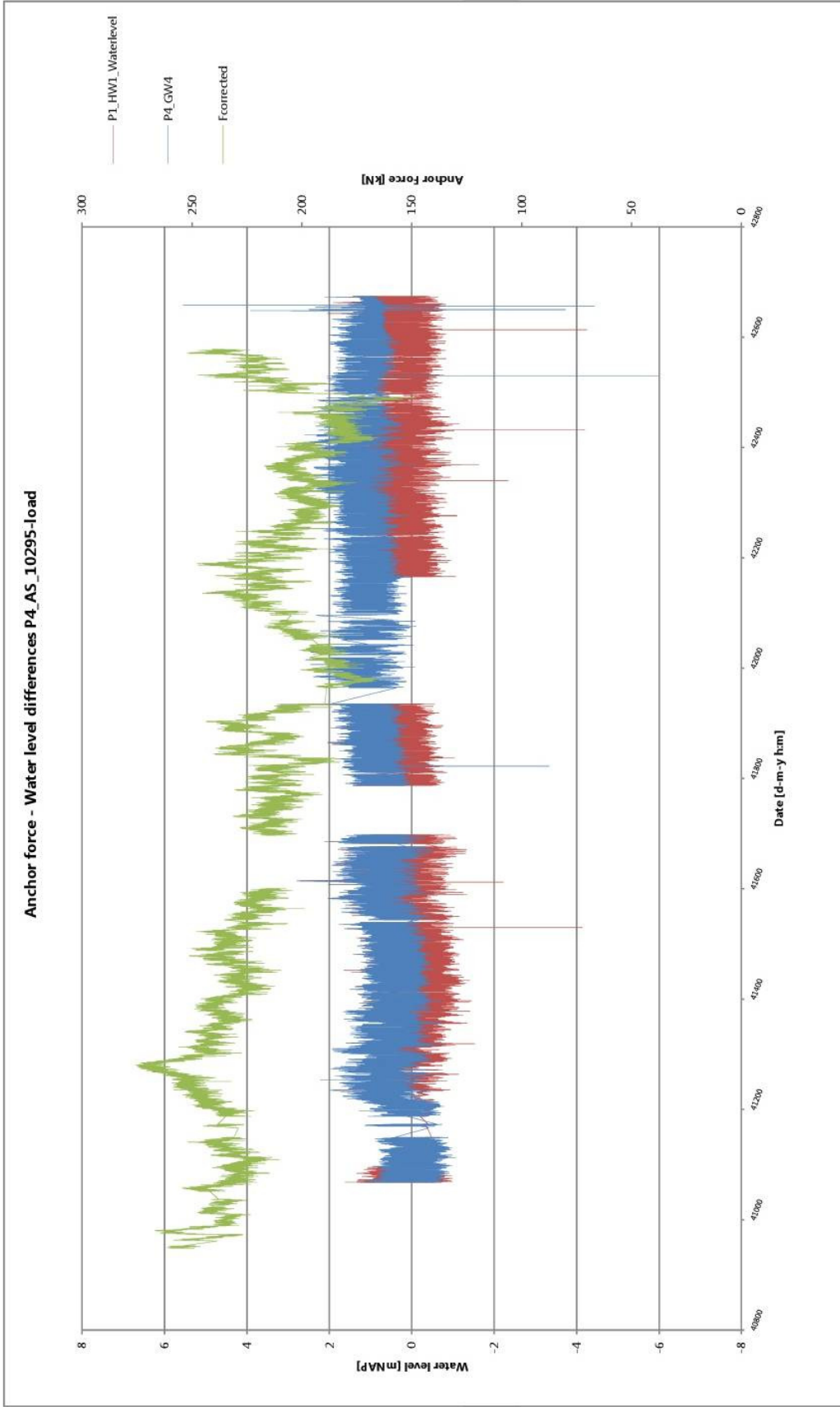
The tables with the exact values of the measurements have been annexed in the digital appendixes.



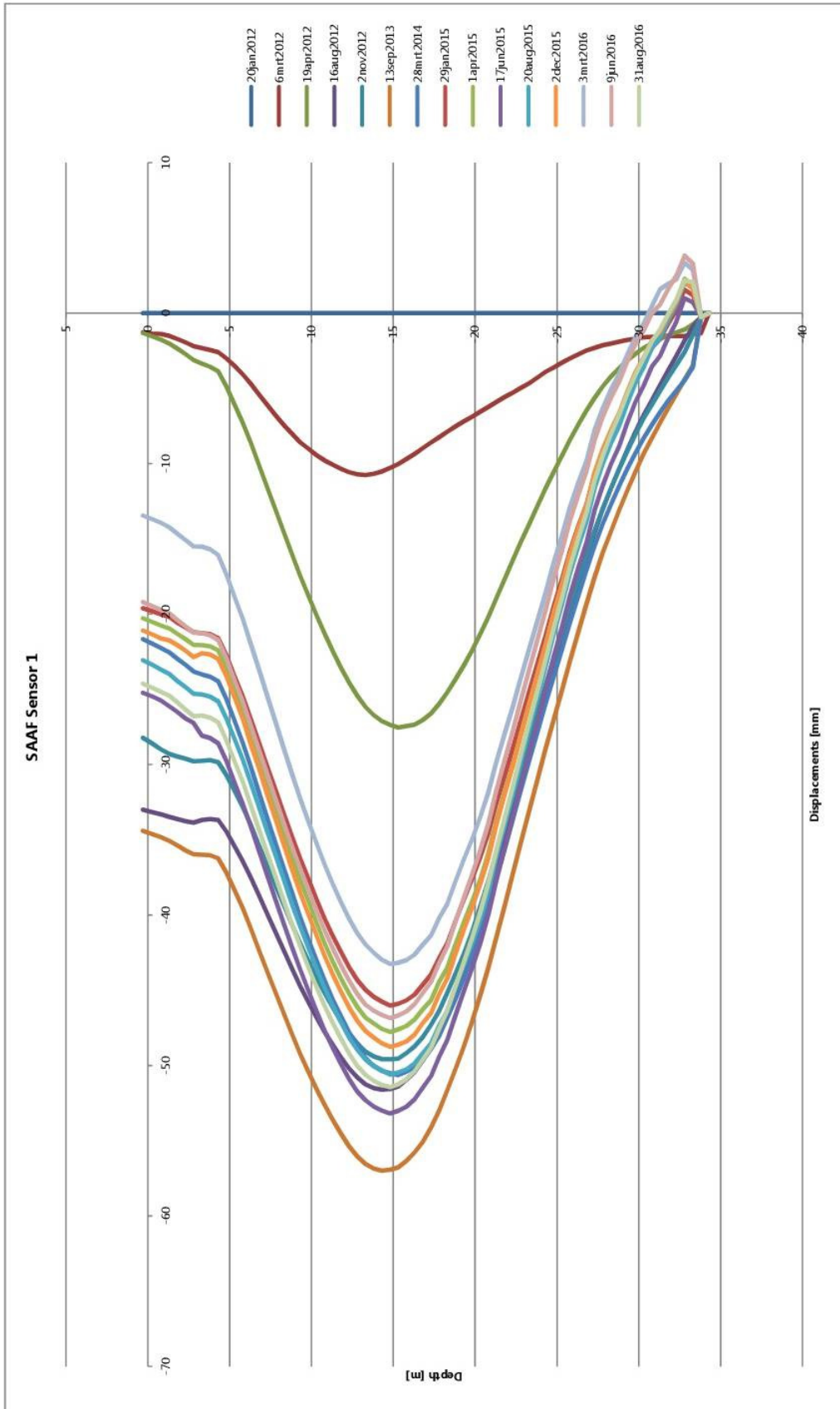
The tables with the exact values of the measurements have been annexed in the digital appendixes.



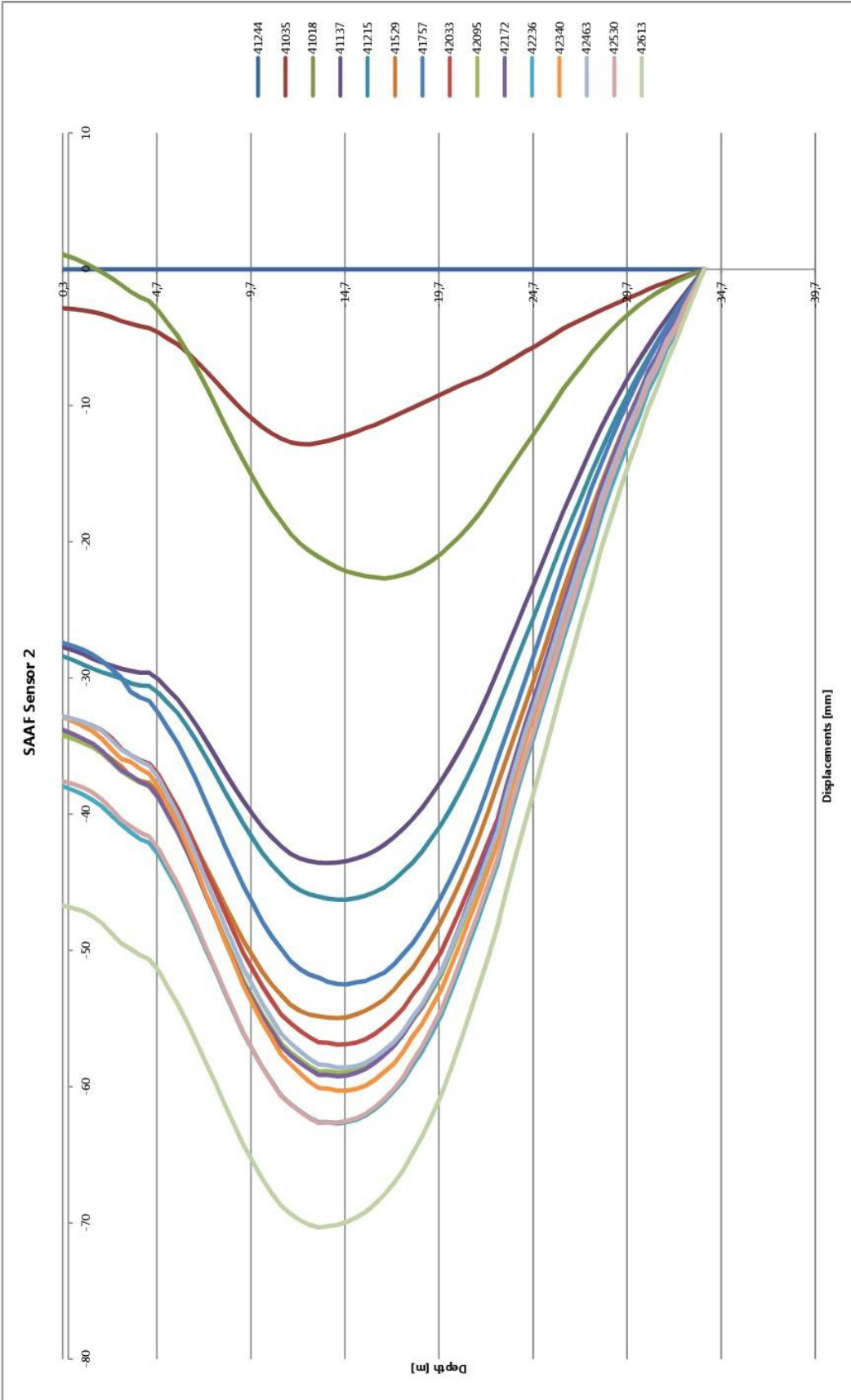
The tables with the exact values of the measurements have been annexed in the digital appendix.



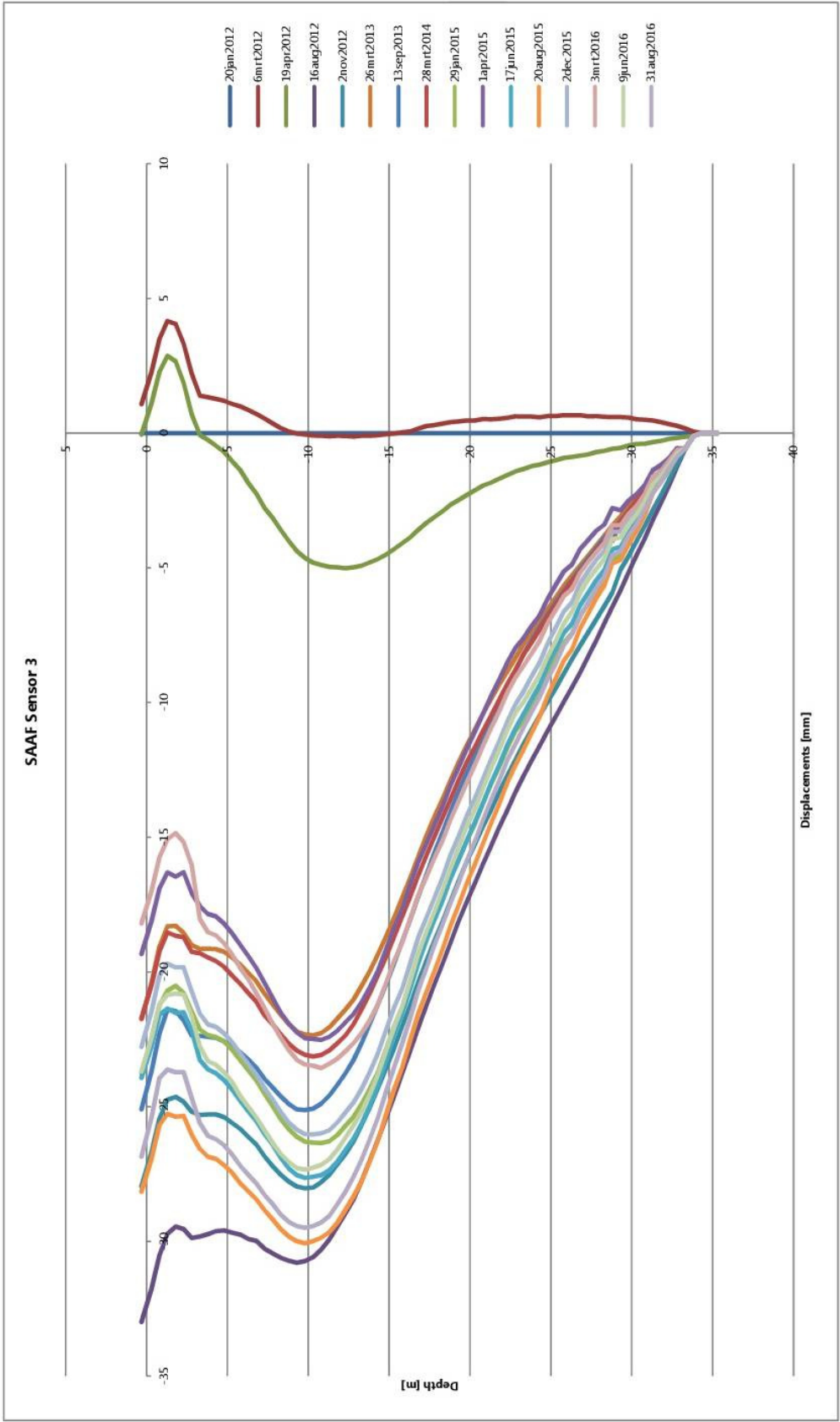
The tables with the exact values of the measurements have been annexed in the digital appendixes.



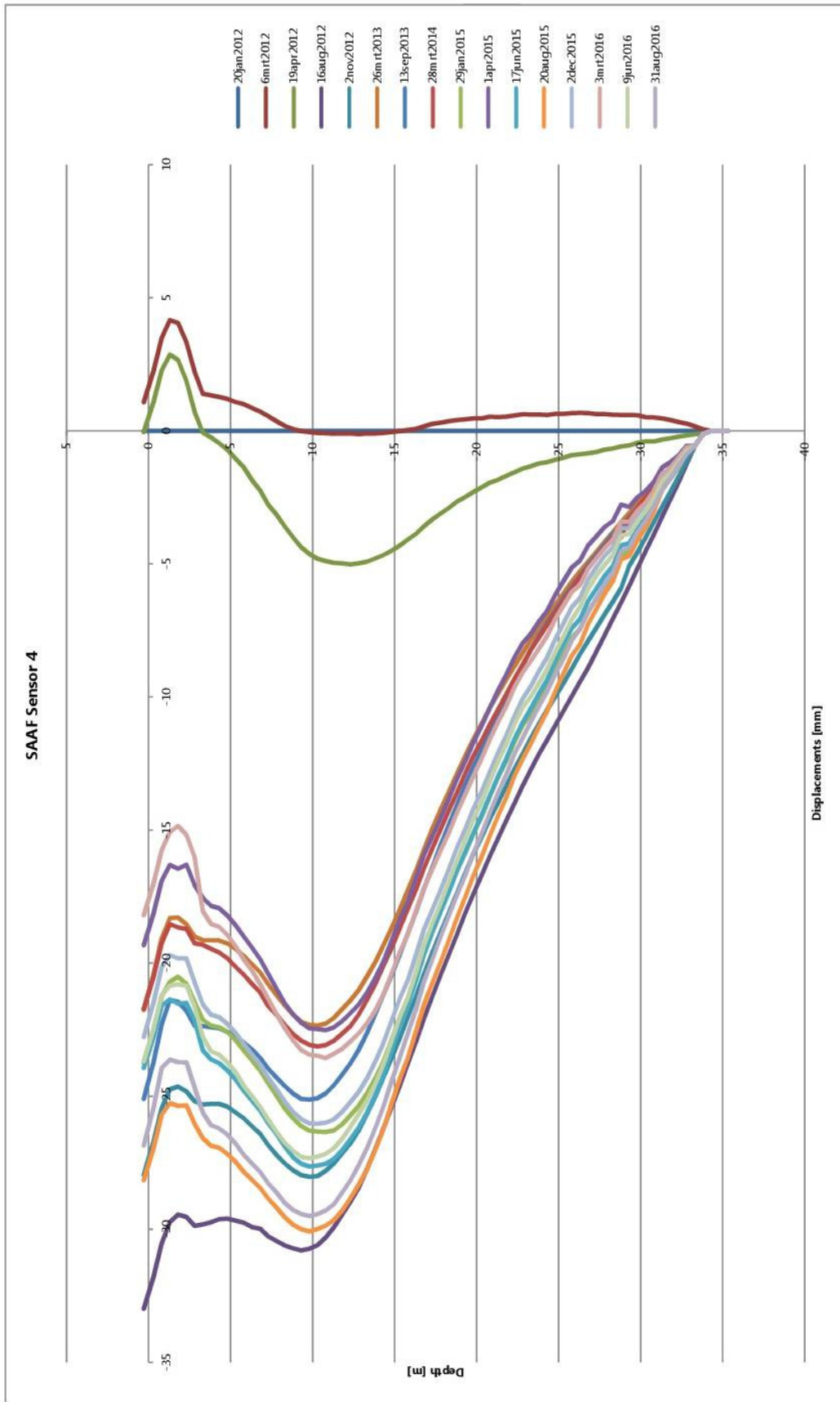
The tables with the exact values of the measurements have been annexed in the digital appendixes.



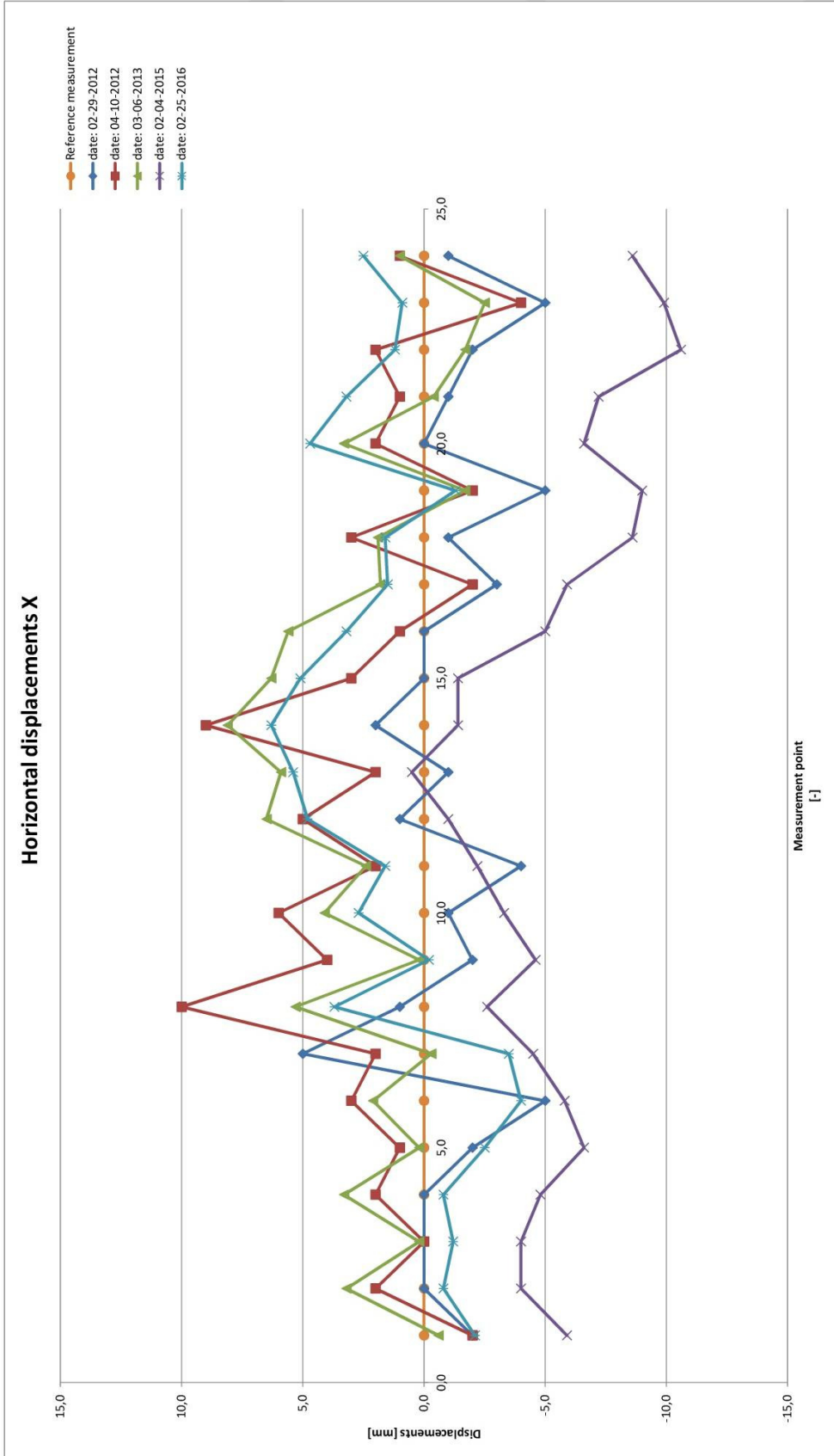
The tables with the exact values of the measurements have been annexed in the digital appendixes.

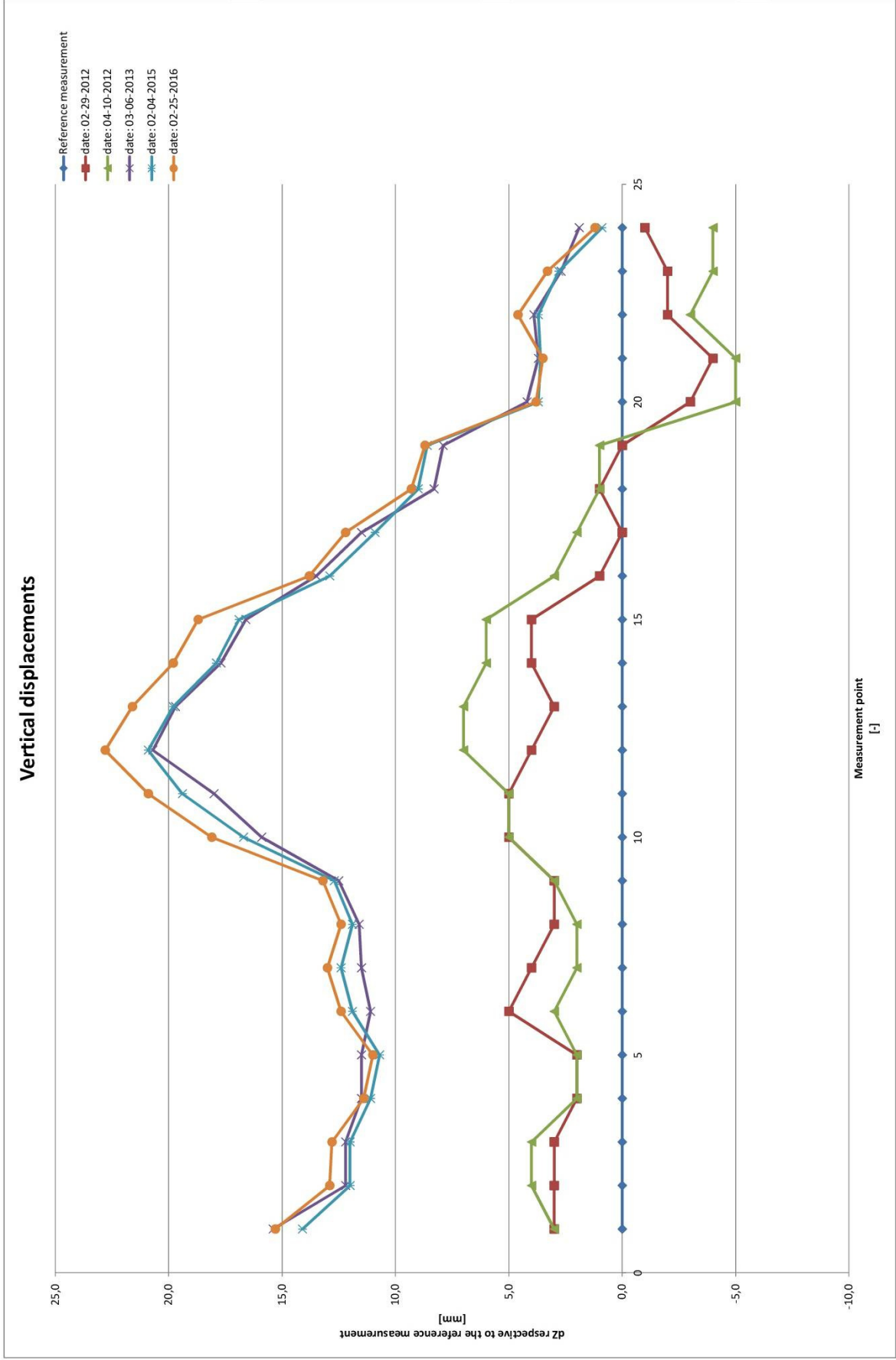


The tables with the exact values of the measurements have been annexed in the digital appendixes.



The tables with the exact values of the measurements have been annexed in the digital appendixes.





H-L-N-MV-072-KAD-011  
 Noordoostzijde  
 Mississippihaven NOz - Kade M5/M6

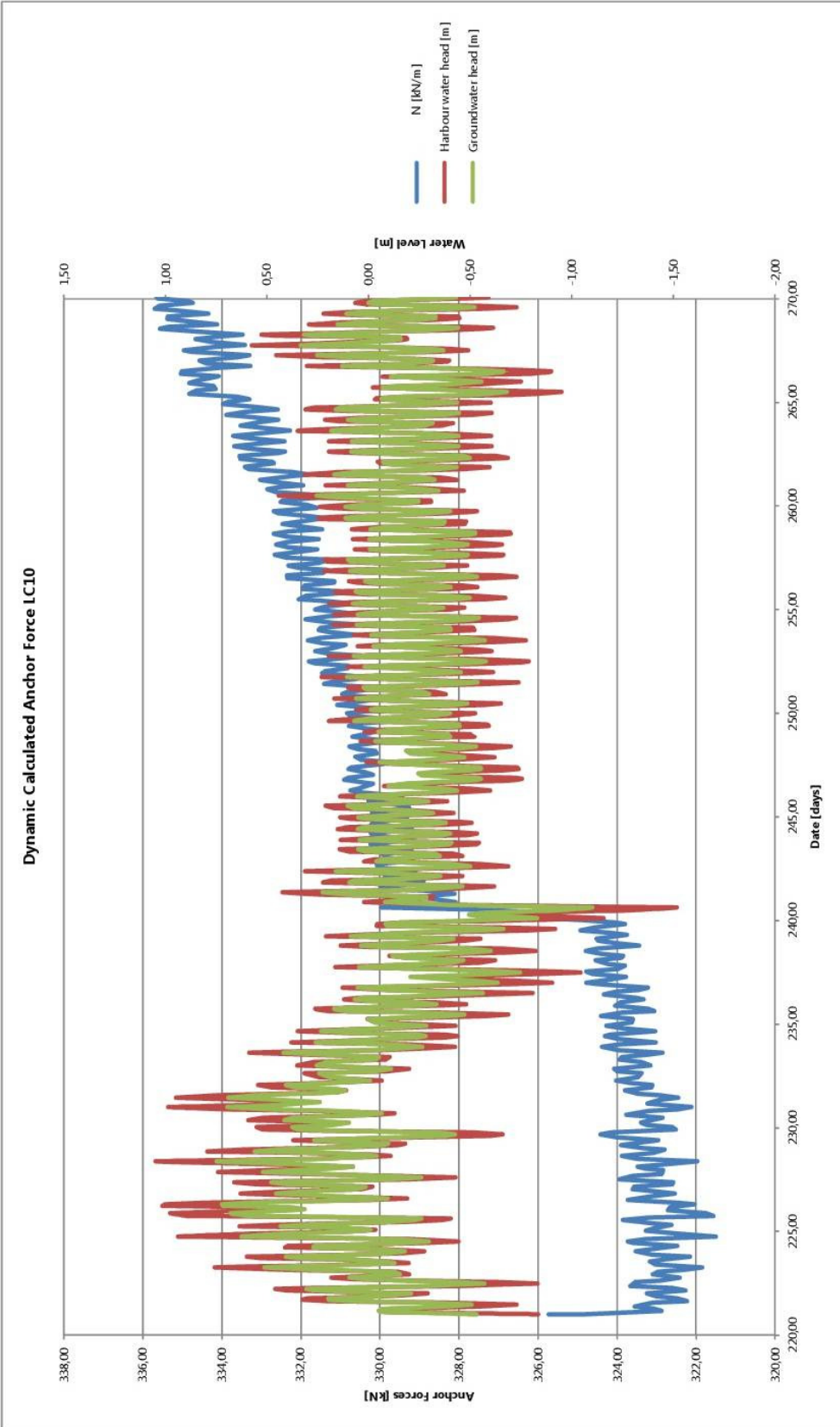
Puntnummer	1st measurement date: 02-29-2012			2nd measurement date: 04-10-2012			3rd measurement date: 03-06-2013			4th measurement date: 02-04-2015			5th measurement date: 02-25-2016			Reference measurement		
	$\Delta X$ in mm	$\Delta Y$ in mm	$\Delta Z$ in mm	$\Delta X$ in mm	$\Delta Y$ in mm	$\Delta Z$ in mm	$\Delta X$ in mm	$\Delta Y$ in mm	$\Delta Z$ in mm	$\Delta X$ in mm	$\Delta Y$ in mm	$\Delta Z$ in mm	$\Delta X$ in mm	$\Delta Y$ in mm	$\Delta Z$ in mm	X in mm	Y in mm	Z in mm
1	-2	4	3.0	-2	4	3.0	-1	3	15.4	-6	9	14.1	-2	-1	15.3	0.0	0.0	0.0
2	0	4	3.0	2	-1	4.0	3	-1	12.2	-4	6	12.0	-1	-2	12.9	0.0	0.0	0.0
3	0	3	3.0	0	-4	4.0	0	-2	12.2	-4	5	12.0	-1	-3	12.8	0.0	0.0	0.0
4	0	3	2.0	2	-4	2.0	3	-2	11.5	-5	5	11.1	-1	-3	11.4	0.0	0.0	0.0
5	-2	2	2.0	1	-5	2.0	0	-3	11.5	-7	4	10.7	-2	-4	11.0	0.0	0.0	0.0
6	-5	1	5.0	3	-8	3.0	2	-5	11.1	-6	-2	11.9	-4	-7	12.4	0.0	0.0	0.0
7	5	-1	4.0	2	-14	2.0	0	-7	11.5	-5	-3	12.4	-3	-8	13.0	0.0	0.0	0.0
8	1	6	3.0	10	-2	2.0	5	-7	11.8	-3	-3	11.9	4	-5	12.4	0.0	0.0	0.0
9	-2	4	3.0	4	-4	3.0	0	-7	12.5	-5	-4	12.7	0	-6	13.2	0.0	0.0	0.0
10	-1	4	5.0	6	1	5.0	4	-12	15.9	-3	-9	16.7	3	-12	18.1	0.0	0.0	0.0
11	-4	4	5.0	2	0	5.0	2	-11	18.0	-2	-6	19.4	2	-9	20.9	0.0	0.0	0.0
12	1	6	4.0	5	-2	7.0	7	-9	20.7	-1	-2	20.9	5	-7	22.8	0.0	0.0	0.0
13	-1	5	3.0	2	-3	19.7	6	-11	19.7	1	-3	19.8	5	-7	21.6	0.0	0.0	0.0
14	2	6	4.0	9	2	6.0	8	-6	17.7	-1	2	17.9	6	-3	19.8	0.0	0.0	0.0
15	0	4	4.0	3	1	6.0	6	-10	16.6	-1	1	16.9	5	-4	18.7	0.0	0.0	0.0
16	0	3	1.0	1	1	3.0	6	-3	13.5	-5	5	12.9	3	-1	13.8	0.0	0.0	0.0
17	-3	3	0.0	-2	-1	2.0	2	-5	11.5	-6	7	10.9	1	-2	12.2	0.0	0.0	0.0
18	-1	4	1.0	3	2	1.0	2	1	8.3	-9	11	9.0	2	5	9.3	0.0	0.0	0.0
19	-5	-1	0.0	-2	-1	1.0	-2	-4	7.9	-9	7	8.6	-1	1	8.7	0.0	0.0	0.0
20	0	3	-3.0	2	8	-5.0	3	2	4.2	-7	13	3.7	5	8	3.8	0.0	0.0	0.0
21	-1	1	-4.0	1	2	-5.0	0	-1	3.7	-7	11	3.6	3	6	3.5	0.0	0.0	0.0
22	-2	0	-2.0	2	4	-3.0	-2	5	3.9	-11	12	3.7	1	6	4.6	0.0	0.0	0.0
23	-5	-1	-2.0	2	2	-4.0	-3	2	2.7	-10	11	2.8	1	6	3.3	0.0	0.0	0.0
24	-1	1	-1.0	1	5	-4.0	1	5	1.9	-9	10	0.9	3	10	1.2	0.0	0.0	0.0



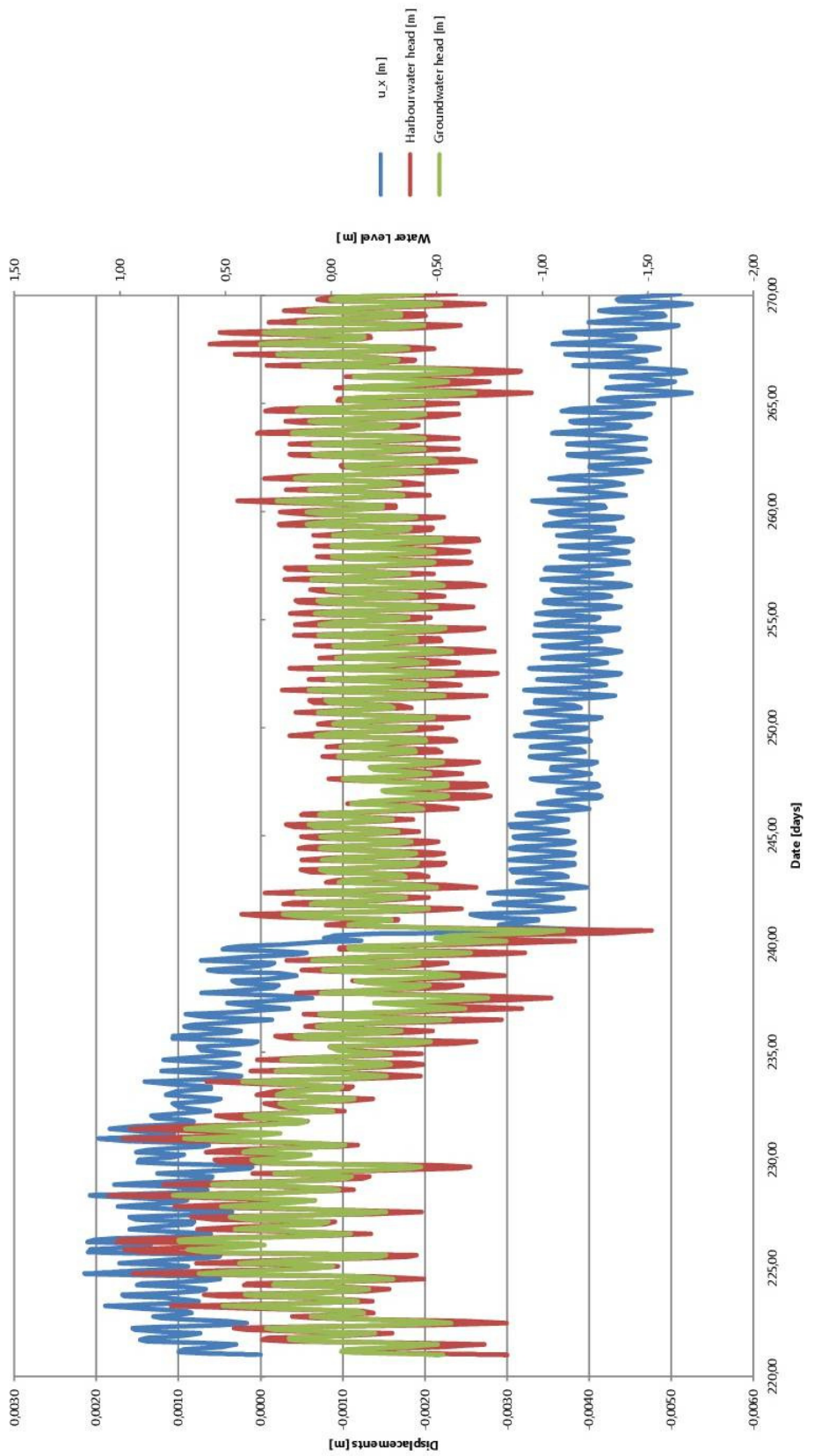
# V

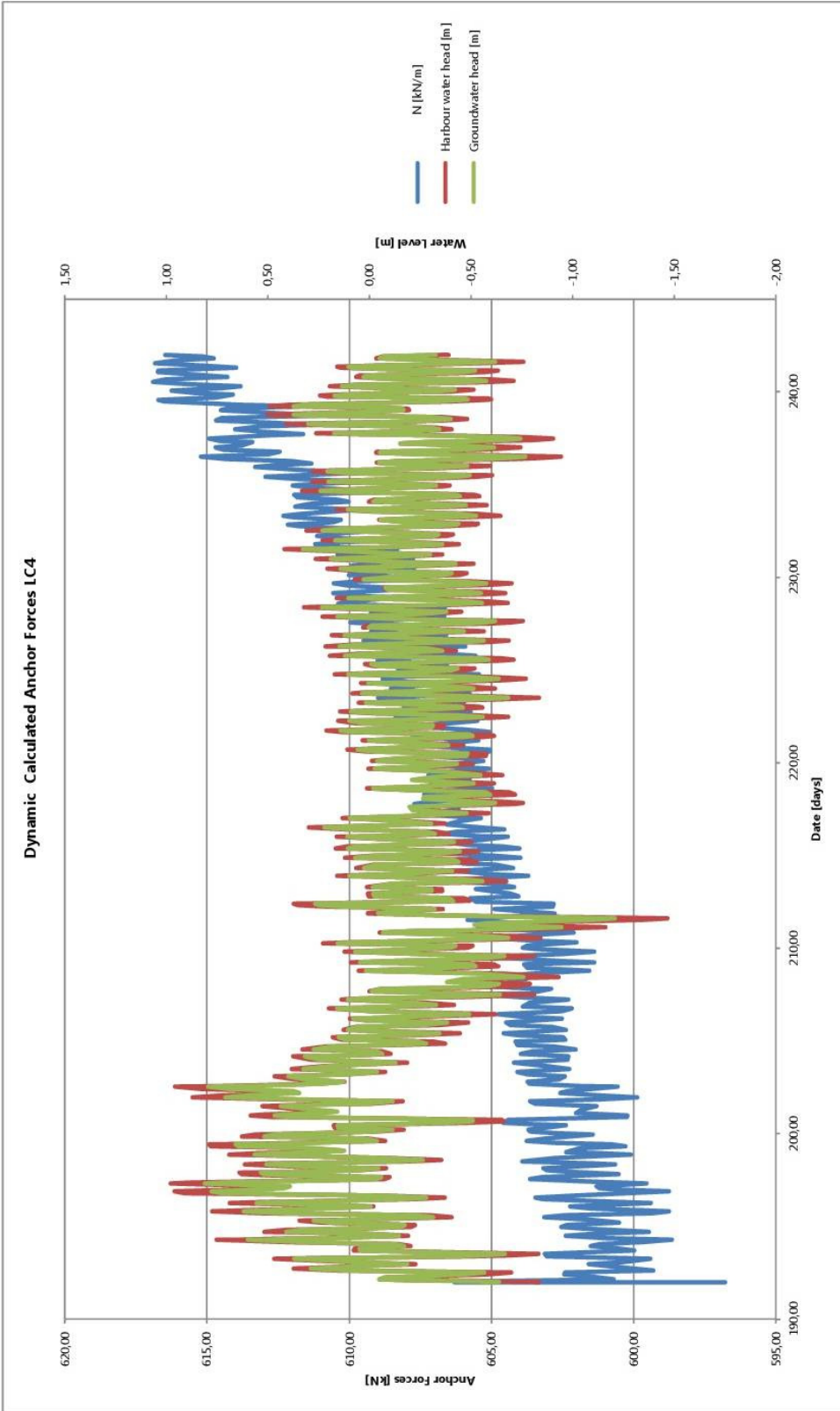
## Appendix: Static and Dynamic Calculation Results

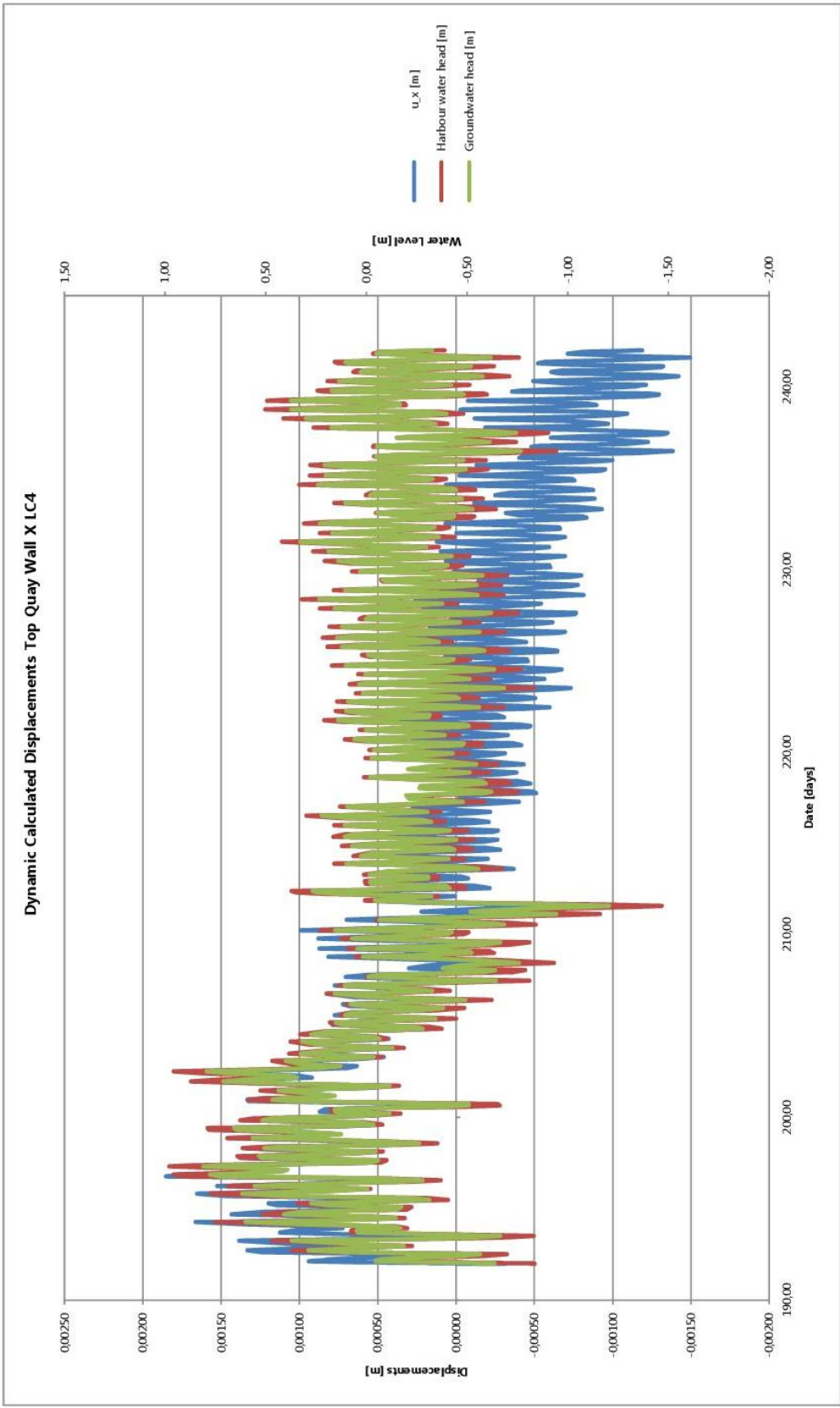




Dynamic Calculated Displacements Top Quay Wall X1C10





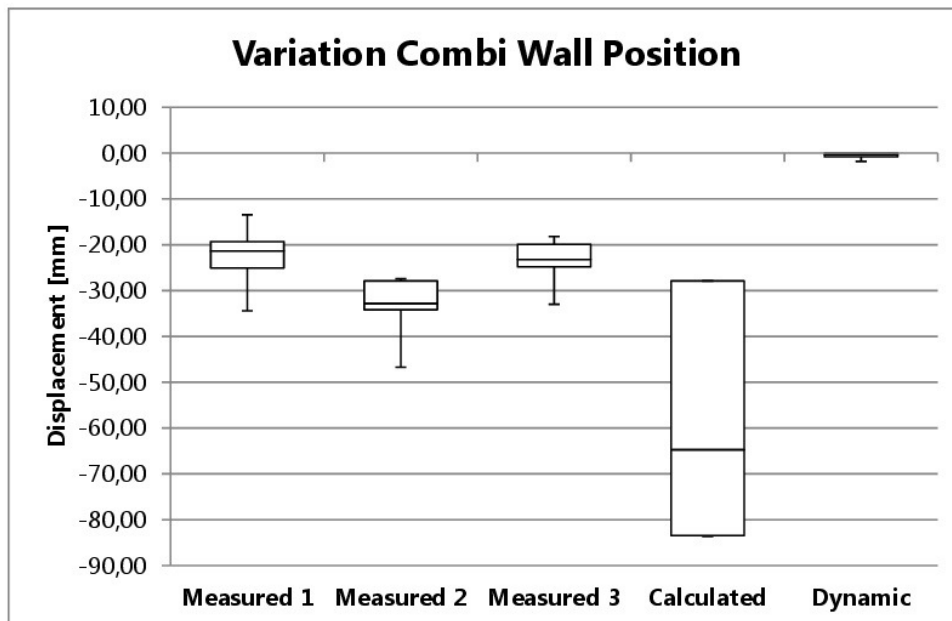


# VI

## Appendix: Statistics of the measured and Calculated Results



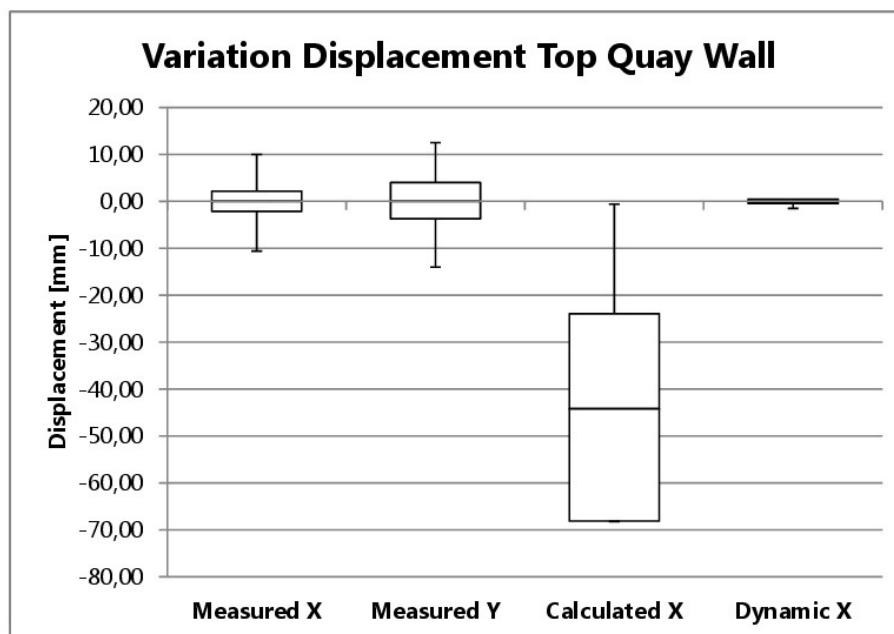
Statistics Inclinometer							
Quartiles	Measured 1	Measured 2	Measured 3	Calculated	Dynamic m	Dynamic mm	
Max	-13,5	-27,4	-18,2	-27,9	0,0017	1,739545936	
75%	-19,3	-27,9	-19,9	-27,9	0,0003	0,298700445	
Median	-21,4	-32,9	-23,2	-64,8	-0,0003	-0,303715608	
25%	-25,1	-34,2	-24,8	-83,5	-0,0008	-0,793213657	
Min	-34,4	-46,7	-33,0	-83,6	-0,0018	-1,818542203	
	Measured 1	Measured 2	Measured 3	Calculated	Dynamic		
Blank							
Bottom 25%							
25-50%							
50-75%					0,2987		
Top 25%					1,4408		
Blank	-13,46	-27,43	-18,20	-27,89			
Top 25%	-5,85	-0,46	-1,73	-0,02			
50-75%	-2,08	-4,96	-3,31	-36,85	-0,3037		
25-50%	-3,70	-1,32	-1,57	-18,72	-0,4895		
Bottom 25%	-9,32	-12,53	-8,18	-0,15	-1,0253		
Plot		0,00	0,00	0,00			
Upper boundary	-5,85	-0,46	-1,73	-0,02	0,44		
Lower boundary	-9,32	-12,53	-8,18	-0,15	-1,03		



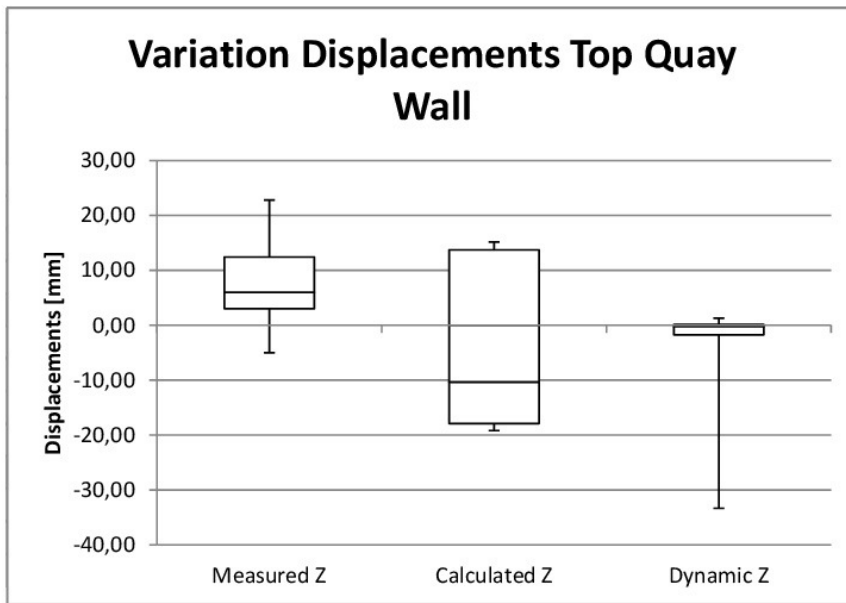
Statistics Displacements XY						
Quartiles	Displacements	Displacements Y	Calculated X	Dynamic m	Dynamic m m	
Max		10	12,5	-0,593	0,0019	1,85
	75%	2	4,0	-23,945	0,0005	0,46
Median		0	0,0	-44,199	-0,0001	-0,08
	25%	-2	-3,7	-68,116	-0,0005	-0,48
Min		-11	-14,0	-68,193	-0,0015	-1,50

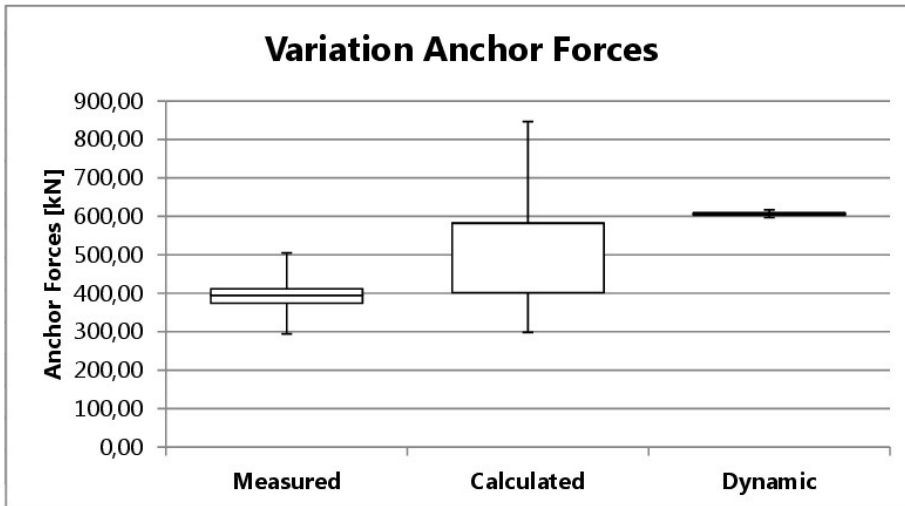
	Measured X	Measured Y	Calculated X	Dynamic X
Blank				
Bottom 25%				
25-50%				
50-75%	2,18	4,00		0,46
Top 25%	7,82	8,50		1,39
Blank			-0,59	
Top 25%			-23,35	
50-75%			-20,25	-0,08
25-50%	-2,13	-3,70	-23,92	-0,40
Bottom 25%	-8,47	-10,30	-0,08	-1,02
Plot				
Upper boundary	7,82	8,50	-23,35	
Lower boundary	8,47	10,30	0,08	1,02



Statistics Displacements XY					
Quartiles	Measured Z	Calculated Z	Dynamic Z		
Max	22,8	15,158	1,3	0,00128	
75%	12,425	13,73	0,1	0,00013	
Median	6	-10,385	-0,2	-0,00024	
25%	3	-17,9	-1,7	-0,00175	
Min	-5	-17,904	-33,3	-0,03334	
	Measured Z	Calculated Z	Dynamic Z		
Blank					
Bottom 25%	3,00				
25-50%	3,00				
50-75%	6,43	13,73	0,13		
Top 25%	10,37	1,43	1,15		
Blank		0,00	0,00		
Top 25%		0,00	0,00		
50-75%		-10,39	-0,24		
25-50%	0,00	-7,52	-1,51		
Bottom 25%	-5,00	0,00	-31,59		



Statistics Anchor Forces					
Quartiles	Measured	Calculated	Dynamic		
Max	505,0	846,6	616,90	225,56	
75%	411,4	582,9	609,24	222,76	
Median	394,6	581,7	605,91	221,54	
25%	374,1	401,6	603,15	220,53	
Min	294,4	298,1	596,79	218,20	
	Measured	Calculated	Dynamic		
Blank	294,39	298,10	596,79		
Bottom 25%	79,67	103,49	6,36		
25-50%	20,53	180,11	2,76		
50-75%	16,80	1,20	3,33		
Top 25%	93,60	263,70	7,66		
Blank					
Top 25%					
50-75%					
25-50%					
Bottom 25%					

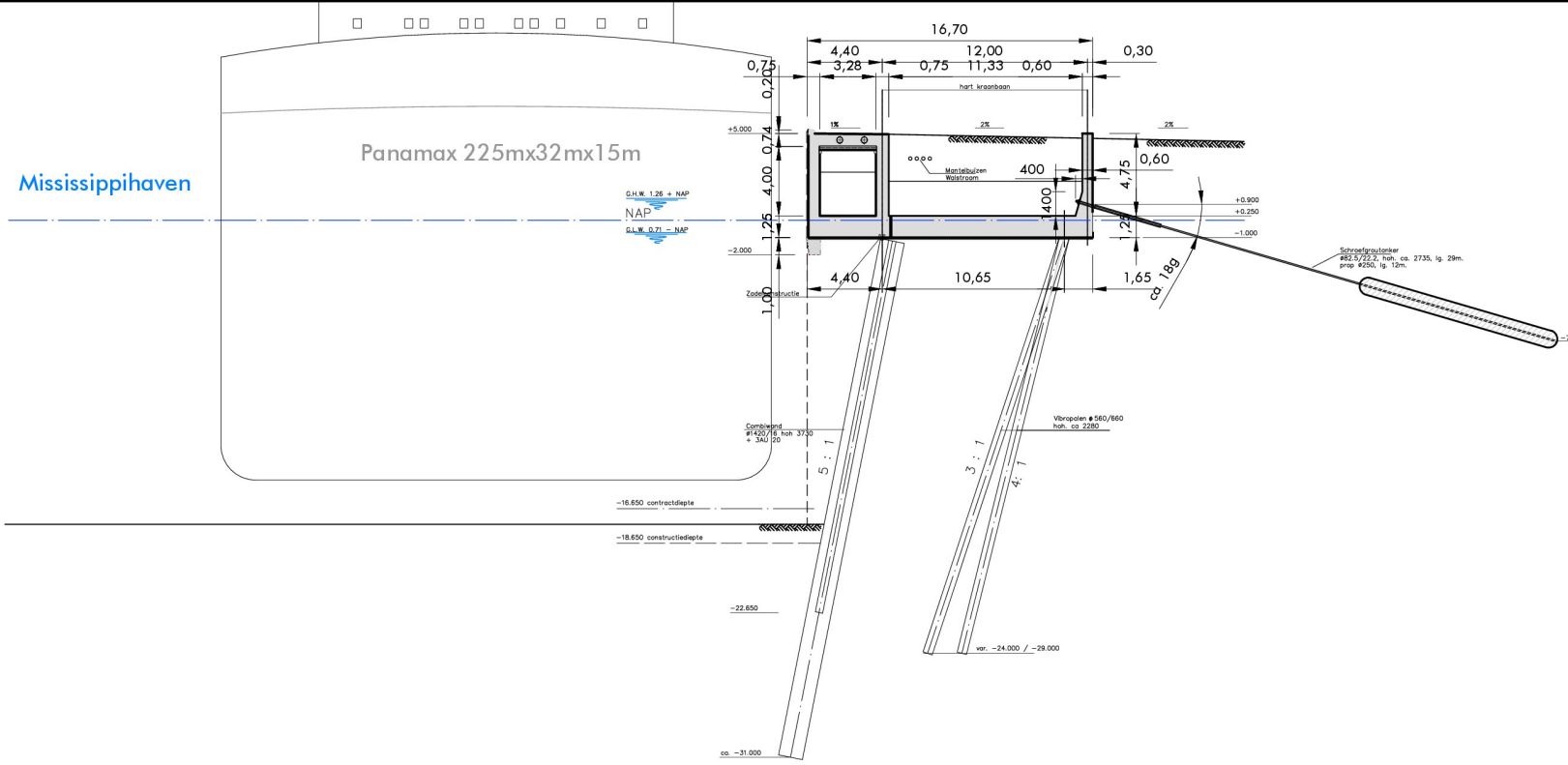


# VII

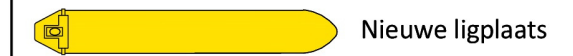
## Appendix: As-built Drawing EMO Quay Wall

# Doorsnede A

Schaal 1: 200



## Legenda



Nieuwe ligplaatsen

**A** Type Panamax (225mx32mx15m)

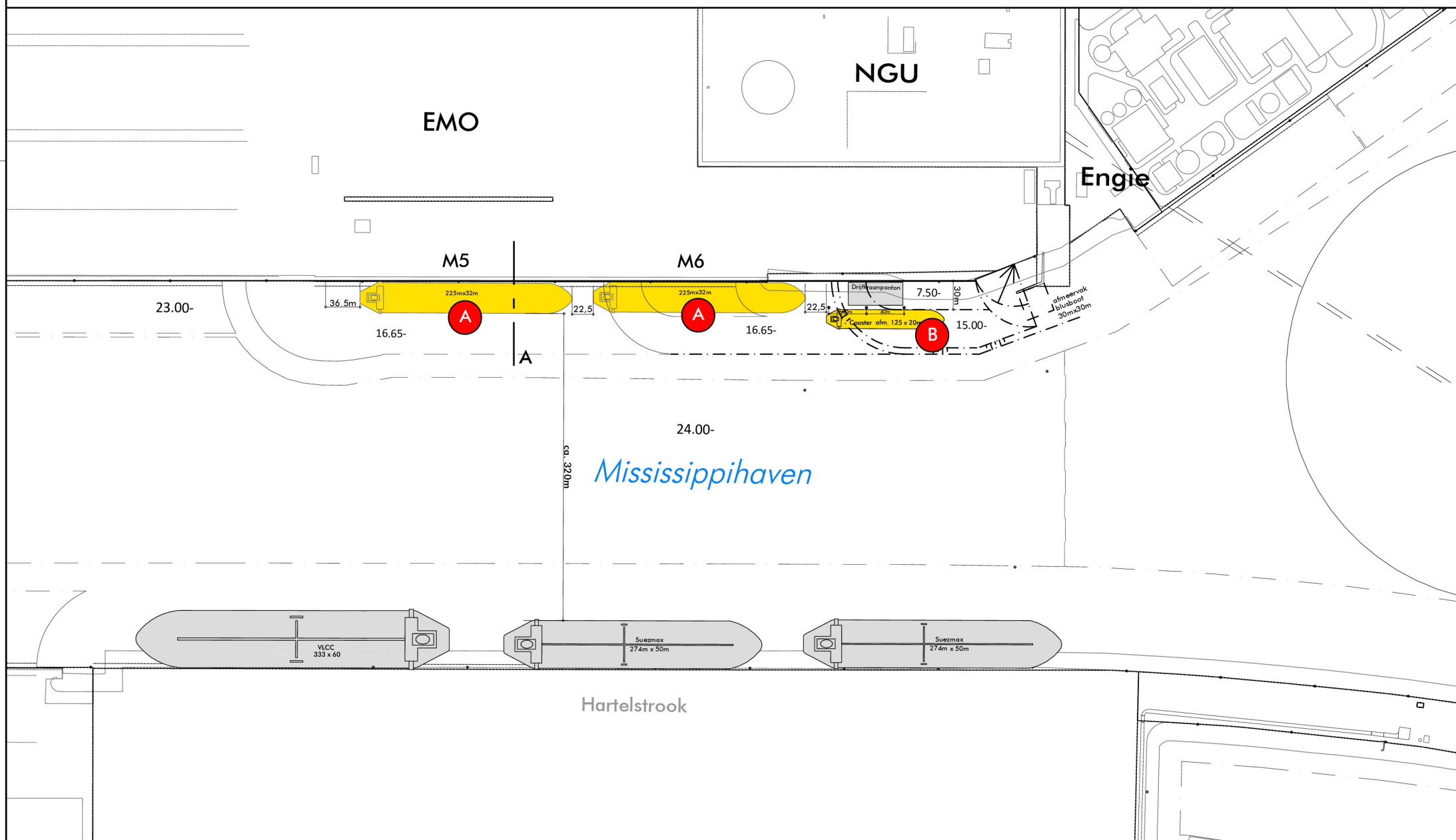
**B** Coaster (125mx20m)

— Bestaande kademuur

— Nieuwe kademuur

— Bestaande baggerlijn

— Nieuwe baggerlijn



<p>Port of Rotterdam</p> <p>Havenbedrijf Rotterdam NV Postbus 6622 3002 AP Rotterdam 010 - 252 10 10 www.portofrotterdam.com</p>	<p>onderwerp</p> <p>Indeling ligplaatsen M5 t/m M7 2 x Panamax + 1 Coaster</p>	<p>tekeningnummer</p> <p>2016-072</p>	<p>uitgave</p> <p>01</p>
	<p>project</p> <p>MV- Engie-aanpassing</p> <p>gebied</p> <p>Maasvlakte</p> <p>opdrachtgever</p> <p>T. Broeken</p> <p>ontwerper / tekenaar</p> <p>R. Mangal</p>	<p>projectnummer</p> <p>1.000511</p> <p>datum aanmaak</p> <p>04-02-2016</p> <p>datum wijziging</p> <p>25-05-2016</p> <p>status</p> <p>CONCEPT</p> <p>schaal</p> <p>1:2500</p>	<p>formaat</p> <p>A1</p>





